Applying large scale genomic and proteomic analysis to identify potential determinants of yeast pseudohyphal growth

by

Qingxuan Song

A dissertation submitted in partial fulfillment
of the requirements for the degree of
Doctor of Philosophy
(Molecular, Cellular and Developmental Biology)
in The University of Michigan
2014

Doctoral Committee:

Associate Professor Anuj Kumar, Chair
Professor Daniel J. Klionsky
Professor Laura J. Olsen
Associate Professor Tomas E. Wilson
Associate Professor Trisha Wittkopp

Acknowledgements

I would like to dedicate my sincere gratitude to my advisor, Dr. Anuj Kumar for his guidance during my research here. He has always been accessible and eager to help with any problems I might have encountered. He has an open mind to my interests and is always sharing his advice in research and life. I also thank members of the Kumar lab, both past and present, for their generous help. I'd like to thank former member Dr. Tao and Dr. Bahrucha for their help in the project. It was a great experience cooperating with those excellent people. I'd like to thank current lab members, especially Cole and Christian. We joined the Kumar lab at the same time and experienced a wonderful life in the past four years. I also thank to members in the Klionsky lab, for their generous help and joyful discussion for my project.

I'd especially like to thank my thesis committee members, Dr. Daniel J. Klionsky, Dr. Laura Olsen and Dr. Patricia Wittkopp and Dr. Tomas E. Wilson for their invaluable advice and thoughtful insights on my research projects as well as interest in furthering my career prospects.

I'd also like to thank Mary Carr for all her help and other members of the MCDB staff. She is one of the main reason I joined this program. My final gratitude goes to my beautiful wife, for her limitless support and encourage during this journey.

Chapter II of this dissertation has been published as:

Song Q, Johnson C, Lyons R, Wilson T, and Kumar A. (2013). Pooled Linkage Analysis with Next-Generation Sequencing to Identify the Genetic Determinants of Yeast Pseudohyphal Growth. Manuscript submitted.

Conceived and designed the experiments: QS, TEW and AK. Performed the experiments: QS, CJ and RL. Analyzed the data: QS, TEW and AK. Wrote the paper: QS and AK.

Chapter III of this dissertation has been published as:

Xu T, Shively CA, Jin R, Eckwahl MJ, Dobry CJ, Song Q, Kumar A. (2010). A Profile of Differentially Abundant Proteins at the Yeast Cell Periphery During Pseudohyphal Growth. J Biol Chem. 2010 May 14;285(20):15476-88.

Conceived and designed the experiments: TX and AK. Performed the experiments: TX, CAS, QS RJ, MJE, CJD. Analyzed the data: TX, CAS, QS. Wrote the paper: TX and AK.

Chapter IV of this dissertation has been published as:

Bharucha, N., Charbrier-Rosello, Y., Xu, T., Johnson, C., Sobczynski, S., Song, Q., Dobry, C., Echwahl, M., Anderson, C., Benjamin, A., Kumar, A., Krysan, D. (2011). A Large-Scale Complex Haploinsufficiency-Based Genetic Interaction Screen in Candida Albicans: Analysis of the RAM Network during Morphogenesis. PLoS Genetics 7(4), e1002058.

Conceived and designed the experiments: NB YC-R AK DJK. Performed the experiments: NB YC-R TX CJ SS QS CJD MJE CPA AJB DJK. Analyzed the data: NB YC-R TX CJ SS AK DJK. Contributed reagents/materials/analysis tools: NB YC-R TX CJ SS QS CJD MJE CPA AJB DJK. Wrote the paper: YC-R AK DJK.

Other publications:

Song Q and Kumar A. (2012). An Overview of Autophagy and Yeast Pseudohyphal Growth: Integration of Signaling Pathways during Nitrogen Stress. *Cells* 2012, *1*(3), 263-283

Wittkopp PJ, Smith-Winberry G, Arnold LL, Thompson EM, Cooley AM, Yuan DC, Song Q, McAllister BF. (2011). Local adaptation for body color in Drosophila americana. Heredity. 2011 Apr;106(4):592-602.

TABLE OF CONTENTS

LIST OF FIGURES

LIST OF TABLES

CHAPTER 1

Introduction

1.1. Yeast as a model organism

Yeasts are unicellular fungi, with precise classifications derived from characteristics related to the cell, ascospore and colony. Variants of different yeast strains have long been used to ferment the sugars of rice, wheat, barley, and corn to produce alcoholic beverages. The fermentation of wine is initiated by naturally occurring yeasts in the vineyards. Many wineries still use nature strains, although they have started to use modern methods of strain maintenance and isolation [1]. Besides the importance of yeasts in wine-making and baking, yeasts are also medically important as causative agents in disease-related infections. In particular, the yeast-like fungus, *Candida albicans*, is commonly found in the mouth, vagina, and intestinal tract as one of the major causes of fungal infection[2]. Candidiasis of the mucous membranes of the mouth is known as thrush, while infection in the vagina is called vaginitis. Both types of *C. albicans* infections are problematic, with oral thrush being a particular problem in immunocompromised individuals and premature infants[3,4].

The Yeast *Saccharomyces cerevisiae* is the most ideal eukaryotic microorganism for biological studies. It has been widely used in biological research and is a popular model organism for genomics and proteomics, cell biology and biochemistry[5-7]. It has a small size, minimal nutritional requirements, and is non-pathogenic in nature. *S. cerevisiae* has a short doubling time of 90 minutes, easing experimental data collection. The size of the haploid genome is 1.2×10^7 bp, consisting of sixteen chromosomes ranging in size from 230,000 bp to 2,352,000 bp[8]. Its genome was the first to be successfully sequenced in 1996[9]. Despite the complexity of the yeast genome in comparison to *E. coli*, both genomes offer many technical advantages for applications

and developments in modern molecular genetics. Some of these properties, including rapid growth, dispersed cells, and mutant isolation systems, make yeast particularly suitable for biological analysis. In addition, *S. cerevisiae* is stable in both haploid and diploid forms[2], which largely facilitates genetic manipulation. Recessive mutations can be conveniently isolated and manifested in haploid strains, and plasmids can be easily introduced into different strain background by transformation. Moreover, there are various markers available from cloning and chromosome modifications. The overall virtues of yeast are highlighted by the fact that mammalian genes can be introduced into yeast for systematic analyses for the functions of the corresponding gene products.

1.2. Yeast Genomics and Proteomics

1.2.1. Yeast Genomics

The *Saccharomyces cerevisiae* genome was first sequenced in 1996[9]. Only a few years later, more cooperative efforts were organized to produce a nearly complete set of deletions of every open reading frame, with each gene replaced by a drug-resistance gene and marked with synthetic barcode sequences[10,11]. This gave the yeast research community the power to screen entire libraries of deletion mutants for biological processes of interest. These libraries of deletion mutants and derivatives over the years have been exploited to great effect in genome-scale experiments. Other comprehensive mutant libraries have been constructed and widely applied in the yeast community to explore protein function and localization[12,13]. The construction of green fluorescent protein (GFP) fusions to the majority of yeast genes have been used to provide localization information for most yeast proteins[14]. Libraries of fusions to other sequence tags have been constructed that facilitate immunoprecipitation and detection of protein interactions[15]. One collection was designed where each of the included 5,573 yeast strains carries a multicopy plasmid bearing a unique yeast ORF tagged C-terminally with a tandem affinity tag that includes a hemagglutination (HA) tag and driven by an inducible *GAL1* promoter. This collection allows the targeted over-expression of most yeast genes and was recently used in a genome-wide study to identify novel regulators of

filamentous growth in *S. cerevisiae*. Collectively, these libraries greatly facilitated the development of a broader yeast biology knowledgebase in the past decade.

The Kumar lab has previously used these tools to study filamentous growth in *S. cerevisiae*. Jun *et al*. used an overexpression library to screen autophagy genes in filamentous growth condition, and discovered that overexpression of 10 autophagy-related genes (*ATG1*, *ATG3*, *ATG4*, *ATG6*, *ATG7*, *ATG17*, *ATG19*, *ATG23*, *ATG24*, and *ATG29*) inhibits filamentous growth[16]. Consistent with these results, the deletion of *ATG1* and *ATG7* results in exaggerated filamentous growth and the premature initiation of filamentous growth under less severe conditions of nitrogen stress. As a simple model to consider these results, the Kumar laboratory proposed previously that the inhibition of autophagy resulting from deletion of *ATG1* and *ATG7* may result in an increased degree of nitrogen stress, manifested as exaggerated filamentous growth[17]. Another overexpression screen conducted by Jin *et al*. in the filamentous Σ1278b strain encompassed 3,627 integrated transposon insertion alleles and 2,043 overexpression constructs[18]. Collectively, the Kumar laboratory analyzed 4,528 yeast genes with these reagents and identified 487 genes conferring mutant filamentous phenotypes upon transposon insertion and/or gene overexpression. This screen identified a variety of genes and pathways affecting filamentous growth, and highlighted mitochondrial function during filamentous growth and retrograde signaling pathway. In total, this filamentous growth gene set represents a wealth of yeast biology, highlighting 84 genes of uncharacterized function and an underappreciated role for the mitochondrial retrograde signaling pathway as an inhibitor of filamentous growth. More recently, Bharucha *et al*. constructed a unique set of 125 kinase-yellow fluorescent protein chimeras in the filamentous Σ1278b strain for this study[19]. In total, we identified six cytoplasmic kinases (Bcy1p, Fus3p, Ksp1p, Kss1p, Sks1p, and Tpk2p) that localize predominantly to the nucleus during filamentous growth. These kinases form part of an interdependent, localization-based regulatory network: deletion of each individual kinase, or loss of kinase activity, disrupts the nuclear translocation of at least two other kinases. This study highlights a previously unknown function for the kinase Ksp1p, indicating the essentiality of its nuclear translocation during yeast filamentous growth. Collectively, these studies took advantage of the yeast genomic tools, and successfully identified genes that are

related to filamentous growth, and represented an overlooked regulatory component of this stress response.

1.2.2. Global analysis of protein-protein interaction

1.2.2.1. Yeast two-hybrid system

One of the advantages of using yeast as a model for study is that it allows biologists to apply powerful tools to interpret the functions of uncharacterized genes and the proteins they encode. Protein-protein interactions are fundamental to all cellular processes, and in many cases, the function of an unknown protein can be inferred from the proteins with which it interacts. The first is the well-developed yeast two-hybrid system, and the second involves the purification of protein complexes coupled with mass spectrometry (MS). The versatility and sensitivity of two-hybrid and MS-based approaches has led to their application in the growing field of proteomics (the global analysis of all the proteins encoded by a genome). This use is perhaps best illustrated by ambitious projects to map the entire yeast interaction network, using systematic, high-throughput two-hybrid technologies.

The yeast two-hybrid system was first developed by Fields and Song in the 1980s and was quickly applied to different types of work around the world[20]. The discovery that the DNA-binding domain (BD) and transcription activation domain (AD) of many proteins are functionally and physically separable, with the BD localizing proteins to specific DNA sequences within the genome, and the AD contacting the transcription machinery to activate gene transcription, inspired Fields and Song to realize that it was possible to bring the BD and AD of a transcription factor together by fusing each to one of a pair of physically interacting proteins (**Figure 1.3**). They used the interacting proteins Snf1p and Snf4p to reconstitute activity of the yeast *Gal4* transcription factor, by generating two plasmid constructs[21]. The first encoded *SNF1* fused to the C-terminus of the Gal4 BD (BD constructs are referred to as the bait), and the second construct encoded the *Gal4 AD-SNF4* fusion protein. With two plasmids transformed into a yeast

strain that carries a *LacZ* reporter gene under the control of a Gal4-reponsive element, the interaction between Snf1p and Snf4p can be detected by β-galactosidase activity[21].

The yeast two-hybrid system has been rapidly developed in numerous ways and used extensively for high throughput applications. To date, two independent large-scale studies have been performed to identify protein-protein interactions across the *S. cerevisiae* proteome. The first study by Uetz *et al.* identified 957 protein-protein interactions involving 1,004 proteins[22], whereas the second study by Ito *et al*. identified 4,549 two-hybrid interactions among 3,278 proteins generating a network linking most of the yeast proteins across the proteome[23,24]. In addition to yeast studies, the yeast two-hybrid system can also be applied to study protein-protein interaction within higher-level model organisms. Matthews *et al*. randomly selected 72 yeast interactions identified by the large-scale two-hybrid approaches, and tested the corresponding *Caenorhabditis elegans* proteins to determine whether similar interaction partnerships were formed[25]. Thirty-one percent of the interactions detected between the yeast proteins were also detected between the corresponding *C. elegans* proteins. After more than 20 years, the yeast two-hybrid system is still one of the most popular and powerful tools to study protein-protein interactions.

1.2.2.2. Mass spectrometry in yeast study

The yeast two-hybrid system is one of many ways in which protein–protein interactions can be investigated (**Figure 1.4**). Although the two-hybrid system is an *in vivo* genetic assay, numerous *in vitro* protocols are also commonly used, such as co-immunoprecipitation, pull-down assays, affinity chromatography, protein-array chips, and surface plasmon resonance (SPR). The combination of these methods with mass spectrometry (MS) enhances the power to examine protein interactions. Instead of detecting binary interactions between proteins, MS-based approaches are effective in characterizing large protein complexes. Gavin *et al.* expressed 1,739 genes with the TAP tag, allowing a tandem purification regime[26]. The tagged ORFs were expressed in yeast cells, and were allowed to form more natural complexes under appropriate physiological

conditions. Protein complexes were purified from the cell lysates of 1,167 yeast strains that expressed the modified proteins to detectable levels; first with mild elution using a high-affinity purification step, followed by a second affinity step. After analyzing the sample with MALDI-TOF MS, 589 protein complexes were purified and 232 were unique. Using the similar approach, Ho *et al.* expressed 725 proteins modified to carry the FLAG epitope[27]. Again, the proteins were expressed in yeast cells and complexes were purified, using a single immunoaffinity purification step. After rendering the sample to LC-MS/MS, they detected 3,617 interactions that involved 1,578 different proteins. Among their set of baits were 86 proteins involved in the DNA-damage response (DDR), which are potentially biological significant.

A major innovation to the quantification of LC-MS/MS is the technique of stable-isotope dilution. This approach applies the fact that a stable isotope-labeled peptide is chemically identical to its native equivalent, and behaves identically in downstream analyses. Mass spectrometers can detect the mass differences between the peptides permitting accurate quantification of unlabeled to labeled peptides. Many variations of stable-isotope tagging have been introduced. Godoy *et al*. introduced 'stable-isotope labeling with amino acids in cell culture', or SILAC in 2008, which offers a simple and effective means to label all peptides for proteomic analysis[28]. In this method, labeled, essential amino acids are added to amino acid-deficient media. Cells grown in the SILAC media metabolically incorporate the labeled amino acids into their proteins as they are produced. They successfully achieved unambiguous identification of more than 2,000 proteins, including very low abundant ones. Effective dynamic range was limited to about 1,000 and effective sensitivity to about 500 femtomoles, far from the subfemtomole sensitivity possible with single proteins. This method has been used for multiple large-scale studies, including a proteomic comparison of haploid and diploid yeast and a genome-wide analysis of protein phosphorylation in mammalian cells. However, the cost and time associated with creating the cell lines often negates the value of information provided, though the ease of yeast genetic manipulation make it an exceptional organism for this methodology.

1.3. Filamentous growth in yeast

1.3.1. Filamentous growth in *Saccharomyces cerevisiae*

Filamentous growth in budding yeast was first discovered by Fink *et al*. in the context of studying cell polarity. It has been studied more intensively than corresponding modes of filamentous growth in other fungi[29]. Most laboratory strains are non-filamentous, and only a handful of laboratory strains can develop filaments under induction (e.g., strains of the Σ1278b and SK1 genetic backgrounds). Filamentous growth can be induced by nutrient scarcity in the form of nitrogen or glucose deprivation[30,31]. Moreover, growth in the presence of short-chain alcohols such as butanol and ethanol can stimulate filamentation in certain strains. The short-chain alcohols are end products of amino acid catabolism under nitrogen-deprivation conditions and likely constitute a mimic of nitrogen stress, although distinctions exist regarding the genetic complement necessary for the induction of filamentous growth by each condition[18,30].

In Σ1278b and SK1 strains, both haploid and diploid cells can undergo filamentous growth, however the morphological changes are slightly different between the two. In diploid cells, nitrogen stress or short-chain-alcohol stress induces the formation of surface-spread filaments from a spotted culture or colony and invasive filaments that extend downward into a solid substrate below (**Figure 1.5**). In haploid strains, surface-spread filamentation is less extensive, but invasive filaments do form on both rich medium and under conditions of glucose deprivation[30]. Typically, the surface-spread filamentation exhibited by diploids under conditions of nitrogen stress is referred to as pseudohyphal growth. Either in haploids or in diploids, the cell morphology is similar. During filamentous growth, yeast cells delay in progression of G2/M[32], result in a prolonged period of apically directed polarized growth, and exhibit an elongated cell shape[33]. The budding pattern changes from axial (in haploid cells) and bipolar (in diploid cells) to a unipolar budding pattern[34]. Moreover, cells remain connected after cytokinesis during filamentous growth, forming a multicellular filament[35].

1.3.2. Cellular processes contributing to yeast filamentous growth

In order for yeast cells to effectively form pseudohyphal filaments, critical processes of budding, polarized growth, and cell cycle progression must be appropriately regulated and coordinated. These processes are related, and the molecular machinery of cell cycle progression and cellular morphogenesis has been intensively studied. In terms of cellular budding components, two bud site selection genes, *BUD6 and BUD14* have been found to be responsible for filamentous growth phenotypes of defective surface filamentation upon gene disruption in a haploid genetic background under conditions of butanol treatment[18]. A larger set of budding genes, including *BUD3, BUD4, BUD6, BUD7, BUD8 and BUD25* are involved in haploid invasive growth, diploid pseudohyphal filametation, and biofilm formation. Similarly, in addition to the genes above, the key polarisome components *SPA2* and *PEA2* also yield defects in surface spread filamentation in a haploid strain upon butanol treatment[36,37]. Genes that regulate the G2/M transition in yeast also affect filamentous growth, leading to the general observation that genetic perturbations resulting in delayed G2/M progression and an extended period of apical growth promote yeast filamentation. However, this generalization must be considered with caution, as many genetic perturbations that affect cell cycle regulators modulate events that impact processes outside of G2/M progression. Thus, it can be difficult to predict the resulting filamentous growth phenotype in such mutant strains.

1.3.3. Signaling pathways regulating filamentous growth in Saccharomyces

Filamentous growth in *S. cerevisiae* is mediated by several signaling pathways. Classic studies from numerous laboratories have identified at least three signaling pathways that regulate filamentous growth: 1) the MAPK pathway, 2) the Ras/PKA pathway, and 3) the Snf1p kinase pathway. While these essential signaling pathways play key roles in regulating filamentous growth transition in *S. cerevisiae*, the full genetic basis of yeast filamentation is very broad. Large-scale phenotypic screens using transposon-mutagenized yeast strains have identified 309 genes that are required for

wild-type filamentous growth in a haploid genetic background under conditions of butanol induction[18]. An overexpression screen in the same background identified 199 genes that yielded filamentous growth phenotypes, while microarray-based expression profiling studies have identified an extensive transcriptional program of 874 genes differentially expressed during filamentous growth[38]. The bulk of these genes are components of cellular processes required for wild-type filamentous growth.

Among those genes discovered, enhanced cell-cell adhesion during filamentous growth is a well-established hallmark of the process[39]. Genetic studies have identified a set of genes required for calcium-dependent aggregation, or flocculation. These flocculation genes comprise a multi-gene family of largely sub-telomeric sequences encoding several lectin-like proteins, with *FLO8* and *FLO11* being most critically associated with filamentous growth[39,40]. Flo8p is a transcriptional factor that regulates the expression of *FLO11* and many other genes contributing to filamentous growth; approximately 230 such gene promoters bound by Flo8p have been identified through chromatin immunoprecipitation-microarray analyses[41]. Interestingly, deletion of *FLO8* yields a strong filamentous growth defect, and the *FLO8* sequence is in fact a pseudogene in strains derived from the common non-filamentous S288c genetic background. Flo8p also functions as a downstream effector of the PKA signaling pathway[42]. *FLO11* has been studied most intensively for its large promoter, which integrates transcriptional signals from Flo8p, Ste12p and Mss1p[43]. Thus, Flo11p is a GPI-anchored cell surface glycoprotein required for invasive growth, pseudohyphal formation, and biofilm formation.

1.3.3.1. Tor Complex I (TORC1) and MAPK pathway

Tor is a critical regulator for multiple cellular mechanisms. The Tor kinase functions in two distinct multi-protein complexes: TORC1 (Tor complex 1) and TORC2 (Tor complex 2). Of these two complexes, TORC1 fulfills the primary role in regulating filamentous growth in *S. cerevisiae*, through two distinct mechanisms. First TORC1 regulates transcript level of *FLO11* via the transcriptional factor Gcn4p. It has been

shown that expression levels of a *FLO11-LacZ* reporter are significantly decreased in a *gcn4Δ* mutant, while overexpression of *GCN4* is sufficient to induce filamentous growth and elevated *FLO11* expression[44](**Figure 1.6**). These results suggest that Gcn4p contributes to the transcriptional regulation of *FLO11*. Second, recent studies have identified multiple proteins associated with the Kog1p/TORC1 complex, such as Mks1p, Kap123p, Hef3p, Ksp1p and Uba3p[45]. Deletion mutants of *KSP1, KAP123* and *UBA4* exhibit impaired invasive growth, and the diploid deletion strains show reduced spread filamentation compared to a wild-type strain[19]. The fact that *FLO11* transcript levels are reduced in these mutants provides more evidence that TORC1 does indeed contribute to the regulation of *FLO11*. Furthermore, the proteins Tap42p and Sit4p have been found to yield filamentous growth phenotypes upon generic perturbation[46]. Overexpression of *TAP42* restores filamentous growth in cells treated with rapamycin, and deletion of the Sit4p phosphatase impairs filamentous growth and shows rapamycin hyperactivity. These results indicate a model where TORC1 changes the association of Tap42p and Sit4p by phosphorylating Tap42p to regulate filamentous growth in yeast.

1.3.3.2. The Ras/PKA pathway

In addition to TORC1 and the MAPK pathway, the Ras/PKA pathway is another conserved signaling network regulating filamentous growth in yeast. Nutrient limitation increases intracellular cAMP levels, which then activates PKA. Yeast PKA contains one regulatory subunit, Bcy1p, and three catalytic subunits, Tpk1p, Tpk2p and Tpk3p[47]. Cellular levels of cAMP are increased by activation of the adenylate cyclase Cyr1p through the Ras GTPase[48].

Under conditions of nutrient sufficiency, two redundant small GTPases, Ras1p and Ras2p, are activated by upstream signals and then stimulate adenylyl cyclase Cyr1p to enhance cAMP levels in the cell. Though Ras2p is responsible for the majority of Ras function, both of there are actually controlled by the guanine nucleotide exchange factors (GEFs), Cdc25p and Sdc25p, as well as the GTPase Activating Proteins (GAPs), Ira1p and Ira2p[49,50]. cAMP binds to the PKA regulatory subunit Bcy1p to release its

catalytic subunits Tpk1p, Tpk2p and Tpk3p, resulting in activation of PKA. Interestingly, the functions of these three catalytic subunits are distinct from each other in regulating filamentous growth (**Figure 1.7**). Whereas deletion of *TPK2* impairs filamentous growth, deletion of *TPK1* and *TPK3* actually enhances filamentous growth. These results suggest that Tpk2p is an activator of filamentation, while Tpk1p and Tpk3p may posses an inhibitory function[42,51]. Although there is still evidence showing that Tpk1p regulates the dual specificity tyrosine-regulated kinase Yak1p, which positively regulates filamentous growth through the transcriptional factors *SOK2* and *PHD1[52]*. The key filamentous growth transcription factor Flo8p is a direct substrate of Tpk2p, and deletion of *FLO8* abolishes filamentous growth in the Σ1278b genetic background.

1.3.3.3. The nutrient-sensing Snf1p pathway

In addition to nitrogen stress, glucose deprivation is known to act as another trigger of filamentous growth. Several studies have shown that the depletion of fermentable carbon sources like sucrose and glucose can trigger filamentous growth[53]. Snf1p can regulate filamentous growth through its beta subunit Gal83p. The Snf1p kinase is a member of the highly conserved Snf1/AMP-activated protein kinase (AMPK) family. The proteins that act upstream of Snf1p are not yet well understood. To date, there are three known kinases Sak1p, Elm1p, Tos3p and the Reg-Glc7 protein phosphatase I[54]. Snf1p-Gal83p antagonizes the zinc-finger proteins Ngr1p and Ngr2p to de-repress transcription of *FLO11[55]*. Snf1p also acts to regulate filamentous growth through another beta subunit, Sip2p, as well as other substrates[56]. These observations significantly establish Snf1p as a consistent connection between the many nutritional states required for filamentous growth.

1.3.4. Morphogenesis and virulence in *Candia albicans*

Candida albicans is the most prominent fungal pathogen in humans. *C. albicans* belongs to the fungal kingdom and shares multiple similarities with *Saccharomyces*

cerevisiae. *C. albicans* is a major cause of candidiasis, which is difficult to treat. It is usually a benign colonizer of human mucosal surfaces and highly specialized for life in a human host. However, a mildly compromised immune system or a minor imbalance of the microbiota can result in its transition from a commensal to a pathogen, permitting infection of virtually every organ of the human body and resulting in severe infections[57]. Oral and oesophageal candidiasis are particularly common in HIV-positive individuals, even in up to 90% of HIV patients without highly active antiretroviral therapy[58]. In addition, cancer patients receiving chemotherapy or organ and bone marrow transplant could easily develop blood stream, kidney, liver, and central nervous system *C. abicans* infections[59].

Candida albicans is known to exist in multiple growth forms: yeast, pseudohyphal and true hyphal forms. Morphogenesis is triggered by a number of environmental factors, such as temperature, pH levels and nutrition supply. Yeast and hyphal forms are found in clinical isolates. Yeast-form cells usually exist at acidic and relatively lower-temperature (30°C) environment. The morphology of yeast-form cells mimics *S. cerevisiae*; the cell shape is oval, and cells divide by budding[60]. In higher pH and high-temperature environments, yeast cells form pseudohyphae, which consist of chains of elongated cells with distinct cell walls. Hyphae are formed from yeast cells in response to many different conditions such as the presence of serum, N-acetylglucosamine, higher temperatures at 37°C and neutral pH, and microaerophillic conditions[61](**Figure 1.8**).

The virulence of *Candida albicans* is strongly associated with its ability to switch between yeast and hyphal growth[62]. It has been suggested that the yeast form is important for dissemination, and the hyphal form is required to invade host tissue. Non-filamentous *C. albicans* mutants are avirulent in animal models. One line of evidence supporting this is that the deletion of the *C. albicans* gene *ACE2* results in defects in cell separation, increased invasion of solid agar medium and inappropriate pseudohyphal growth. The *ACE2* deletion strain is also avirulent in a mouse model[63].

1.3.5. Regulating pathways leading to hyphal growth in *C. albicans*

1.3.5.1. MAPK pathway

The mitogen-activated protein kinase (MAPK) cascade has been shown to regulate hyphal or pseudohyphal growth in *S. cerevisiae* and *C. albicans[32,43,64]*. In *C. albicans*, the MAP Kinase cascade consists of the MAP kinase homologue Cek1p, the MAP or extracellular signal-regulated kinase homologue, Hst7p, the MEK kinase homologue Ste11p and the p21-activated kinase homologue, Cst20p[65]. The protein phosphatase Cpp1p phosphorylates and activates Cek1p, which then leads to the stimulation of the putative transcriptional factor, Cph1p[66]. In addition, a recent study showed that the mitogen-activated protein kinase Mkc1p, which has been reported to be a part of the fungal cell integrity pathway, also affects hyphal growth and biofilm formation. The *mkc1Δ/Δ* null mutant was defective in producing filamentous colonies when cells were embedded within agar medium. And introduction of wild-type Mkc1p can rescue the phenotype. Also, defects in biofilm formation are present in the *mkc1Δ/Δ* null mutant, indicating that normal biofilm formation requires Mkc1p[67].

1.3.5.2. cAMP/PKA pathway

The cAMP-dependent PKA pathway has been shown to regulate hyphal development in *C. albicans*. Activation of this signaling cascade occurs via the GTP binding protein Ras1p, which is in turn activated by the GEF Cdc25p and stimulates production of cAMP by activation of the adenylate cyclase Cdc35p[68]. Deletion of both *CDC35* alleles completely abolishes detectable levels of intracellular cAMP. The mutant cells grow more slowly than wild-type cells, and they are unable to switch from yeast to hyphal forms in the hyphae-induction conditions. There are two PKA calalytic subunit isoforms in *C. albicans*, Tpk1p and Tpk2p. Deletion of both alleles of *TPK2* results in changes in morphogenesis in some environmental conditions and partially reduced virulence in a mouse model, suggesting that Tpk1p also functions in this signaling cascade[69]. Epistatic analysis and biochemical studies indicate that when cAMP binds to Tpk2p, Tpk2p dissociates, phosphorylates and mediates the downstream signal via the

transcription factor, Efg1p[70], which is a key regulator of morphogenesis in *C. albicans*, including the yeast-hyphae switch.

Shapiro et al. have shown that one of the HSP family proteins, Hsp90p[71], functions in the cAMP-PKA pathways to regulate hyphal development in *C. albicans*. Pharmacological inhibition of *Hsp90* with geldanamycin induced filamentation, indicating that relief of *Hsp90*-mediated repression is required for induction of filamentous growth. This could be the reason why a requirement of most conditions that induce filamentation is an elevated temperature of 37°C. The mutants of positive regulators of the Ras1-PKA pathway, such as *cdc25Δ, ras1Δ, cdc35Δ,* failed to form hyphae in response to *HSP90* inhibition, suggesting that *HSP90* regulates morphogenesis via the cAMP-PKA cascade[72].

1.3.5.3. RAM pathway

The regulation of Ace2p transcription factor and polarized morphogenesis (RAM) signaling network consists six genes present in both *C. albicans* and *S. cerevisiae*: *CBK1, MOB1, KIC1, HYM1, PAG1* and *SOG1* (**Figure 1.9**). The RAM network regulates the maintenance of cell polarity, cell wall integrity, and daughter-cell-specific nuclear localization of Ace2p, which in turn activates cell separation genes during mitotic exit[73,74].

Kelly *et al*. have found that the *ACE2* gene affects morphogenesis, adherence, and virulence in *C. albicans*. Deleting both *ACE2* alleles results in a defect in cell separation, increased invasion of solid agar medium and inappropriate pseudohyphal growth. The loss-of-function mutants are also avirulent in a mouse model. Mulhern *et al*. have shown that Ace2p is required for hyphal development under hypoxic conditions and regulates a large number of metabolic genes during this process[63]. They also used microarray approaches to identify 20 genes involved in cell wall metabolism or the regulation of expression of cell wall genes whose expression level was reduced in the *ace2Δ/Δ* strain. They subsequently identified a candidate consensus DNA binding site for Ace2p (MMCCASC), although this site has not been confirmed.

Cbk1p is a serine/threonine protein kinase in the Ndr/LATS family, and has been most intensively studied in *S. cerevisiae[75]*, where it phosphorylates Ace2p in a process that is required for asymmetric localization of Ace2p to daughter cells. Song *et al*. analyzed the role of the RAM network by focusing on the Cbk1p binding partner Mob2p. They showed that interaction between Cbk1p and Mob2p is critical for hyphal growth in *C. albicans[73]*. Their results indicate that the SMA domain of Cbk1p and the Mob1p/phocein domain of Mob2p are essential for proper function of the Cbk1p-Mob2p complex and suggest that this complex might be involved in regulating a subset of Tup1p/Nrg1p-controlled hyphae-specific genes under hyphae-inducing conditions[76].

1.3.6. Genomic and proteomic studies of filamentous growth in yeast

Since the discovery of yeast pseudohyphal growth in the 1980s, numerous studies have applied genomic and proteomic approaches to explore the detailed mechanisms regulating filamentous growth in *S. cerevisiae* and *C. albicans*. Deletion and overexpression libraries are currently available in the filamentous Σ1278b genetic background. Previous studies have applied genetic screening using these libraries to identify potential regulators in the filamentous growth process. Through this, the key components regulating filamentous signaling pathways, such as PKA, MAPK and Ste12p, have been identified. A thorough screen using deletion libraries was recently finished by the Boone lab, and they have successful identified a large set of genes whose deletion mutants affect different forms of filamentous growth. Jun *et al*. used an overexpression library to screen autophagy genes in filamentous growth condition, and discovered that overexpression of 10 autophagy-related genes (*ATG1*, *ATG3*, *ATG4*, *ATG6*, *ATG7*, *ATG17*, *ATG19*, *ATG23*, *ATG24*, and *ATG29*) inhibits filamentous growth[16]. Another overexpression screen conducted by Jin *et al*. in the filamentous Σ1278b strain encompassed 3,627 integrated transposon insertion alleles and 2,043 overexpression constructs[18]. Collectively, the Kumar laboratory analyzed 4,528 yeast genes with these reagents and identified 487 genes conferring mutant filamentous phenotypes upon transposon insertion and/or gene overexpression. Similar libraries were also available in *C. albicans*. The Krysan and Kumar labs presented the first large-scale

synthetic genetic interaction screen in *C. albicans*. This work involved a CHI-based screening strategy applied to the identification of genes that interact with the RAM signaling network during *C. albicans* filamentation.

In terms of studies in proteomics, different forms of mass spectrometry are widely used to screen proteins that change abundance during filamentation. For example, SILAC-MS has been used to detect changes in abundance of proteins on the cell periphery. Also, mass spectrometry has been used to screen potential targets of kinases required for wild-type pseudohyphal growth in yeast. Network analyses of proteins differentially phosphorylated in these kinase mutants identify multiple cellular processes and mechanisms, such as RNA processing components and cellular respiratory components. These findings have broadened our understanding of pseudohyphal growth beyond the initial signaling pathways identified as important regulatory factors.

To date, filamentous growth is considered as a drastic cellular morphological change induced by nutrient limitation. During filamentous growth, yeast cells exhibit an elongated shape due to a delay in progression through G2/M, resulting in a prolonged period of apically directed polarized growth. The mode of cell division switches from being asymmetric and asynchronous to a symmetric and synchronous form. The budding pattern changes from axial (in haploid cells) or bipolar (in diploid cells) to a unipolar pattern. Classic studies from numerous laboratories have identified at least three signaling pathways that regulate filamentous growth in *S. cerevisiae*: 1) the MAPK pathway, 2) the Ras/PKA pathway, and 3) the Snf1p kinase pathway. The RAM pathway, MAPK pathway and cAMP/PKA pathways are generally recognized as key regulators of hyphal growth in *C. albicans*. As a form of morphological change, filamentous growth is closely related to other cell mechanisms regulating morphology, such as apical cell growth, budding pattern selection and cell-cell adhesion regulating mechanisms. Moreover, since it is induced by nutrient limitation in the surrounding environment, filamentous growth has been found to be related to cellular energy-providing system, such as mitochondrial metabolism and RNA processing mechanisms. Although these findings are thrilling and insightful, the detailed mechanisms of these processes remain to be identified. Some general questions need to be answered, such as: 1) what is the profound difference

between filamentous strains and non-filamentous strains; 2) how can filamentous growth be considered in an evolutionary context; and 3) what are the molecular connections that connect filamentous growth and other cellular mechanisms?

Figure 1.1. Genetic relationship of *S. cerevisiae* strains in wine industry. Cladogram of various *S. cerevisiae* strains produced from whole-genome sequence alignments[1].

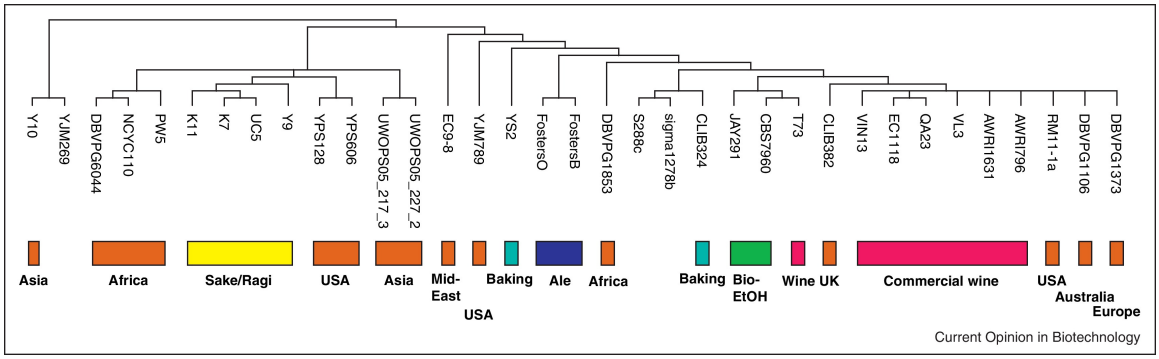

Figure 1.2. *S. cerevisiae* naturally exist in both haploid and diploid forms. The *MAT* locus in *S. cerevisiae* exists as either of two alleles, a and α, that determine the mating type of haploid cells through expression of distinct sets of transcriptional regulators. a type cells, which possess the *MAT* a allele, can mate only with α type cells, which possess the *MATα* allele, and vice versa. The product of mating is a diploid cell that is heterozygous at the *MAT* locus and cannot mate. Instead, under appropriate environmental conditions, diploid cells undergo meiosis, thereby recreating haploid cells of a and α mating types[2].

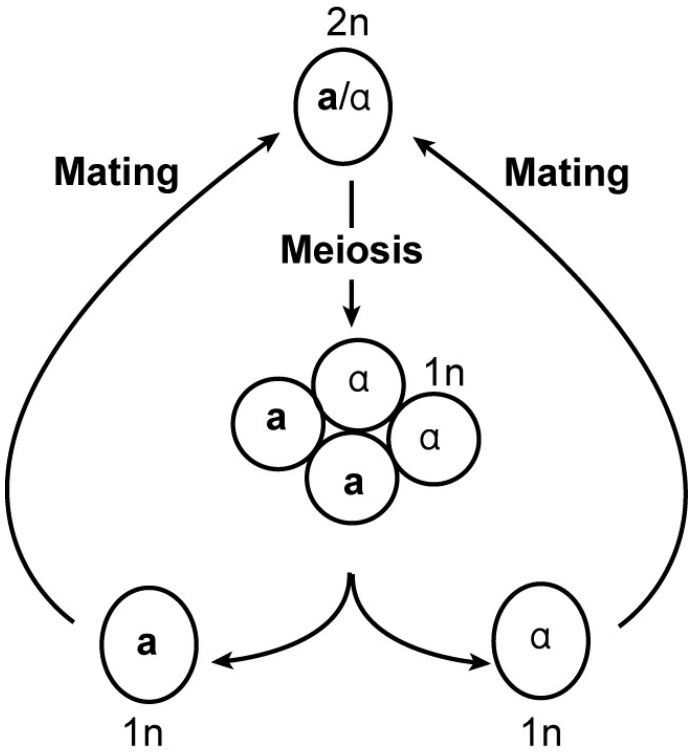

Figure 1.3. The principle of the yeast two-hybrid system. The bait-encoding protein X fused to the C-terminus of a transcription factor DNA-binding domain (BD) and the prey-encoding protein Y fused to an activation domain (AD). Alternatively, the prey can consist of proteins encoded by an expression library. Each plasmid is introduced into an appropriate yeast strain either by co-transformation, sequential transformation, or by yeast mating. Only if proteins X and Y physically interact with one another are the BD and AD brought together to reconstitute a functionally active transcription factor that binds to upstream specific activation sequences (UAS) in the promoters of the reporter genes, and to activate their expression[77].

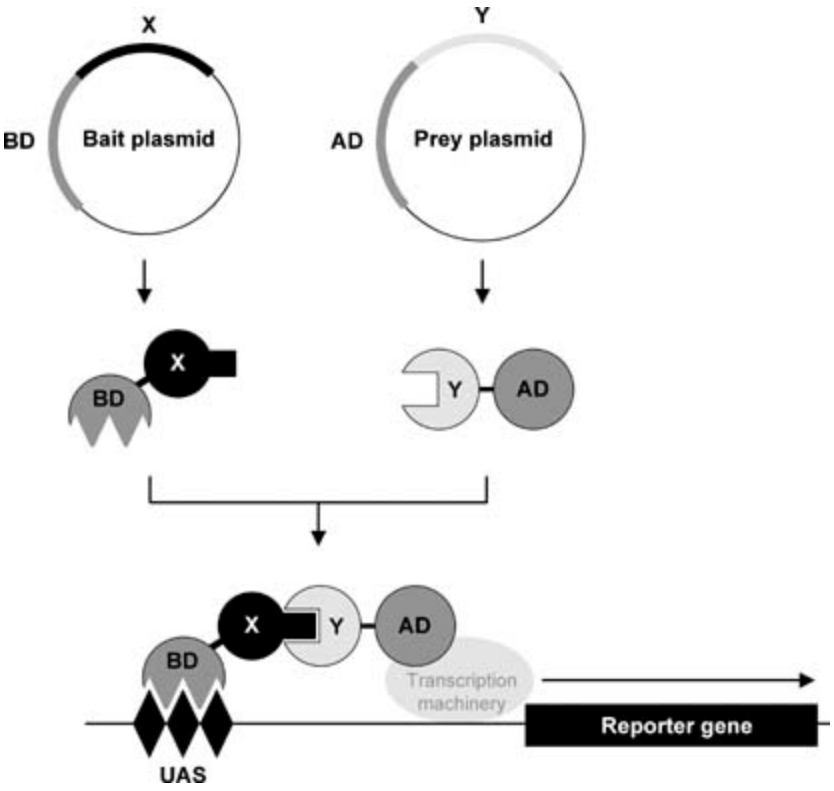

Figure 1.4. Large-scale analysis of yeast protein complexes using mass spectrometry (MS). Bait proteins were generated that carried a particular affinity tag, and the tandem affinity purification (TAP)-tag or FLAG epitope were used. Tagged proteins were expressed in yeast, and were allowed to form physiological complexes. Those complexes were affinity-purified using the appropriate tag, and the complex components were resolved by SDS–polyacrylamide gel electrophoresis (PAGE). Resolved proteins were excised from the gel and were treated with trypsin; the resultant peptides were analyzed and identified, using MS and bioinformatics[26,27].

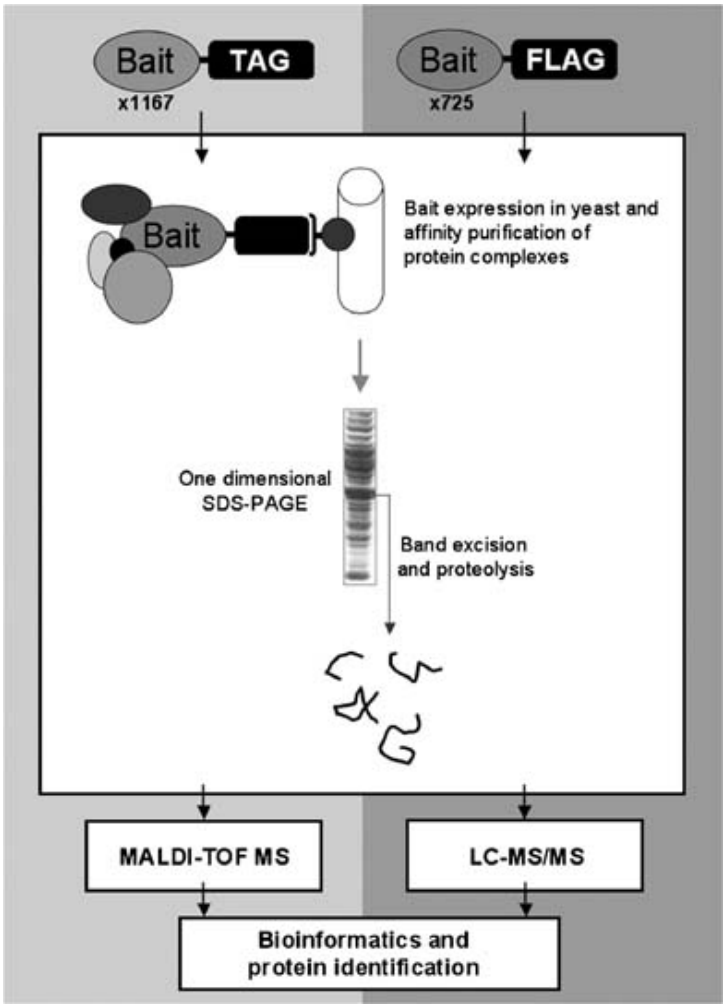

Figure 1.5. Filamentous growth in *S. cerevisiae*. Filaments can form in both diploid and haploid cells in *S. cerevisiae*. Due to the different behavior of colonies, the filamentous growth in diploid is called pseudohyphal growth; and it is called invasive growth in hapoid [30].

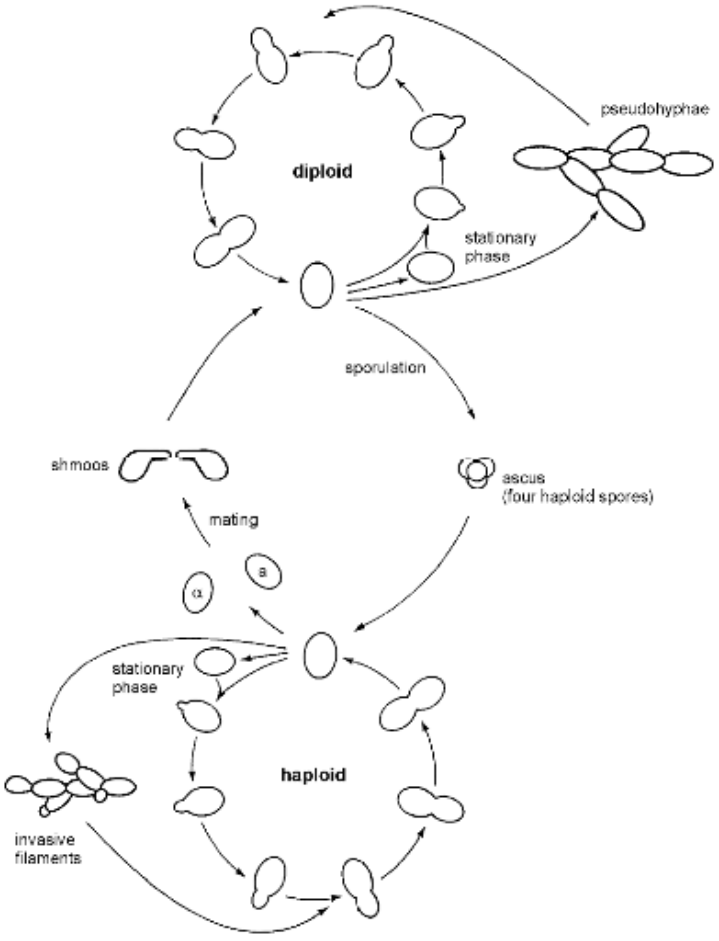

Figure 1.6. Model of TORC1 module of filamentous growth signaling pathway. TORC1 regulates transcript level of *FLO11* via the transcriptional factor Gcn4p. the proteins Tap42p and Sit4p have been found to yield filamentous growth phenotypes upon generic perturbation. It is likely that these two proteins transduce the signal from Tor1 to the downstream components.

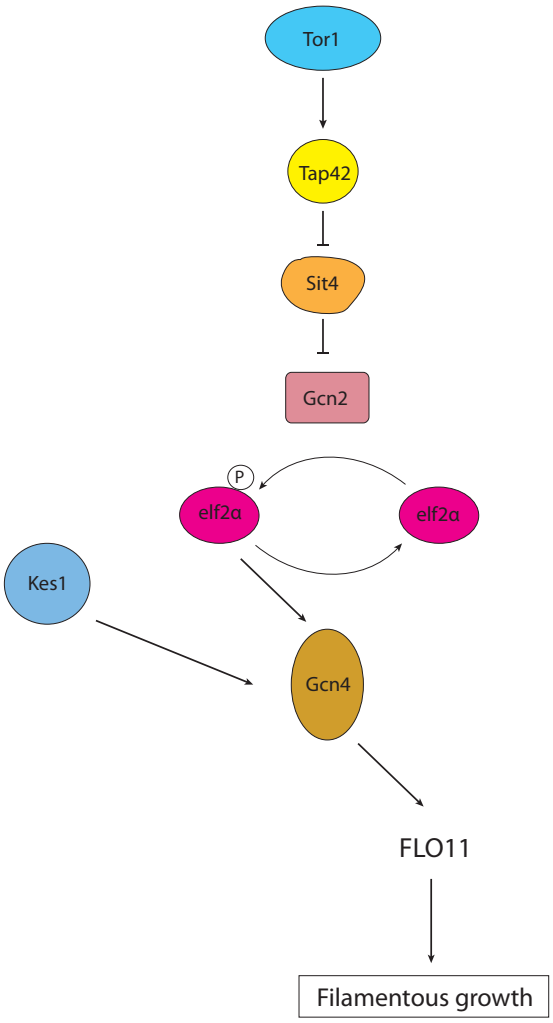

Figure 1.7. The RAS/PKA pathway. The G-protein coupled receptor (GPCR) Gpr1 and its associated heterotrimeric G protein regulate the Ras2 GTPase activating proteins (GAPs), Ira1 and Ira2. Ras2 regulates adenylate cyclase, which produces cAMP. cAMP binds to Bcy1, inactivating the protein, and releasing Tpk1, Tpk2, and Tpk3 to activate Flo8 and other targets that contribute to nutrient-regulated filamentous growth. Filled hexagons represent sucrose and other sugars.

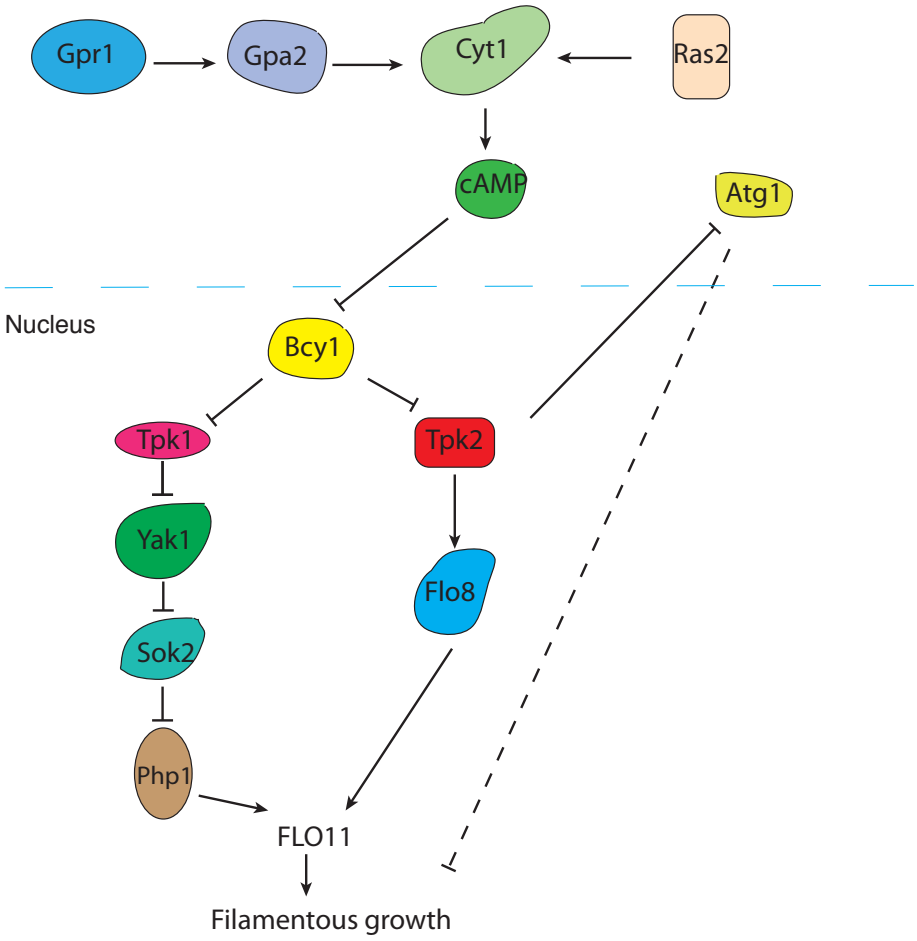

Figure 1.8. Morphological change of *Candida albicans*. *C. albicans* has three distinct cell forms: yeast, pseudohyphal, and true hyphal form. Switching between the pseudohyphal and true hyphal form is less frequent [78].

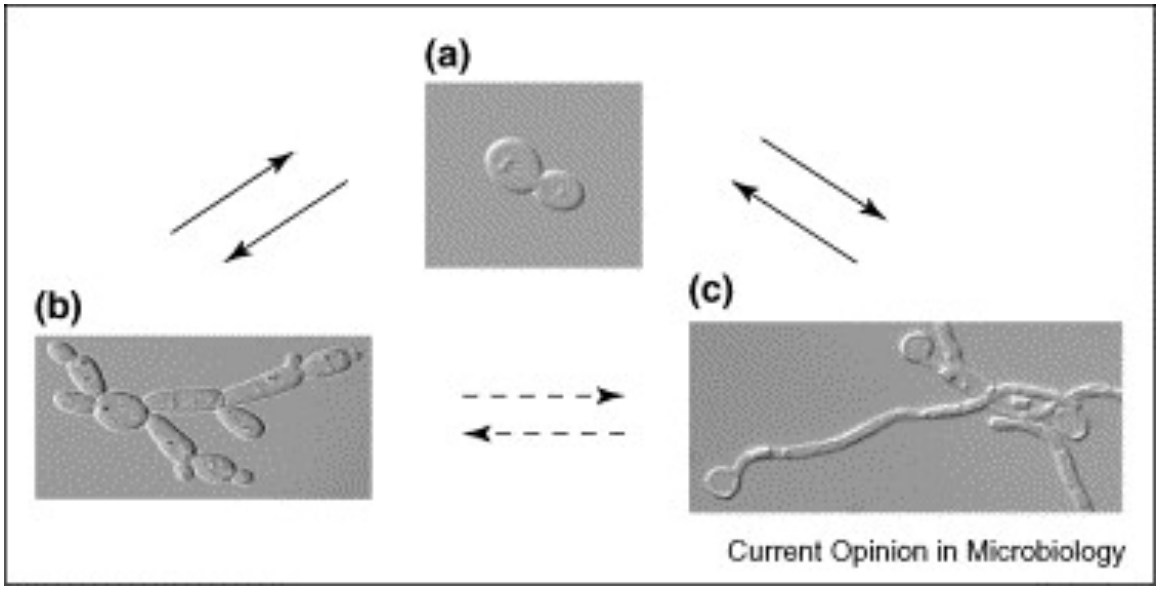

Figure 1.9. Regulation of Ace2p and Morphogenesis (RAM) pathway. Interaction of the network proteins leads to activation of the kinase Cbk1p, which phosphorylates the transcription factor Ace2p. This leads to activation of downstream target genes.

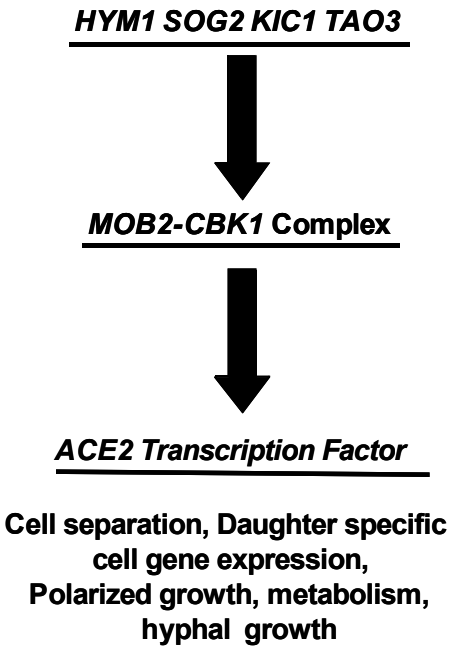

Reference

1. Borneman AR, Pretorius IS, Chambers PJ (2013) Comparative genomics: a revolutionary tool for wine yeast strain development. Current Opinion in Biotechnology 24: 192-199.
2. Noble SM, Johnson AD (2007) Genetics of Candida albicans, a Diploid Human Fungal Pathogen. Annual Review of Genetics 41: 193-211.
3. Junqueira J (2012) Models Hosts for the Study of Oral Candidiasis. In: Mylonakis E, Ausubel FM, Gilmore M, Casadevall A, editors. Recent Advances on Model Hosts: Springer New York. pp. 95-105.
4. Rosa MI, Silva BR, Pires PS, Silva FR, Silva NC, et al. (2013) Weekly fluconazole therapy for recurrent vulvovaginal candidiasis: a systematic review and meta-analysis. European Journal of Obstetrics & Gynecology and Reproductive Biology 167: 132-136.
5. Enserink JM (2012) Chemical Genetics: Budding Yeast as a Platform for Drug Discovery and Mapping of Genetic Pathways. Molecules 17: 9258-9273.
6. Rees J, Lilley K (2011) Enabling Technologies for Yeast Proteome Analysis. In: Castrillo JI, Oliver SG, editors. Yeast Systems Biology: Humana Press. pp. 149-178.
7. Martínez-Pastor M, Llanos R, Romero A, Puig S (2013) Post-Transcriptional Regulation of Iron Homeostasis in Saccharomyces cerevisiae. International Journal of Molecular Sciences 14: 15785-15809.
8. Suter B, Auerbach D, Stagljar I (2006) Yeast-based functional genomics and proteomics technologies: the first 15 years and beyond. Biotechniques 40: 625-644.
9. Goffeau A, Barrell BG, Bussey H, Davis RW, Dujon B, et al. (1996) Life with 6000 genes. Science 274: 546, 563-547.
10. Winzeler EA, Shoemaker DD, Astromoff A, Liang H, Anderson K, et al. (1999) Functional characterization of the S. cerevisiae genome by gene deletion and parallel analysis. Science 285: 901-906.
11. Giaever G, Chu AM, Ni L, Connelly C, Riles L, et al. (2002) Functional profiling of the Saccharomyces cerevisiae genome. Nature 418: 387-391.
12. Huh WK, Falvo JV, Gerke LC, Carroll AS, Howson RW, et al. (2003) Global analysis of protein localization in budding yeast. Nature 425: 686-691.
13. Ghaemmaghami S, Huh WK, Bower K, Howson RW, Belle A, et al. (2003) Global analysis of protein expression in yeast. Nature 425: 737-741.
14. Chong Y, Cox M, Andrews B (2012) Proteome-Wide Screens in Saccharomyces cerevisiae Using the Yeast GFP Collection. In: Goryanin II, Goryachev AB, editors. Advances in Systems Biology: Springer New York. pp. 169-178.

15. Ross-Macdonald P, Coelho PS, Roemer T, Agarwal S, Kumar A, et al. (1999) Large-scale analysis of the yeast genome by transposon tagging and gene disruption. Nature 402: 413-418.
16. Ma J, Jin R, Jia X, Dobry CJ, Wang L, et al. (2007) An interrelationship between autophagy and filamentous growth in budding yeast. Genetics 177: 205-214.
17. Ma J, Jin R, Dobry CJ, Lawson SK, Kumar A (2007) Overexpression of Autophagy-Related Genes Inhibits Yeast Filamentous Growth. Autophagy 3: 604-609.
18. Jin R, Dobry CJ, McCown PJ, Kumar A (2008) Large-Scale Analysis of Yeast Filamentous Growth by Systematic Gene Disruption and Overexpression. Molecular Biology of the Cell 19: 284-296.
19. Bharucha N, Ma J, Dobry CJ, Lawson SK, Yang Z, et al. (2008) Analysis of the Yeast Kinome Reveals a Network of Regulated Protein Localization during Filamentous Growth. Molecular Biology of the Cell 19: 2708-2717.
20. Fields S, Sternglanz R (1994) The two-hybrid system: an assay for protein-protein interactions. Trends Genet 10: 286-292.
21. Fields S, Song O (1989) A novel genetic system to detect protein-protein interactions. Nature 340: 245-246.
22. Uetz P, Giot L, Cagney G, Mansfield TA, Judson RS, et al. (2000) A comprehensive analysis of protein-protein interactions in Saccharomyces cerevisiae. Nature 403: 623-627.
23. Ito T, Tashiro K, Muta S, Ozawa R, Chiba T, et al. (2000) Toward a protein–protein interaction map of the budding yeast: A comprehensive system to examine two-hybrid interactions in all possible combinations between the yeast proteins. Proceedings of the National Academy of Sciences 97: 1143-1147.
24. Ito T, Chiba T, Ozawa R, Yoshida M, Hattori M, et al. (2001) A comprehensive two-hybrid analysis to explore the yeast protein interactome. Proceedings of the National Academy of Sciences 98: 4569-4574.
25. Matthews LR, Vaglio P, Reboul J, Ge H, Davis BP, et al. (2001) Identification of Potential Interaction Networks Using Sequence-Based Searches for Conserved Protein-Protein Interactions or “Interologs”. Genome Research 11: 2120-2126.
26. Gavin AC, Bosche M, Krause R, Grandi P, Marzioch M, et al. (2002) Functional organization of the yeast proteome by systematic analysis of protein complexes. Nature 415: 141-147.
27. Ho Y, Gruhler A, Heilbut A, Bader GD, Moore L, et al. (2002) Systematic identification of protein complexes in Saccharomyces cerevisiae by mass spectrometry. Nature 415: 180-183.
28. de Godoy LM, Olsen JV, Cox J, Nielsen ML, Hubner NC, et al. (2008) Comprehensive mass-spectrometry-based proteome quantification of haploid versus diploid yeast. Nature 455: 1251-1254.

29. Gimeno CJ, Ljungdahl PO, Styles CA, Fink GR (1992) Unipolar cell divisions in the yeast S. cerevisiae lead to filamentous growth: regulation by starvation and RAS. Cell 68: 1077-1090.
30. Cullen PJ, Sprague GF (2012) The Regulation of Filamentous Growth in Yeast. Genetics 190: 23-49.
31. Cullen PJ, Sprague GF, Jr. (2000) Glucose depletion causes haploid invasive growth in yeast. Proc Natl Acad Sci U S A 97: 13619-13624.
32. Ahn SH, Acurio A, Kron SJ (1999) Regulation of G2/M progression by the STE mitogen-activated protein kinase pathway in budding yeast filamentous growth. Mol Biol Cell 10: 3301-3316.
33. Edgington NP, Blacketer MJ, Bierwagen TA, Myers AM (1999) Control of Saccharomyces cerevisiae filamentous growth by cyclin-dependent kinase Cdc28. Mol Cell Biol 19: 1369-1380.
34. Kron SJ, Styles CA, Fink GR (1994) Symmetric cell division in pseudohyphae of the yeast Saccharomyces cerevisiae. Mol Biol Cell 5: 1003-1022.
35. Li W, Mitchell AP (1997) Proteolytic activation of Rim1p, a positive regulator of yeast sporulation and invasive growth. Genetics 145: 63-73.
36. Gehrung S, Snyder M (1990) The SPA2 gene of Saccharomyces cerevisiae is important for pheromone-induced morphogenesis and efficient mating. The Journal of Cell Biology 111: 1451-1464.
37. Valtz N, Herskowitz I (1996) Pea2 protein of yeast is localized to sites of polarized growth and is required for efficient mating and bipolar budding. The Journal of Cell Biology 135: 725-739.
38. Shively CA, Eckwahl MJ, Dobry CJ, Mellacheruvu D, Nesvizhskii A, et al. (2013) Genetic Networks Inducing Invasive Growth in Saccharomyces cerevisiae Identified Through Systematic Genome-Wide Overexpression. Genetics 193: 1297-1310.
39. Guo B, Styles CA, Feng Q, Fink GR (2000) A Saccharomyces gene family involved in invasive growth, cell-cell adhesion, and mating. Proc Natl Acad Sci U S A 97: 12158-12163.
40. Liu H, Styles CA, Fink GR (1996) Saccharomyces cerevisiae S288C Has a Mutation in FL08, a Gene Required for Filamentous Growth. Genetics 144: 967-978.
41. Fichtner L, Schulze F, Braus GH (2007) Differential Flo8p-dependent regulation of FLO1 and FLO11 for cell–cell and cell–substrate adherence of S. cerevisiae S288c. Molecular Microbiology 66: 1276-1289.
42. Pan X, Heitman J (1999) Cyclic AMP-Dependent Protein Kinase Regulates Pseudohyphal Differentiation in Saccharomyces cerevisiae. Molecular and Cellular Biology 19: 4874-4887.

43. Rupp S, Summers E, Lo HJ, Madhani H, Fink G (1999) MAP kinase and cAMP filamentation signaling pathways converge on the unusually large promoter of the yeast FLO11 gene. EMBO J 18: 1257-1269.
44. Braus GH, Grundmann O, Bruckner S, Mosch HU (2003) Amino acid starvation and Gcn4p regulate adhesive growth and FLO11 gene expression in Saccharomyces cerevisiae. Mol Biol Cell 14: 4272-4284.
45. Pan X, Heitman J (1999) Cyclic AMP-dependent protein kinase regulates pseudohyphal differentiation in Saccharomyces cerevisiae. Mol Cell Biol 19: 4874-4887.
46. Cutler NS, Pan X, Heitman J, Cardenas ME (2001) The TOR signal transduction cascade controls cellular differentiation in response to nutrients. Mol Biol Cell 12: 4103-4113.
47. Toda T, Cameron S, Sass P, Zoller M, Wigler M (1987) Three different genes in S. cerevisiae encode the catalytic subunits of the cAMP-dependent protein kinase. Cell 50: 277-287.
48. Santangelo GM (2006) Glucose signaling in Saccharomyces cerevisiae. Microbiol Mol Biol Rev 70: 253-282.
49. Kataoka T, Powers S, McGill C, Fasano O, Strathern J, et al. (1984) Genetic analysis of yeast RAS1 and RAS2 genes. Cell 37: 437-445.
50. Busti S, Coccetti P, Alberghina L, Vanoni M (2010) Glucose signaling-mediated coordination of cell growth and cell cycle in Saccharomyces cerevisiae. Sensors (Basel) 10: 6195-6240.
51. Robertson LS, Causton HC, Young RA, Fink GR (2000) The yeast A kinases differentially regulate iron uptake and respiratory function. Proc Natl Acad Sci U S A 97: 5984-5988.
52. Malcher M, Schladebeck S, Mosch HU (2011) The Yak1 protein kinase lies at the center of a regulatory cascade affecting adhesive growth and stress resistance in Saccharomyces cerevisiae. Genetics 187: 717-730.
53. Celenza JL, Carlson M (1986) A yeast gene that is essential for release from glucose repression encodes a protein kinase. Science 233: 1175-1180.
54. Hedbacker K, Carlson M (2008) SNF1/AMPK pathways in yeast. Front Biosci 13: 2408-2420.
55. Vyas VK, Kuchin S, Berkey CD, Carlson M (2003) Snf1 kinases with different beta-subunit isoforms play distinct roles in regulating haploid invasive growth. Mol Cell Biol 23: 1341-1348.
56. Orlova M, Ozcetin H, Barrett L, Kuchin S (2010) Roles of the Snf1-activating kinases during nitrogen limitation and pseudohyphal differentiation in Saccharomyces cerevisiae. Eukaryot Cell 9: 208-214.

57. Wilson D, Thewes S, Zakikhany K, Fradin C, Albrecht A, et al. (2009) Identifying infection-associated genes of Candida albicans in the postgenomic era. FEMS Yeast Res 9: 688-700.
58. Berman J, Sudbery PE (2002) Candida Albicans: a molecular revolution built on lessons from budding yeast. Nat Rev Genet 3: 918-930.
59. Enoch DA, Ludlam HA, Brown NM (2006) Invasive fungal infections: a review of epidemiology and management options. J Med Microbiol 55: 809-818.
60. Sudbery P, Gow N, Berman J (2004) The distinct morphogenic states of Candida albicans. Trends Microbiol 12: 317-324.
61. Whiteway M, Oberholzer U (2004) Candida morphogenesis and host-pathogen interactions. Curr Opin Microbiol 7: 350-357.
62. Jayatilake JA, Samaranayake YH, Cheung LK, Samaranayake LP (2006) Quantitative evaluation of tissue invasion by wild type, hyphal and SAP mutants of Candida albicans, and non-albicans Candida species in reconstituted human oral epithelium. J Oral Pathol Med 35: 484-491.
63. Kelly MT, MacCallum DM, Clancy SD, Odds FC, Brown AJ, et al. (2004) The Candida albicans CaACE2 gene affects morphogenesis, adherence and virulence. Mol Microbiol 53: 969-983.
64. Kang CM, Jiang YW (2005) Genome-wide survey of non-essential genes required for slowed DNA synthesis-induced filamentous growth in yeast. Yeast 22: 79-90.
65. Csank C, Schroppel K, Leberer E, Harcus D, Mohamed O, et al. (1998) Roles of the Candida albicans mitogen-activated protein kinase homolog, Cek1p, in hyphal development and systemic candidiasis. Infect Immun 66: 2713-2721.
66. Csank C, Makris C, Meloche S, Schroppel K, Rollinghoff M, et al. (1997) Derepressed hyphal growth and reduced virulence in a VH1 family-related protein phosphatase mutant of the human pathogen Candida albicans. Mol Biol Cell 8: 2539-2551.
67. Navarro-Garcia F, Alonso-Monge R, Rico H, Pla J, Sentandreu R, et al. (1998) A role for the MAP kinase gene MKC1 in cell wall construction and morphological transitions in Candida albicans. Microbiology 144 (Pt 2): 411-424.
68. Rocha CR, Schroppel K, Harcus D, Marcil A, Dignard D, et al. (2001) Signaling through adenylyl cyclase is essential for hyphal growth and virulence in the pathogenic fungus Candida albicans. Mol Biol Cell 12: 3631-3643.
69. Zelada A, Passeron S, Lopes Gomes S, Cantore ML (1998) Isolation and characterisation of cAMP-dependent protein kinase from Candida albicans. Purification of the regulatory and catalytic subunits. Eur J Biochem 252: 245-252.
70. Sonneborn A, Bockmuhl DP, Gerads M, Kurpanek K, Sanglard D, et al. (2000) Protein kinase A encoded by TPK2 regulates dimorphism of Candida albicans. Mol Microbiol 35: 386-396.

71. Wandinger SK, Richter K, Buchner J (2008) The Hsp90 chaperone machinery. J Biol Chem 283: 18473-18477.
72. Shapiro RS, Uppuluri P, Zaas AK, Collins C, Senn H, et al. (2009) Hsp90 orchestrates temperature-dependent Candida albicans morphogenesis via Ras1-PKA signaling. Curr Biol 19: 621-629.
73. Song Y, Cheon SA, Lee KE, Lee SY, Lee BK, et al. (2008) Role of the RAM network in cell polarity and hyphal morphogenesis in Candida albicans. Mol Biol Cell 19: 5456-5477.
74. Nelson B, Kurischko C, Horecka J, Mody M, Nair P, et al. (2003) RAM: a conserved signaling network that regulates Ace2p transcriptional activity and polarized morphogenesis. Mol Biol Cell 14: 3782-3803.
75. Sharkey LL, McNemar MD, Saporito-Irwin SM, Sypherd PS, Fonzi WA (1999) HWP1 functions in the morphological development of Candida albicans downstream of EFG1, TUP1, and RBF1. J Bacteriol 181: 5273-5279.
76. Jansen JM, Barry MF, Yoo CK, Weiss EL (2006) Phosphoregulation of Cbk1 is critical for RAM network control of transcription and morphogenesis. J Cell Biol 175: 755-766.
77. Causier B (2004) Studying the interactome with the yeast two-hybrid system and mass spectrometry. Mass Spectrom Rev 23: 350-367.
78. Berman J (2006) Morphogenesis and cell cycle progression in Candida albicans. Curr Opin Microbiol 9: 595-601.

CHAPTER 2

Linkage analysis with Next-Generation Sequencing to identify the genetic determinants of yeast pseudohyphal growth

2.1 Introduction

Under normal growth conditions with sufficient nitrogen availability and glucose as a carbon source, the baker's yeast *Saccharomyces cerevisiae* maintains its oval cell shape and divides mitotically by budding, forming two independent and separate daughter cells from a single mother cell. However, under conditions of limited nutrient availability, some strains of *S. cerevisiae* are capable of forming multicellular filamentous chains of cells that remain physically connected after cytokinesis. This latter mode of growth is referred to as filamentous or pseudohyphal growth[1-5]. Specifically, filamentous growth can be induced by nitrogen or glucose deprivation. Additionally, growth in the presence of short-chain alcohols such as butanol and ethanol can stimulate filamentation in certain strains[6-8]. The short-chain alcohols are end products of amino acid catabolism under nitrogen-deprivation conditions and likely constitute a mimic of nitrogen stress, although distinctions exist regarding the genetic complement necessary for the induction of filamentous growth by each condition. In general, the filamentous growth response is viewed as a foraging mechanism allowing immobile yeast to scavenge for nutrients under stressful conditions.

Filamentous growth in *S. cerevisiae* is mediated by several signaling pathways. Classic studies from numerous laboratories have identified at least three signaling pathways that regulate filamentous growth: 1) the MAPK pathway[5,9], 2) the Ras/PKA pathway[10], and 3) the Snf1p kinase pathway[11]. The filamentous growth mitogen-activated protein kinase (MAPK) cascade is regulated by Ste20p and consists of Ste11p, Ste7p, and the MAPK Kss1p[9,12]. Ste11p is a substrate of Ste20p, and Ste20p is itself

regulated by the small rho-like GTPase Cdc42p[13], and the GTP-binding protein Ras2p[2,14-16]. In yeast, PKA consists of the regulatory subunit Bcy1p and one of three catalytic subunits Tpk1p, Tpk2p and Tpk3p[17-19]. Tpk2p is an activator of pseudohyphal growth, while Tpk1p and Tpk3p are considered as inhibitors[5,20]. The adenylate cyclase Cyr1p is also regulated by Ras2p; thus Ras2p can be placed upstream of both the filamentous growth MAPK and PKA pathways[15,21,22]. The serine/threonine kinase Snf1p regulates transcriptional changes associated with glucose derepression, mediates several stress responses, and is required for pseudohyphal growth[11,23-25].

During filamentous growth, yeast cells exhibit an elongated shape due to a delay in progression through G2/M, resulting in a prolonged period of apically directed polarized growth[26-28]. The budding pattern changes from axial (in haploid cells) or bipolar (in diploid cells) to a unipolar pattern[1,29]. In order for yeast cells to effectively form pseudohyphal filaments, critical processes of budding, polarized growth, and cell cycle progression must be appropriately regulated and coordinated. In terms of budding patterns, deletion mutants of *BUD2, BUD4,* and *BUD6*, genes that regulate budding pattern selection, yield filamentous growth phenotypes of defective surface filamentation upon gene disruption in a haploid genetic background under conditions of butanol treatment[30]. Similarly, Spa2p, a key polarisome component is also required for filamentation in *S. cerevisiae[31-33]*. The fact that G2/M transition components also affect pseudohyphal growth, leads to the general observation that genetic perturbations resulting in delayed G2/M progression and an extended period of apical growth promote an elongated cell shape and yeast filamentation.

Another large group of proteins contributing to filamentous growth is the plasma membrane and cell wall proteins that mediate cell-cell and cell-substrate adhesion[10,30,34]. Genetic studies have identified a set of genes required for calcium-dependent aggregation, or flocculation, in yeast, and many of these genes contribute to the yeast filamentous growth transition, particularly in response to conditions of nitrogen stress[35]. For example, the cell surface mannoprotein Flo11p is required for pseudohyphal growth, invasive growth, and biofilm formation in filamentous strains of *S.*

cerevisiae[12,36,37]. Flo11p contributes to cell-substrate adhesion *in vivo*, exhibits homotypic adhesion *in vitro*, and is the only flocculin family member expressed in filamentous strains of *S. cerevisiae[38,39]*, and it has been studied most intensively for its large promoter, which integrates transcriptional signals from Flo8p, Ste12p/Tec1p and Mss11p[10,40,41]. Another example of a cell membrane protein that is required for wild-type pseudohyphal growth is *PUN1*. The *PUN1* gene encodes a protein that localizes in the membrane compartment of Can1 (MCC)[42,43], and transcript levels of *PUN1* increase in abundance during filamentous growth. The fact that *PUN1* is also subject to transcriptional regulation by the filamentous growth factors Mss11p and Flo8p suggests that it functions downstream of both the MAPK and PKA pathways.

In addition to nutrient stress, oxygen availability seems to be an important external environmental signal. Previous studies have shown that yeast cells lose the ability to form pseudohyphae under anaerobic conditions[44,45]. This suggests an important role of mitochondria in signaling pathways governing filamentous growth. In accordance with this, it was reported that cells without mitochondrial DNA lose the ability to form pseudohyphae[8,46]. In general, two subpopulations of mitochondria are required for filamentous growth: one with high transmembrane potential and another mitochondrial subpopulation with low transmembrane potential. These mitochondria-activated signaling pathways appear to converge at the Swe1p protein kinase and Mih1p protein phosphatase, the two essential regulators of the cell G2/M transition[8,47].

Since the *Saccharomyces cerevisiae* genome sequence was completed in 1996[48], it has served as a powerful tool for yeast researchers and provided a model for functional genome analysis[37,49-51]. However, in order to comprehensively discover new or interesting genetic differences in an unbiased manner, it is advantageous to apply repeated rounds of DNA sequencing on the whole-genome scale in related strains with varied genetic backgrounds. The emergence of high-throughput short-read sequencing technologies has dramatically overcome the obstacles in these approaches caused by finance and labor. We present here the first pooled linkage analysis of yeast pseudohyphal growth using next-generation sequencing (NGS) technology. For this study, we systematically generated genetic pools with 224 spores and identified 522 allelic

differences within 201 genes that relate to haploid invasive growth. The data set was analyzed computationally to identify enriched pathways and signaling cascades, highlighting networks mediating MAPK signaling, cell cycle progression as well as mitochondrial function. Subsequent studies address a function for the cell polarisome protein, Pea2p in regulating filamentous growth by altering cell budding pattern along with Spa2p. Further studies of Pea2p suggest that it acts downstream of the MAPK pathway. Our results indicate that allelic differences in *PEA2* result in protein-protein interaction differences between Pea2p and Spa2p. In a parallel linkage analysis study of another strain capable of undergoing invasive growth, we identified that allelic differences in the *MDM32* gene encoding a mitochondrial structural protein are linked with filamentation phenotypes through the regulation of mitochondrial function. Collectively, the work provides a valuable information resource for studies of yeast pseudohyphal growth.

2.2 Materials and Methods

2.2.1 Yeast strains and growth conditions

Haploid mating strains used in this study are derived from the filamentous strains HLY337 (derived from Σ1278b), SK1 and the standard non-filamentous strain S288c. The genotype of haploid HLY337 is *MATα ura3-52 trp1*-1; the genotype of haploid Y826 is *MATa ura3-52 leu2Δ0[30,52]*; the genotype of the haploid SK1 strain is *MATα ura3-52 trp1Δ0[53]*. The genotype of BY4741 is *MATa his3Δ1 leu2Δ 0 met15Δ 0 ura3Δ0*. Haploid deletion mutants were constructed in strain Y826 and SK1 using PCR-mediated gene disruption with pFA6a-KanMX6 or pUG72[54,55] (**Table 2.1**).

Yeast strains were propagated on rich YPD medium (1% yeast extract, 2% polypeptone and 2% glucose) medium or synthetic medium as described. Yeast invasive growth was assayed on YPD medium.

2.2.2 Pooling and Sequencing

The statistical assessments and modeling used to derive the probabilities of identifying causative alleles are described by Birkeland *et al[56]*. To generate two genetic pools, we crossed HLY337 to BY4741 (of the S288c background) as well as SK1 to BY4741. Following mating, the resulting strains were sporulated and asci were dissected. The dissected spores were grown overnight at 30°C and were each individually tested for mating type by standard protocols. Spores resulting from complete meiosis were then used for whole genome sequencing. Each spore was assigned to invasive or non-invasive pools based on its filamentous growth phenotype. To make sure the pooled linkage strategy contains an equal representation of all segregants in a pooled population, each haploid strain was grown overnight at 30°C in individual 4 ml YPD cultures. The OD_{600} of the cultures was determined and used to calculate the appropriate volume of each strain so that upon mixing, we would achieve equal numbers of cells. Sequencing was performed on the Illumina Genome Analyzer by the University of Michigan DNA Sequencing Core. Sequence image analysis and based calling were performed using the Illumina Firecrest and Bustard algorithms.

2.2.3 Identifying allelic change

All subsequent sequence data analyses were performed using the VAMP platform[56]. LOD score of 3 and 4 were used to identify causative alleles in the HLY337/BY4741 and SK1/BY4741 crosses, respectively.

2.2.4 Yeast invasive growth assays

Invasive growth of haploid strains was determined by the standard plate washing assay[1]. Mid-log phase cultures were spotted onto YPD plates and incubated for 7 days at 30 °C, and surface cells were subsequently washed off under a gentle stream of water. The mark on the plates was then photographed using a NIKON Fluorescence microscope.

2.2.5 Plasmids construction

For expression of Σ1278b alleles in null mutants, yeast ORFs of the Y826 background with 1 kb of upstream sequence and 300 bp of downstream sequence were cloned into Gateway vecter using Gateway cloning Kit (Invitrogen).

For tagging enhanced green fluorescent protein (eGFP) and tandem affinity purification (TAP) cassettes to the carboxyl-terminal residues of the budding yeast Mdm31p and Mdm32p proteins, Gateway plasmids 416-GPD-ccdB-EGFP and 414-GPD-ccdB-TAP were used[57].

Plasmid pCu-Spa2-3HA-Ura and pCu-Bud6-GFP-His were modified from pCu-3HA-Ura and pCu-GFP-His (from Dr. Klisonsky), using standard restriction enzyme digestion and ligation-based techniques. The *SalI* and *HindIII* restriction sites of these plasmids were used to integrate the *SPA2* and *BUD6* open reading frames between the copper-inducible *CUP1* promoter and 3xHA/GFP tag.

2.2.6 Integrated point mutations

Allelic variants of *PEA2* were generated as integrated point mutations. A *URA3* cassette was amplified from the pUG6 plasmid and then used to replace the *PEA2* open reading frame in Y826. Subsequently, 5-FOA-mediated counter selection[58] was applied to replace the integrated *URA3* cassette with a 500 bp cassette covering the *PEA2* allelic change (*M409L*), recreating the S288c allele in the Σ1278b background. The integrated point mutation was confirmed by sequencing of an amplified PCR fragment using the University of Michigan Sequencing Core.

2.2.7 FRE-LacZ assays

Plasmids pLG669-Z FLO11 6/7 and 9/10 were transformed into designated yeast strains[46]. Cells were grown in SC medium overnight, and then inoculated into fresh SC medium to an OD_{600} of ~0.2. Cultures were subsequently grown for 3-4 hours to an OD_{600} of ~0.8-1.0. β-galactosidase activity was determined with the use of ortho-nitrophenyl-β-galactoside as a substrate[46,59] (Sigma Aldrich)

2.2.8 Assay for respiratory activity

Respiratory ability was assessed using YPG plates with glycerol as a non-fermentable carbon source[60]. Cells were pre-grown overnight and then inoculated into fresh SC medium to an OD_{600} of ~0.2; culture were subsequently incubated an additional 3 hours to an OD_{600} of ~0.8. The same amount of cells were serial diluted and spotted onto YPD and YPG (1% yeast extract, 2% polypeptone and 2% glycerol) plates, and incubated for 2 days at 30 °C.

2.2.9 Fluorescence microscopy and image processing

For live-cells imaging, spotted cultures were grown in YPD plates for 7 days at 30 °C. After washing surface cells from the YPD plates, cells that had invaded the YPD agar were dug out using a steel scalpel, and the extracted cells were washed twice with distilled water. Images were taken using a NIKON upright fluorescence microscope. To determine budding patterns, cells were stained with Calcofluor White as previously described[61]. Over 250 cells were counted twice for each strain. Statistics were analyzed using the ANOVA approach.

To reveal mitochondrial morphology, living cells were stained with 50nM MitoTracker Red, and the staining pattern was visualized by fluorescence microscopy[60].

2.2.10 Immunoprecipitation

The binding affinity between selected proteins was detected by co-immnoprecipitation[62]. For native immunoprecipitation, 2 OD units of cells were lysed in 1 ml lysis buffer (50 mM Tris-HCl [pH 7.5], 150 mM NaCl, 2 mM EDTA, 0.5% Triton X-100, 1 mM PMSF, and Complete EDTA-free protease inhibitor [Roche]) with glass beads. After centrifugation at 13,000 × g for 10 min, the resulting supernatant was incubated with protein G-Sepharose 4 Fast Flow (GE Life Tech) for 2 hr at 4°C. After washing the Sepharose with lysis buffer six times, the bound materials were eluted by boiling the Sepharose in SDS-PAGE loading buffer. The resulting eluate was analyzed by Western blotting with designated antibodies (anti-HA, anti-Protein A and anti-GFP). Blots were developed using the SuperSignal West Dura Extended Duration Substrate (Thermo Scientific).

2.3 Results

2.3.1 A pooled segregant approach for linkage of filamentous growth in yeast

To identify the genetic alterations underlying filamentous growth through an approach utilizing next-generation sequencing, the causative alleles should be both positively identified and distinguished from sequencing errors or strain polymorphisms. For this study, we applied a single cross, generating a large set of asci that we dissected and analyzed in parallel. Here, haploid spores were segregated by invasive growth phenotypes, and genomic DNA was prepared from the pooled segregants; a library of the DNA was then prepared for next-generation sequencing. The libraries of pooled filamentous and non-filamentous segregants were sequenced in two runs. This pooled parallel approach is similar to methods for bulk segregant analysis and is a powerful linkage tool to distinguish causative alleles underlying a specific phenotype from unlinked incidental alleles, as well as sequencing errors[56]. As compared to traditional serial crossing strategies, the pooled parallel strategy employed here has two major advantages: first, it has much greater discriminatory power for the exclusion of incidental alleles, because the total information content of every ascus can be used in the analysis.

In addition, it requires less asci for the sampling to exclude the large majority of incidental alleles, mainly because the probability of selecting only parental ditype asci rapidly becomes very small.

For this study, we used two haploid filamentous strains derived from the Σ1278b and SK1 genetic backgrounds, respectively, and one haploid non-filamentous strain derived from the S288C genetic background. Unlike the non-filamentous lab strain S288c, Σ1278b and SK1 can undergo an extensive and easily controlled transition to invasive growth and are the preferred genetic background for filamentous growth studies (**Figure 2.1A**). When cells undergo invasive growth on solid agar, the colony develops pseudohyphal filaments that invade into the agar. This phenotype can be assayed by assessing residual cells within the agar after running a stream of gentle water to remove the cells on the agar surface. In **Figure 4.1**, we can observe that in comparison to S288c strains, Σ1278b and SK1-derived colonies leave behind significant numbers of invasive cells in the agar following washing. Haploid Σ1278b and SK1 strains were crossed with S288c, respectively, to form Σ1278b/S288c and SK1/S288c diploid heterozygotes. The diploid strains were grown in synthetic complete medium to maintain auxotrophic selection, and then were transferred into sporulation medium, and were grown for 5 days at 25°C to facilitate sporulation. Sporulated cells were harvested from both strains, and each tetrad was dissected using standard techniques to separate 4 daughter spores (**Figure 2.1B**). To test that the dissected tetrads were formed by complete meiosis, we applied a pheromone assay to determine each respective mating type. If the four isolated spores were formed by complete meiosis, then these offspring should contain two *MATa* and two *MATα* mating types[63]. Dissected tetrads with missing spores or mismatched mating type were not included in the following analyses. Dissected spores were grown in YPD medium overnight and then were plated onto YPD solid plates to test invasive growth phenotypes by the wash assay described previously (**Figure 2.2**).

2.3.2 Identifying causative alleles affecting filamentous growth in *S. cerevisiae*

To identify genes and corresponding alleles affecting filamentous growth, we tested our entire collection of 224 spores for alterations in invasive growth by spotting cultures on 96-well format plates in duplicate and incubating them for 5 days. Invasive growth phenotypes were compared to the original Σ1278b and SK1 strains. A loss in invasive growth was detected as a reduction or absence of invasive cells after washing. Intermediate phenotypes were defined as a gentle reduction in the amount of residual invasive cells after washing. A representative plate obtained from the screen is shown in Figure 2.2. After retesting these strains in duplicate as earlier, with the Σ1278b/S288c cross, we collected 37 spores with invasive phenotypes, 63 non-invasive spores, and 24 strains with an intermediate phenotype. With the SK1/S288c cross, we have 51 invasive spores, 24 non-invasive spores, and 25 spores exhibiting an intermediate invasive phenotype. Haploid strains with invasive and non-invasive phenotypes were grouped into 4 pools based on invasive phenotypes, and genomic DNA was prepared from each pool (**Figure 2.1B**). To make sure the dissected strains were equally represented in each DNA pool, asci were grown in YPD on 96-well format plates. Cell density was then determined by measuring the OD_{600}, and the final culture volume was adjusted accordingly such that equal amounts of each strain were combined prior to DNA extraction. Genomic DNA from the pooled cultures was analyzed by sequencing using an Illumina platform at the University of Michigan Sequencing Core. Following next-generation sequencing, the resulting data were analyzed using the VAMP platform developed by Dr. Thomas Wilson[56].

In total, we sequenced four genomic DNA pools from the Σ1278b/S288c and SK1/S288c crosses, and identified 53 and 91 genes respectively with allelic differences linked to filamentation phenotypes (**Table 2.2 and 2.3**). The LOD score (logarithm of odds) is a statistical test often used for linkage analysis in population and genetic research. Here it determines the probability that the identified gene is linked to its filamentous phenotype. By convention, a LOD score greater than 3.0 is often considered evidence for linkage. A LOD score of 3 indicates 1000-to-1 odds that the linkage being observed did not occur by chance. In the Σ1278b x S288c cross, we used an LOD score of 3.0 as the cutoff. Since more genes were identified in the SK1/S288c cross, we decided to use LOD

4.0 as cutoff to maintain a manageable data set. The full gene list is provided in **Table 2.2 and 2.3**

Two well known filamentous growth genes, *FLO11* and *FLO8*, and corresponding alleles were linked with invasive growth in the Σ1278b x S288c cross. Flo8p is a transcription factor acting downstream of the MAPK and PKA signaling pathways. It mediates filamentous growth by regulating transcripts levels of a large set of genes and is well recognized as a key transcriptional regulator enabling invasion and filamentation. Previous studies have established the presence of a premature stop codon in the *FLO8* gene in the non-invasive S288c strain[18]. The resulting non-functional *FLO8* pseudogene was considered to be one of the main reasons why S288c cannot undergo filamentous growth under induction conditions. Supporting the accuracy and utility of our approach, *FLO8* alleles were very strongly linked with filamentation; the allelic difference between the filamentous Σ1278b and non-filamentous S288c alleles resulted in an LOD score of 21, which was the highest such score for any allelic difference identified in the Σ1278b x S288c cross. *FLO11* encodes a cell surface flocculin protein. Flo11p contributes to cell-substrate adhesion *in vivo*, exhibits homotypic adhesion in *vitro*, and is the only flocculin family member expressed in filamentous growth[36,37]. The fact that *FLO11* is transcriptionally regulated by PKA, the Kss1 MAPK and Snf1p makes it another hallmark of filamentous growth[9,10]. Both our crosses have identified *FLO11* alleles as being linked to invasive growth. This is effective validation, indicating the power of pooled linkage analysis in identifying genetic determinants of filamentous growth.

2.3.3 Alleles linked to filamentous growth in Σ1278b and SK1 genetic background

In the Σ1278b/S288c cross, we identified 53 genes potentially linked to invasive growth (LOD>3.0). The identified chromosomal loci are largely concentrated in chromosomes V, IX, XIII, and XIV. Noticeably, there is a large set of genes distributed near *FLO8* and *FLO11* (**Figure 2.3**). We believe this effect is mainly caused by the

dominant *FLO8* and *FLO11* allelic differences, and the LOD values of some genes were potentially exaggerated by their proximity to these key filamentous growth genes. By simple Gene Ontology (GO) term analysis, the invasive growth related gene set was not enriched for any protein-associated subcellular components; however, we did identify several enriched molecular functions and biological process terms (**Figure 2.4**). Genes annotated as contributing to the regulation of metabolic processes associated with chemical responses were enriched in the gene set. This is not surprising since nitrogen availability is an important regulator of pseudohyphal growth. This GO term is broad in scope; among the associated genes are several known pseudohyphal growth regulators, including the *FLO11* and *FLO8* genes that play critical roles in pseudohyphal formation. Another large grouping of identified genes is associated with cytoskeletal organization, including *APP1, PEA2* and *RHO2*. A grouping of identified genes associated with carbohydrate metabolic processes includes *CAT8, GAL80* and *SAK1*.

In the SK1 x S288c cross, we identified 91 genes possibly linked to filamentous growth (LOD>4.0). In contrast to the genes identified in the Σ1278b x S288c cross, the genes from this analysis are mainly distributed on chromosomes V, XIV, XV, and XVI, suggesting that allelic differences among a largely distinct gene set mediate filamentation in strains of the SK1 genetic background. However, as in the Σ1278b screen, a large group of alleles exhibiting high LOD scores concentrated around *FLO8*, and we believe it is still caused by the dominant effect of *FLO8* (**Figure 2.5**). Distinct from the Σ1278b/S288c cross, GO term analysis of the gene set identified in the SK1 cross was enriched for protein-associated subcellular components (**Figure 2.6**). It is obvious that a large set of genes in SK1 with allelic linkage to filamentation is enriched in encoded proteins that localize to mitochondria, including *CAT5, MDM32, IDH2, MAP43,* and *MRPL23*. Some of these genes encode mitochondria structural proteins, like *MDM32* and *CAT5*. Other genes play enzymatic roles in mitochondrial respiratory function. Another set of genes encodes proteins located at the site of polarized growth or the cellular bud. These genes include *BNI1, BOI2, SHO1, PRM1*, and *AFI1*. It is not surprising to see these genes enriched in this analysis. It reflects the close relationship between polarized growth and filamentous growth, as filamentation is indeed a form of polarized growth.

To consider the functional significance of alleles identified in these crosses during filamentous growth, we generated haploid deletion mutants of each corresponding gene in the filamentous growth Σ1278b and SK1 genetic background and assayed each mutant for defects in invasive growth. By our analysis, deletion of *PEA2, RHO2,* and *YIR021W-A* in the Σ1278b genetic background and *MDM32, MRPL23, MPA43, SHO1, VPS17* and *GCY1* in the SK1 genetic background result in reduced filamentous growth on solid YPD plates. Outside of *FLO8* mutants, deletion mutants of the common components in both crosses, *sfl1Δ* and *sak1Δ*, show wild type invasive growth. Because of its role in polarized growth and its significant associated LOD score, we were particularly interested in the allelic differences observed in *PEA2*. The *PEA2* gene encodes a protein of 420 amino acids with a C-terminal coiled-coiled domain. Our linkage analysis shows strong linkage to invasive growth for a single C-to-A transversion in the coding sequence of the *PEA2* gene, converting leucine in the S288c strains to methionine in the Σ1278b genetic background. Mdm32p is a mitochondrial structural protein located in the inner membrane of mitochondria. There are two allelic changes in *MDM32* within the SK1 background strains: G-C and A-T transitions, converting cysteine to serine, and leucine to phenylalanine, respectively. The contributions of *PEA2* and *MDM32* to the filamentous growth response have not been studied previously and are the focus of the following studies.

2.3.4. Phenotypic analysis of *PEA2*

To further define the *PEA2*-mediated filamentous growth phenotype, we constructed a plasmid with the *PEA2* open reading frame from the S288c genetic background (Pea2-L409) downstream of its endogenous promoter. In parallel, we also constructed a plasmid containing the *PEA2* open reading frame from the Σ1278b genetic background (Pea2-M409). Both plasmids were then transformed into a *PEA2* deletion mutant of the Σ1278b strain and were assayed for invasive growth. The resulting *pea2Δ* strain with the plasmid-based *pea2-L409* allele is defective in invasive growth on rich medium. However, a *pea2Δ* mutant carrying the plasmid-based *PEA2-M409* allele

exhibits wild type invasive growth on solid YPD rich medium. To further confirm the effect of allelic change at codon 409 in *PEA2*, we implemented an integrated allelic swap in strains of the Σ1278b genetic background (See Materials and Methods). Essentially, we generated an integrated point mutant in the Σ1278b background that represented the S288c allele of *PEA2* within the genetic context of Σ1278b. As observed in our previous plasmid-based analyses, the *pea2-M409L* allelic change is defective in invasive growth on rich medium in the Σ1278b background (**Figure 2.7A**). Cells undergoing invasive growth exhibit an elongated morphology, and consistent with the observed decrease in invasion, *pea2Δ* and *Pea2-M409L* mutants exhibit a smaller fraction of elongated cells (length:width ratio of greater than 2) than is observed in an otherwise isogenic strain. (**Figure 2.7B**). This result indicates that Pea2p function can affect filamentous growth in yeast, and in addition, the allelic change in its coiled-coiled domain is essential for its wild-type function in each respective genetic context. To assess whether this loss of filamentous growth occurs at least in part through decreased activity of the Kss1p MAPK pathway or PKA pathway, we introduced a plasmid-based filamentation and invasion response element (FRE)-driven *lacZ* reporter in the *pea2Δ* and *Pea2-M409L* mutants. The FRE promoter sequence (-2.0kb ~ -1.6kb) is recognized by the Ste12p-Tec1p transcriptional factor complex that acts downstream of the Kss1p MAPK pathway; thus, expression of this reporter is a good indicator of filamentous growth MAPK pathway activity. The cAMP-PKA-responsive *FLO11* promoter fragment contains the Flo8- and Sfl1-binding sites (-1.4 ~ -1.0kb). In total, two *lacZ* fusion plasmids were constructed: plasmids pLG669-Z *FLO11* 6/7 and 9/10. The *FLO11* promoter region of -1400 to -1000 bp from the *FLO11* start codon corresponds to fragment 6/7, and sequence from -2000 to -1600 bp upstream of the transcriptional start site corresponds to fragment 9/10. Thus, pLG669-Z *FLO11* 6/7 is responsive to the PKA pathway, while pLG669-Z *FLO11* 9/10 is responsive to the MAPK pathway. Both plasmids were transformed into *pea2Δ* and *Pea2-M409L* mutants, and induced β-galacosidase activity was measured and then compared against a wild type strain of the Σ1278b genetic background. Here, we observed a significant decrease in *lacZ*-encoded β-galactosidase activity in *FLO11* 9/10 relative to wild type in *pea2Δ* and *Pea2-M409L* mutants, indicating decreased activity of the filamentous growth MAPK pathway upon deletion and allelic change of *PEA2* in

filamentous strains of the Σ1278b genetic background. In contrast, β-galactosidase activity was induced from the PKA response element at nearly wild-type levels in the respective mutants (**Figure 2.8**). Thus, this result indicates that *PEA2* contributes to the yeast pseudohyphal response through Mss11p-MAPK mediated effects, rather than through the PKA pathway.

2.3.5. *PEA2* mediates filamentous growth by affecting yeast apical growth

Here, we identified *PEA2*, and specifically, the methionine 409 residue as being crucial for mediating filamentous growth in strains of the Σ1278b genetic background. Our results also indicate that Pea2p enables filamentous growth through the Kss1p MAPK signaling pathway. However, the mechanism of Pea2p action with respect to M409 is unclear. Previous studies have explored Pea2p functions as an essential component in the polarisome complex. Valz & Herskowitz suggested Pea2p was involved in regulating the bipolar budding pattern in diploids to guarantee proper polarization during mating[61]. This study was conducted within a non-filamentous diploid yeast strain; however, the function of Pea2p in budding has not been well studied in a filamentous yeast background. To determine the contributions of Pea2p towards wild-type budding in the filamentous Σ1278b strain, we visualized bud scars using Calcofluor White staining. Here, we analyzed *pea2Δ* and *Pea2-M409L* mutants as well as a wild-type strain in the Σ1278b genetic background. Overnight cultures were spotted on rich medium (YPD plates), and grown for 5 days at 30°C. To assay the strains undergoing invasive growth on the solid medium, we scrapped off cells from the agar surface, and only analyzed cells that had invaded into the solid agar. These cells were dug out of the agar and were then washed twice prior to imaging. Calcofluor White staining was used to reveal the budding pattern of each strain, as Calcofluor White binds chitin that is easily visualized at the bud site.

Theoretically, non-filamentous haploid yeast strains should undergo axial budding, where the most recent bud scar should appear adjacent to the previous one. However, within the filamentous strain where most cells undergo the pseudohyphal morphological

transition, cells are elongated, and the daughter cells are physically attached to the mother cells. Therefore, the bud scar predominantly appears on the cell pole opposite the birth end, establishing a unipolar budding pattern. In **Figure 2.9**, we observed that the majority of wild type cells in the filamentous Σ1278b strain exhibit a unipolar budding pattern (approximately 70% of the observed cells, n>250). However, in *pea2Δ* and *pea2-M409L* mutants, the observed percentage of cells exhibiting unipolar budding was decreased (48% and 59%, respectively). On the contrary, a significant proportion of *pea2Δ* and *pea2-M409L* cells switched to the axial budding pattern, which is consistent with observed defects in invasive growth. Therefore, these results indicate that the allelic difference in *PEA2* affects the cellular budding pattern, diminishing the degree of unipolar budding in a manner consistent with decreased invasive growth.

Previous studies have found that Pea2p interacts with Spa2p, a scaffold protein, and Bud6p, an actin- and formin-interacting protein, forming part of the polarisome complex that mediates polarized cell growth[31,33,64]. To further investigate the function of Pea2p allelic variants in the polarisome, we generated an integrated *PEA2-ProA* fusion yielding an endogenously expressed Pea2p-ProA chimera. Also, using the same technique, we constructed a Pea2p-M409L-ProA chimera. In addition, both the Σ1278b and S288c genetic alleles of *SPA2* were cloned into vectors such that the genes were under transcriptional control of a copper-inducible promoter. Here, *SPA2* was N-terminally tagged with 3HA and formed a HA-Spa2p fusion. Both *SPA2-HA* plasmids were transformed into *PEA2-ProA* and *PEA2p-M409L-ProA* strains. Using Pea2p-ProA and Pea2p-M409L-ProA as baits in a co-immunoprecipitation assay, we examined the binding affinity between different alleles of Pea2p and Spa2p in strains of the Σ1278b genetic background. In this pull-down assay, we observed that Pea2p-ProA (the Σ1278b *PEA2* allele) was able to pull down more Σ-Spa2p-HA protein (the Σ1278b *SPA2* allele) than Sc-Spa2p-HA (encoded by the S288c *SPA2* allele). Similarly, Pea2p-M409L-ProA (encoded by the S288c *PEA2* allele) was able to pull down more Sc-Spa2p-HA protein (from the S288c *SPA2* allele) than Σ-Spa2p-HA (encoded by the Σ1278b *SPA2* allele). In total, we found that Pea2p was able to interact more effectively with Spa2p from the same genetic background (**Figure 2.10**). A “mismatched” pair of Pea2p and Spa2 from

different alleles would significantly impair this interaction. We also generated plasmids with different alleles of *BUD6*, but by the assays described above, no changes in Pea2p-binding were detected (data not shown). These results suggest that Pea2p regulates filamentous growth by contributing to characteristic cell polarity and budding profiles associated with filamentation; furthermore, allelic variants of Pea2p exhibit altered binding of the polarisome scaffold Spa2p.

2.3.6. *MDM32* and filamentous growth in SK1 strain

From the SK1 x S288c cross, we identified a large set of genes related to mitochondrial structure and function, including *MDM32, MRPL23,* and *MPA43*. Previous studies have revealed a link between mitochondrial function and yeast filamentous growth. Aun *et al*. have found that *rho* mutants lacking in mitochondrial DNA also exhibit defects in filamentous growth[46]. Furthermore, the dysfunctional mitochondria modulate the output of the PKA pathway. Starovoytova *et al*. discovered that retrograde signaling appears to be a positive regulator of butanol-induced pseudohyphal formation[8]. In this study, we choose *MDM32* as a mitochondrial structural gene to study mitochondrial function in yeast filamentation (LOD of 9.0). The SK1 allele of *MDM32* has two differences from the S288c allele: a G to C and A to T change that encodes serine at codon 182 in place of cysteine and phenylalanine at position 262 in place of leucine. As mentioned previously, deletion of *MDM32* in strains of the SK1 genetic background results in an invasive growth defect. To further investigate the *MDM32*-mediated filamentous growth phenotype, we constructed a plasmid with the *MDM32* open reading frame from the S288c genetic background (*MDM32-C182/L262*) downstream of its endogenous promoter. In parallel, we also constructed a plasmid with the *MDM32* open reading frame from the SK1 genetic background (*MDM32-S182/F262*). Both plasmids were then transformed into the *MDM32* deletion mutant, and the resulting strains were then assayed for invasive growth. The resulting *mdm32Δ*-Mdm32-C182/L262 transformant is defective in invasive growth on rich medium. However, the *mdm32Δ*-Mdm32-S182/F262 undergoes wild type invasive growth on solid YPD medium (**Figure 2.11**). Changes in cell morphology were consistent with the invasive

phenotype. Overall, this result suggests that Mdm32p can affect filamentous growth in yeast, and specifically, that residues S182 and F262 are crucial for its function in filamentous growth.

MDM32 encodes a structural protein in the inner membrane of mitochondria. It is an essential protein for normal mitochondrial structure and function[60,65]. Previous studies have found that *MDM32* deletion mutants possess dysfunctional mitochondria, and therefore, are respiratory-deficient. Also, the loss of normal Mdm32p results in abnormal mitochondrial shape; the *MDM32* deletion mutants exhibit enlarged and spherical mitochondria. Here, we used a similar approach to investigate different alleles of *MDM32* in a filamentous strain of the SK1 genetic background. From these studies, we observed that both *mdm32Δ*-Mdm32-C182/L262, and *mdm32Δ*-Mdm32-S182/F262 mutants can grow on nonfermentable carbon sources. Serial dilutions of wild type and mutant cultures were spotted onto plates containing either glucose or glycerol as carbon source and incubated at 37°C. The *mdm32Δ*-Mdm32-C182/L262 mutant strains showed a growth defect on plates containing glycerol as the carbon source, and the *mdm32Δ*-Mdm32-S182/F262 mutant showed a wild type growth phenotype on nonfermentable carbon sources at elevated temperature (**Figure 2.12**). Furthermore, mitochondrial structure in the *mdm32Δ*-Mdm32-C182/L262 mutant appears similar to the *mdm32Δ* deletion mutant; mitochondrial structure was collapsed to a spherical, large complex. However, expressing Mdm32-S182/F262 in the *mdm32Δ* deletion mutant can fully rescue the defective phenotype (**Figure 2.13**). Therefore, these results indicate that the SK1 allele of *MDM32* is essential to regulate the filamentous phenotype, and it is important in maintaining mitochondrial structure and function in SK1 strains. Notably, the S288c allele of *MDM32* (Mdm32-C182/L262) also encodes a fully functional protein; however, we prove in this study that the S288c variant of *MDM32* cannot function well in filamentous strains of the SK1 genetic background.

It is known that Mdm32p interacts with Mdm31p to maintain mitochondrial structure. These proteins both localize to the inner mitochondrial membrane[60]. To examine whether different alleles of *MDM32* alter its encode protein interaction with Mdm31p, we cloned different alleles of *MDM32* from the filamentous Σ1278b and non-

filamentous S288c strains into overexpression plasmids such that the genes formed a carboxy-terminal translational fusion with the protein A tag. The resulting plasmids can express an Mdm32p-ProA chimera. In addition, both the SK1 and S288c genetic alleles of *MDM31* were cloned into a similar overexpression plasmid, generating carboxy-terminal translational fusions with the eGFP tag. Thus, *MDM31* was C-terminally tagged with eGFP, forming an Mdm31p-eGFP fusion chimera. Using Mdm32p-ProA as bait in co-immunoprecipitation assays, we examined the binding affinity between different alleles of Mdm32p and Mdm31p in strains of the SK1 genetic background. Here, we observed that different alleles of Mdm32p can pull-down similar levels of Mdm31p from either the SK1 or S288c background (**Figure 2.14**). This result shows that allelic variants of *MDM32* did not alter the binding affinity of the encoded proteins with respect to Mdm31p.

2.4. Discussion

In this study, we integrated pooled segregant analysis with next-generation sequencing techniques to identify alleles linked with invasive growth. Our analysis focused on allelic variants between two filamentous strains, Σ1278b and SK1, and one non-filamentous strain, S288c, linked with invasive growth phenotypes on rich medium. In total, we identified 522 allelic differences within 201 genes that relate to haploid invasive growth. In particular, our work identified allelic variation in the *PEA2* and *MDM32* genes linked with invasive growth phenotypes in the Σ1278b and SK1 genetic backgrounds, respectively. Pea2p is a component of the cell polarisome complex; it interacts with Spa2p and Bud6p to regulate cell polarity in diploid cells[33,64]. But its function in haploid filamentous strain during filamentation was largely uncharacterized prior to this study. We found that *PEA2* is required for invasive filamentous growth in haploid strains; specifically, its allelic variation at position 409 is crucial for its function in filamentous growth. In S288c-derived strains, *PEA2* encodes leucine at codon 409, while in the filamentous strain Σ1278b, *PEA2* encodes methionine at the same position. Replacement of the Σ1278b allele of *PEA2* with the S288c allele in the Σ1278b genetic

background results in defective invasive growth on rich medium. By the FRE-*lacZ* reporter and β-galactosidase activity assays, Pea2p affects the MAPK-responsive element in the *FLO11* promoter, rather than the PKA-responsive element, indicating it mediates filamentous growth through the Kss1p/MAPK signaling pathway. By budding pattern analysis and co-immunoprecipitation studies, we found that Pea2p primarily interacts with the scaffolding protein Spa2p to alter haploid axial budding to a unipolar pattern during invasive growth in filamentous strains. The fact that Pea2p interacts more effectively with specific alleles of Spa2p from the same genetic background raises the interesting thought that given allelic variants may be specific for partner allelic variants in the same genetic context.

The connection between cell polarity and filamentous growth has been studied extensively over the years. The scaffolding protein Spa2p, for example, has been identified as a filamentous growth regulator in the context of promoting polarized cell growth through regulation of the actin cytoskeleton. Deletion of Spa2p has been found to impair filamentous growth under nitrogen stress conditions. Spa2p interacts with Pea2p and Bud6p to form a multi-protein complex, which in turn coordinates the complex processes of polarized growth. Both Spa2p and Pea2p have conserved coiled-coil segments. The interaction of the Spa2p coiled-coil segments with Pea2p raises the possibility that the two polarity proteins might associate with each other via a coiled-coil interaction. The allelic change found in this study was located inside of the predicted coiled-coil domain, further suggesting that an interaction between Pea2p and Spa2p may be crucial for the function of the polarisome complex. Both yeast two-hybrid and immunoprecipitation studies have revealed an interaction between Spa2p and Mss11p, Ste11p, and Ste7p, suggesting that this multi-protein complex interact with constituents of two MAPK signaling pathways involved in budding, mating, and pseudohyphal formation. Our study is consistent with the conclusion that the Pea2p-mediated filamentous response is through MAPK signaling, rather than PKA signaling.

Within the Σ1278b/S288c cross, A single T-to-G transversion in the coding sequence of the *RHO2* gene, converting phenylalanine at 91 to cysteine in Σ1278b, was strongly linked with invasive growth, and substitution of the S288c *RHO2* allele for the

corresponding gene in Σ1278b results in a loss of invasive growth. *RHO2* encodes a small GTPase of the Rho/Rac family of Ras-like protein. In general, Rho GTPase has been reported to play a critical role in cell polarized growth. Rho2p may play a role in the establishment of cell polarity or in microtubule assembly[66]. In total, our findings strengthen the connection between cell polarized growth and filamentous growth, shedding light on the potential function of the polarisome during filamentation in yeast.

In the SK1/S288c cross, we discovered a large set of mitochondrial genes that regulate filamentous growth in strain of the SK1 genetic background. *MDM32* encodes a mitochondrial structural protein located in the mitochondrial inner membrane. There are two allelic changes in *MDM32* from S288c to SK1: in the encoded protein, cysteine is changed to serine at amino acid 182, and leucine is changed to phenylalanine at amino acid 262. Switching *MDM32* to its S288c allelic form in a strain of the SK1 genetic background results in defective invasive growth. In addition, we found that the resulting *mdm32Δ*-Mdm32-C182/L262 mutant not only affects invasive growth in haploid filamentous strains, but also affects normal mitochondrial structure and function. Previous studies have shown that Mdm32p primarily interacts with Mdm31p to maintain normal mitochondrial shape. By co-immunoprecipitation, we failed to detect changes in the binding affinity between the two with different alleles. Therefore, there must be a third component that potentially interacts with Mdm32p to regulate filamentous growth, or the functional consequences of this allelic variation are not carried out through altered protein interactions.

In addition to genes that are positively related to wild type invasive growth in the filamentous strains, we also identified a large set of genes whose allelic changes correspond to non-invasive offspring. These genes could potentially serve as inhibitors of the filamentous growth transition. Conversely, allelic variants in the non-filamentous S288c strain were also enriched in the pools of invasive offspring. Interestingly, these S288c alleles are actually linked with an invasive phenotype, suggesting that the S288c genetic background is not uniformly repressive with respect to filamentation. Filamentous growth is viewed as a cellular foraging mechanism allowing non-motile yeast to scavenge for nutrients under stressful conditions. It requires multiple cellular

response mechanisms to function efficiently, save energy, and utilize/recycle available nutrients. In this process, non-essential protein synthesis is shut down, some transcription and translation processes are temporarily stopped, cellular degradative processes such as autophagy and endocytosis are modified, and cytokinesis and cytoskeletal processes are regulated in order to change cell morphology. From our understanding, this mechanism is a natural cell adaptation to the changing environment. Therefore, it is not surprising that the filamentous growth mechanism may exist in numerous yeast strains, with remnants present in non-filamentous strains. Such non-filamentous strains may contain many components required for filamentation but lack a few essential components for pseudohyphal growth, such as the genes *FLO8* and *FLO11*. Further study will be needed to more fully determine the functional consequences of the identified instances of allelic variation between filamentous and non-filamentous strains.

In sum, this study is the first to apply pooled segregant analysis for the identification of alleles that are potentially linked to the filamentous growth trait. Even though the complete sequence of the yeast genome has been available since 1996, tracking SNPs (Single-nucleotide polymorphism) in different strains is still cumbersome. A traditional way is to generate custom SNP arrays and to create extensive heterozygosity in order to map SNPs by microarrays. However, the pooled linkage/sequencing strategy has several advantages over traditional methods; in particular, it doesn't require extra SNP arrays or the time needed to perform a series of backcrosses, therefore, saving both time and labor. The pooling approach described here could be applied to other organisms for which the phenotypes of meiotic progeny can be assessed and for which a reference genome is available. Pooling can also be applied to study different cellular mechanisms in yeast, such as autophagy, endocytosis, and oxidative stress. Therefore, it opens many avenues for additional allelic linkage studies in the yeast community.

2.5. Acknowledgements

We thank Dr. Tomas Wilson for helping DNA sequence analysis, and generous

suggestions throughout this project. We also thank Dr. Daniel Klionsky for providing MitoTracker, plasmids and anti-ProA antibodies used in this project.

Figure 2.1. Schematic of pooled linkage analysis in filamentous growth. ***A,*** invasive growth phenotypes of filamentous strains (Σ1278b and SK1) and a non-filamentous strain (S288c). For this analysis, overnight cultures were spotted on YPD solid plates, with growth for 5 days at 30°C. After removing surface cells with a gentle stream of water, the residual cell markers on the agar were recorded to assess invasive growth intensity. ***B,*** pooled segregant strategy. By this approach, we crossed Σ1278b and SK1 with the S288c-derived non-filamentous strain, and after complete meiosis, we separated and grouped the spores based on their filamentous phenotype (invasive or non-invasive in this study). In total, 174 spores were collected. Statistically, the pool size is sufficiently large to allow for the determination of genetic linkage. The resulting genetic pools were then used for next generation sequencing.

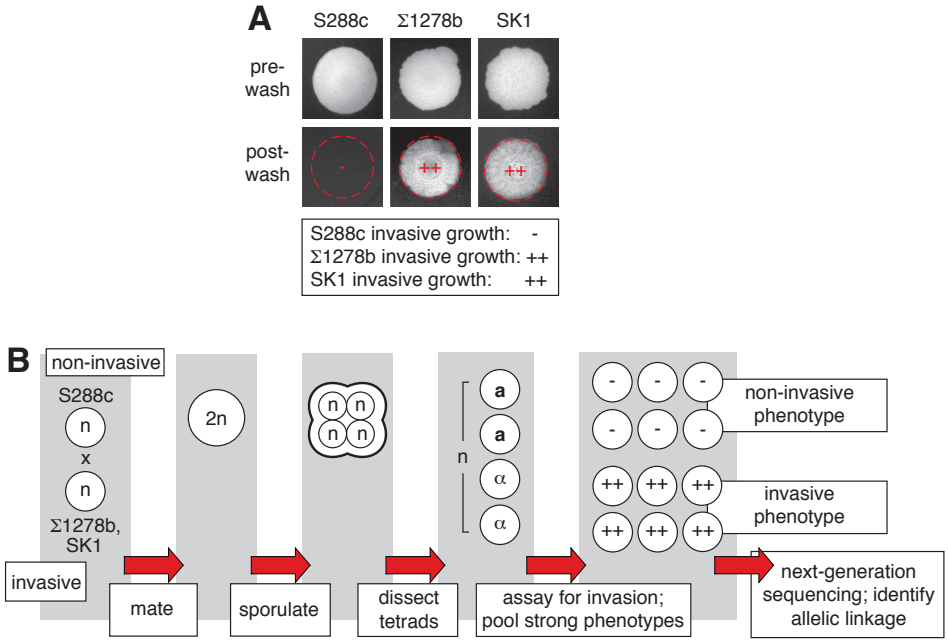

Figure 2.2. **Screening of offspring spores for invasive growth phenotypes on YPD medium.** Offspring spores were grown overnight in rich medium and then spotted in 96-well format using a hand pinning tool on YPD. Plates were incubated at 30°C for 5 days. Colonies showing lost invasive markers as compared to wild type were scored as non-invasive (examples of such colonies are shown by the white pointed arrow). Colonies with wild-type markers were scored as invasive (red pointed arrow). Colonies with reduced invasive markers were scored as intermediate phenotypes (green pointed arrow). Duplicate tests were performed to ensure the positive hits.

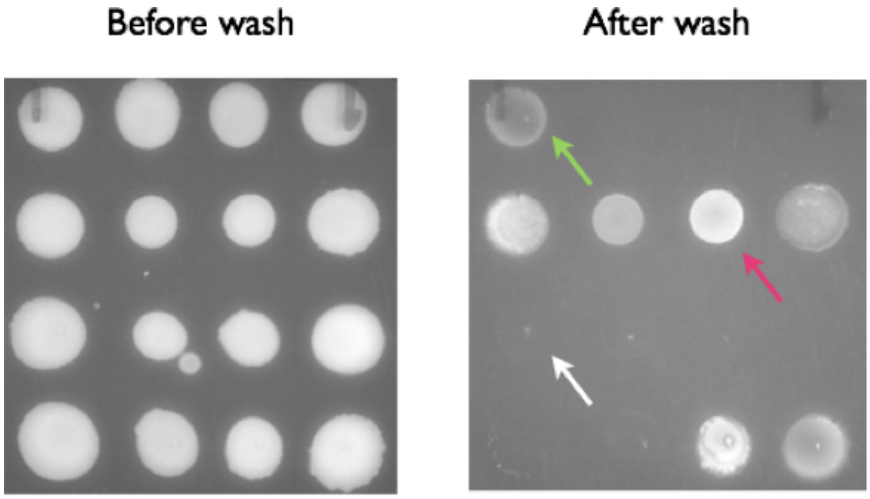

Figure 2.3. Linkage analysis of the Σ1278b/S288c cross. ***A,*** strain of the S288c genetic background was crossed with a derivative strain of Σ1278b. After pheromone assays to determine mating type, 124 offspring spores from complete meiosis were collected. Based on the wash test results, 37 spores were categorized as exhibiting strong invasive phenotypes, while 63 lost the invasive phenotypic traits. The two resulting genetic pools were then sequenced and were compared using the VAMP site. ***B,*** after analyzing the sequence data by VAMP, 53 genes were potentially linked to invasive growth. We used LOD scores larger than 3.0 as the criteria in this analysis. The identified genes were concentrated on chromosomes V, IX, XIII, and XIV, including *FLO8* and *FLO11*. A large set of genes was found near *FLO8*, reflecting the dominant effect of *FLO8*. We identified *PEA2* and *RHO2* on chromosomes V and XIV, respectively.

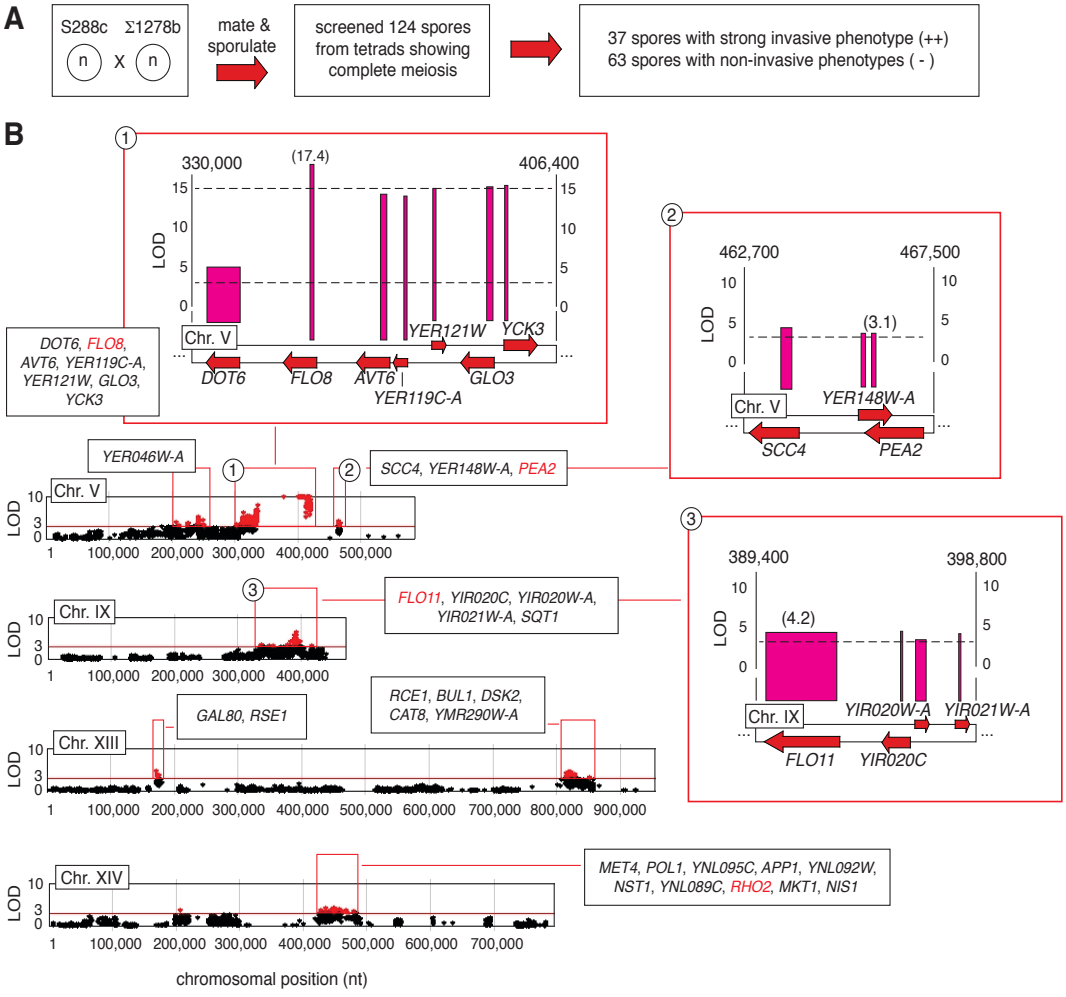

Figure 2.4. GO term analysis of Σ1278b/S288c cross genes. Listing of Gene Ontology (GO) biological process categories enriched in the set of genes identified in the Σ1278b/S288c cross. Identified genes belonging to each category are indicated; extensively overlapping biological process categories are grouped together for convenience.

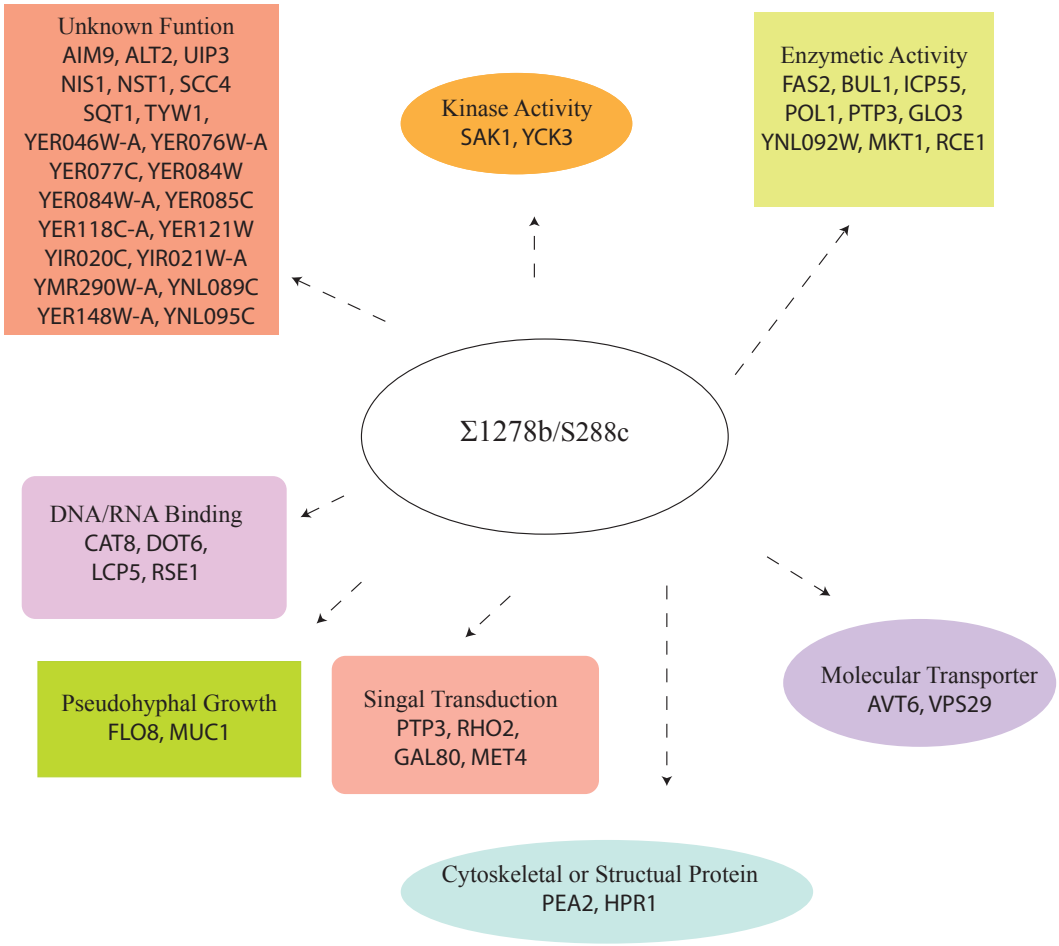

Figure 2.5. Linkage analysis of the SK1/S288c cross. ***A,*** strain of the S288c genetic background was crossed with the SK1 strain. After pheromone testing to determine mating types, 100 offspring spores representing complete meiosis were collected. Based on the wash test result, 51 spores were categorized as having strong invasive phenotypes, while 24 lost the invasive phenotypic trait. The two resulting genetic pools were then sequenced and were compared using tools incorporated in the VAMP site. ***B,*** after analyzing the sequence data, 91 genes were identified with potential linkage to invasive growth. We used LOD scores larger than 4.0 as the criteria in this analysis. Distinct from the Σ1278b/S288c cross, the identified genes are concentrated on chromosomes V, XIV, XV, and XVI, including *FLO8*. *FLO11* was not identified in this analysis. *MDM32* has the second highest LOD score except for FLO8.

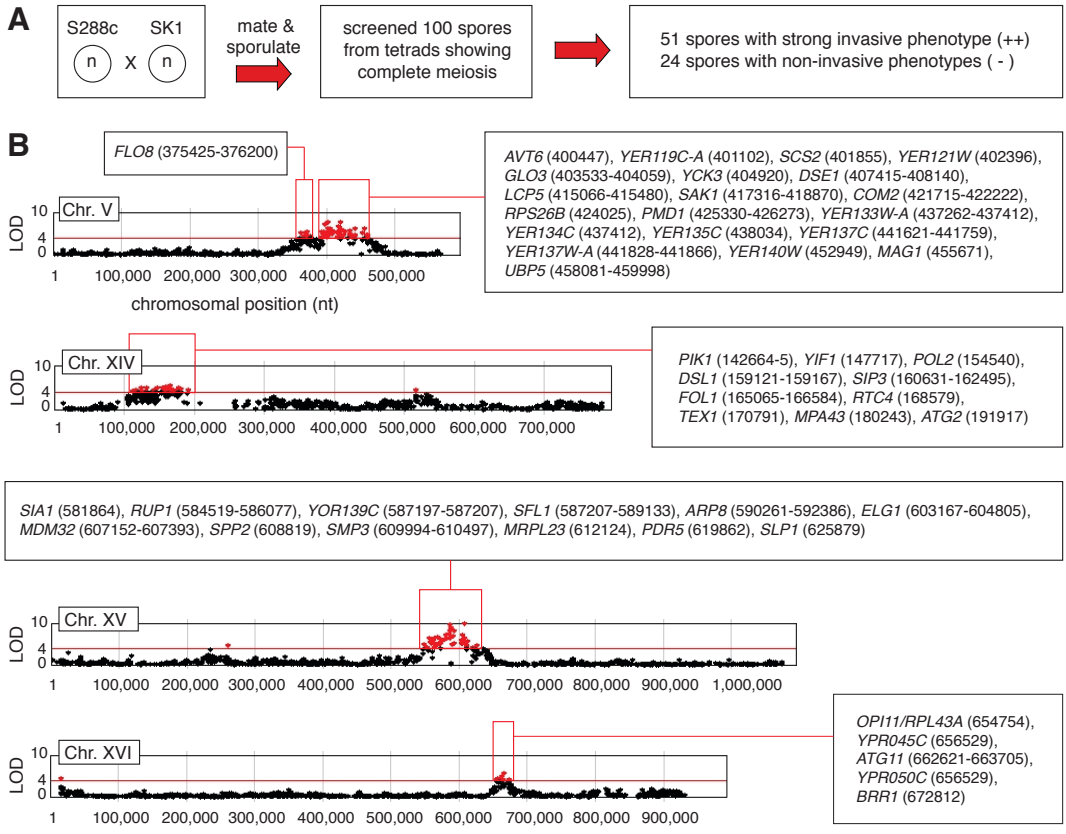

Figure 2.6. GO term analysis of genes identified in theSK1/S288c cross. Listing of Gene Ontology (GO) biological process categories enriched in the set of genes identified in SK1/S288c cross. Identified genes belonging to each category are indicated; extensively overlapping biological process categories are grouped together for convenience.

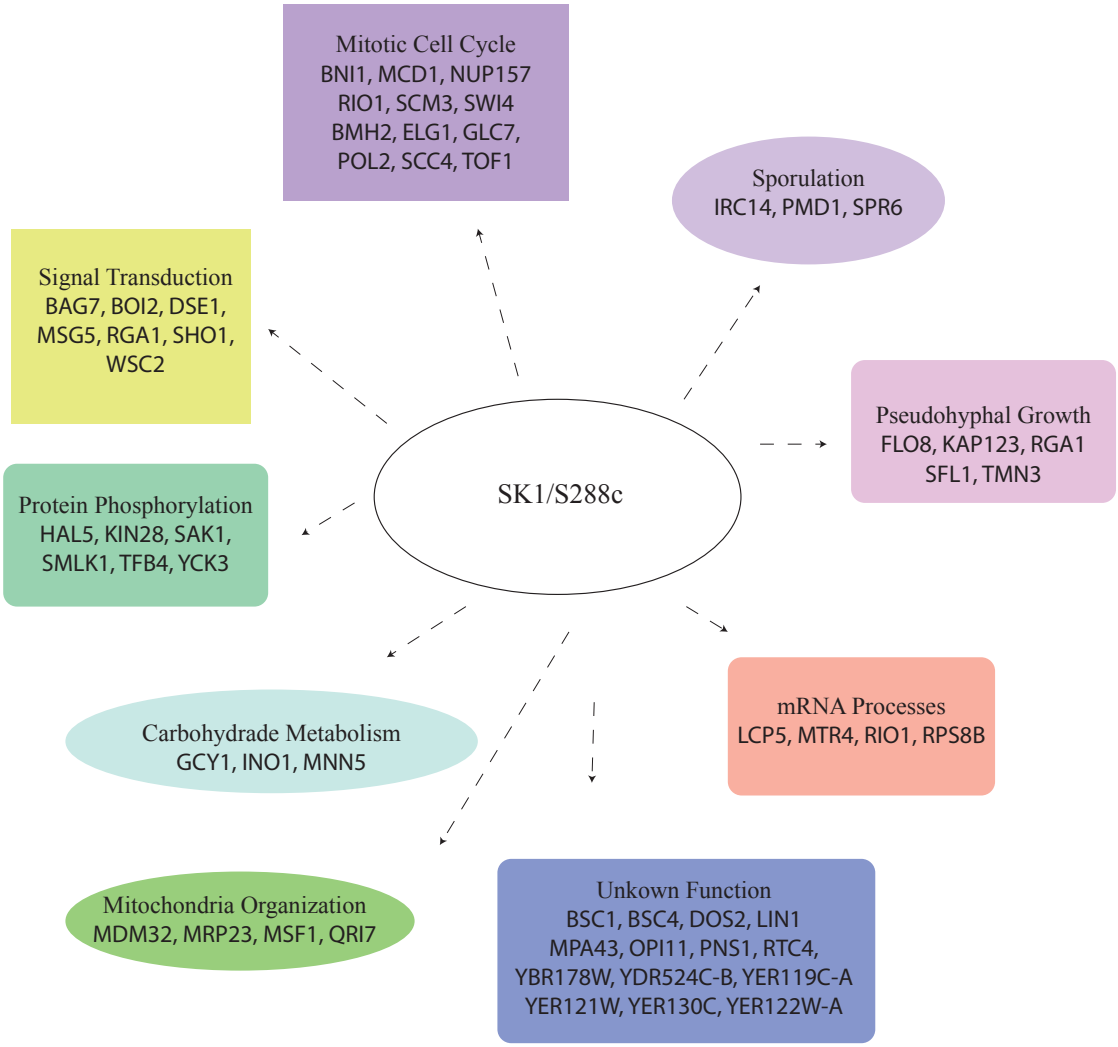

Figure 2.7. Filamentous phenotypic analysis of *PEA2*. *A*, invasive growth assay of *PEA2* in haploid strains with Σ1278b genetic background. Overnight cultures were spotted on YPD medium and grown for 5 days at 30°C. After washing off the cells on the surface of the medium, residual cells were observed and compared to the wild type culture. The *pea2* deletion mutant and *pea2-M409L* strain showed reduced invasive growth phenotypes as compared to wild type. ***B***, cells from these colonies were scraped into a suspension in identical liquid media for analysis of cell morphology by differential interference contrast microscopy. Cell length-to-width ratios were calculated for each strain. The *pea2* deletion strain and *pea2-M409L* mutant displayed a majority of cells with a ratio of less than 1.5, indicating defects in cell elongation.

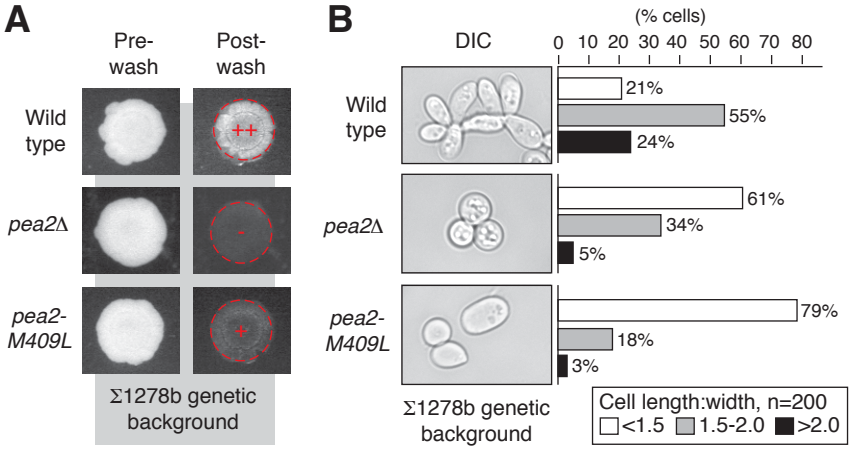

Figure 2.8. *PEA2* affects filamentous growth through MAPK pathway, rather than PKA signaling. Activity of cAMP-PKA and Filamentous growth MAPK-responsive pFLO11 fragment::lacZ reporters in wild type, *pea2Δ* and *pea2-M409L* mutants. Analysis of the *FLO11* locus indicates positions of cAMP-PKA pathway-responsive (21.0 to 21.4 kb from *FLO11* start codon, named 6/7) and MAPK- responsive (21.6 to 22.0 kb from FLO11 start codon, named 9/10) promoter fragments. Numbers mark nucleotides in kilobases. β-galactosidase activity was measured from cells growing exponentially in SC-URA medium and carrying pLG669-Z FLO11 6/7, pLG669-Z FLO11 9/10. Error bars indicate standard deviations of three independent measurements. The MAPK response is reduced in *pea2Δ* and *pea2-M409L* mutants.

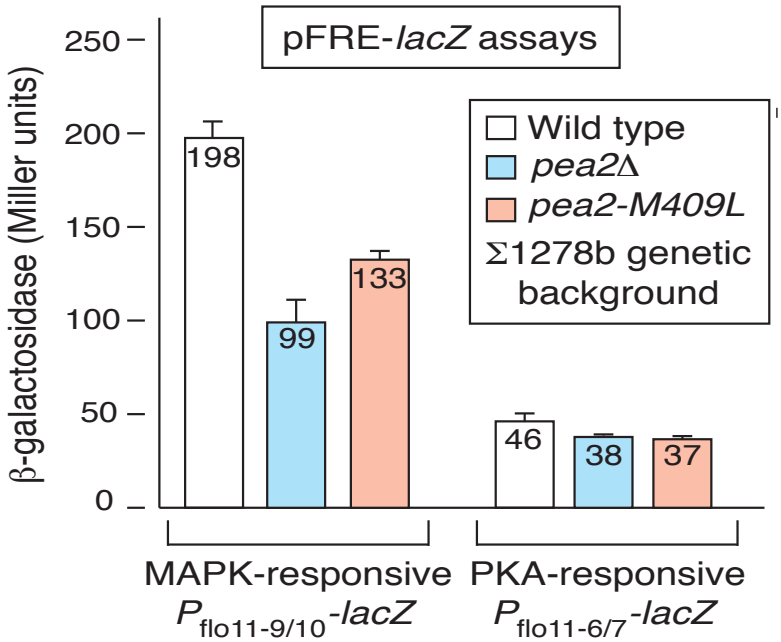

Figure 2.9. *PEA2* affects budding pattern in haploid filamentous strains. Overnight cultures were spotted on YPD medium and grown for 5 days at 30°C. After washing off the cells on the surface of agar, the invaded cells in the agar were collected and washed twice with identical medium. A solution of 17% formaldehyde was used to fix the cells. A solution of 10 mM Calcofluor White was used to stain the cells for 1 hour as previously described. The bud scars can be observed by fluorescence microscopy (DAPI channel). For each strain, more than 250 cells were counted and were categorized into four typical budding patterns. The proportion of each pattern was calculated and compared. *pea2Δ* and *pea2-M409L* mutants have more cells with an axial budding pattern, and less unipolar budding.

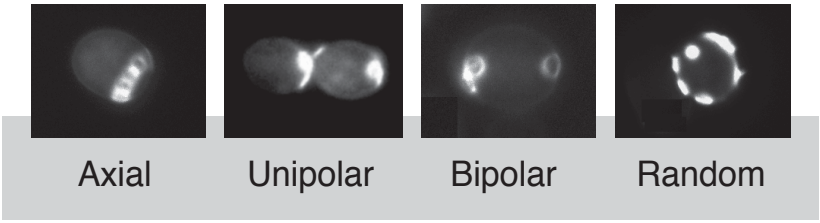

	Axial	Unipolar	Bipolar	Random
Wild type	17%	69%	9%	5%
*pea2*Δ	33%	48%	7%	12%
pea2-M409L	31%	59%	5%	5%

WT: n=259; *pea2*Δ: n=240; *pea2-M409L*: n=296

Figure 2.10. Analysis of Pea2p and Spa2p binding affinity by co-immunoprecipitation. Integrated *PEA2* alleles were generated by tagging with ProA on the C-terminus in wild type and *pea2-M409L* mutants. The *SPA2* ORF was cloned into the pCu-3HA-URA plasmid, which has a copper inducible overexpression promoter and 3HA-tagging on the N-terminus. The resulting plasmids pCu-3HA-ScSpa2p and pCu-3HA-ΣSpa2p were transformed into both wild type and *pea2-M409L* mutants. The binding affinity between Pea2p and Spa2p was revealed by IgG pull-down assay using Pea2p-ProA as bait.

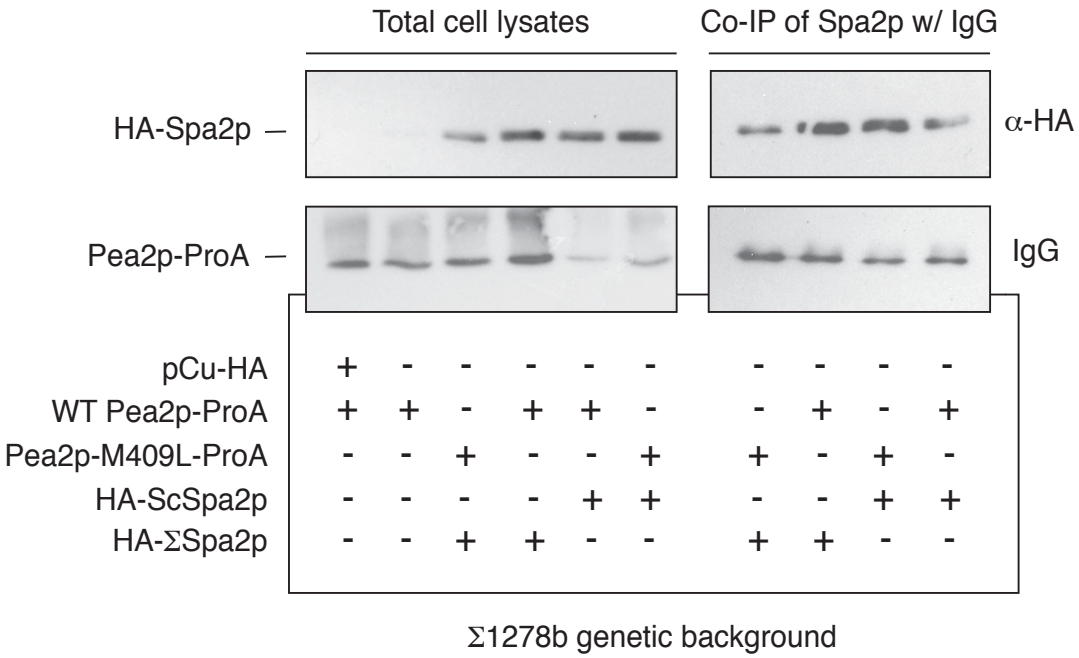

Figure 2.11. Filamentous phenotypic analysis of *MDM2*. *A*, invasive growth assay of *MDM32* in haploid strains with SK1 genetic background. Overnight cultures were spotted on YPD medium and grown for 7 days at 30°C. After washing off the cells on the surface of the medium, residual cells were observed and compared to the wild type culture. The *mdm32* deletion mutant, *mdm32Δ-SCMDM32* and *mdm32Δ-SK1MDM32* strains showed reduced invasive growth phenotypes as compared to wild type. ***B***, cells from these colonies were scraped into a suspension in identical liquid media for analysis of cell morphology by differential interference contrast microscopy. Cell length-to-width ratios were calculated for each strain.

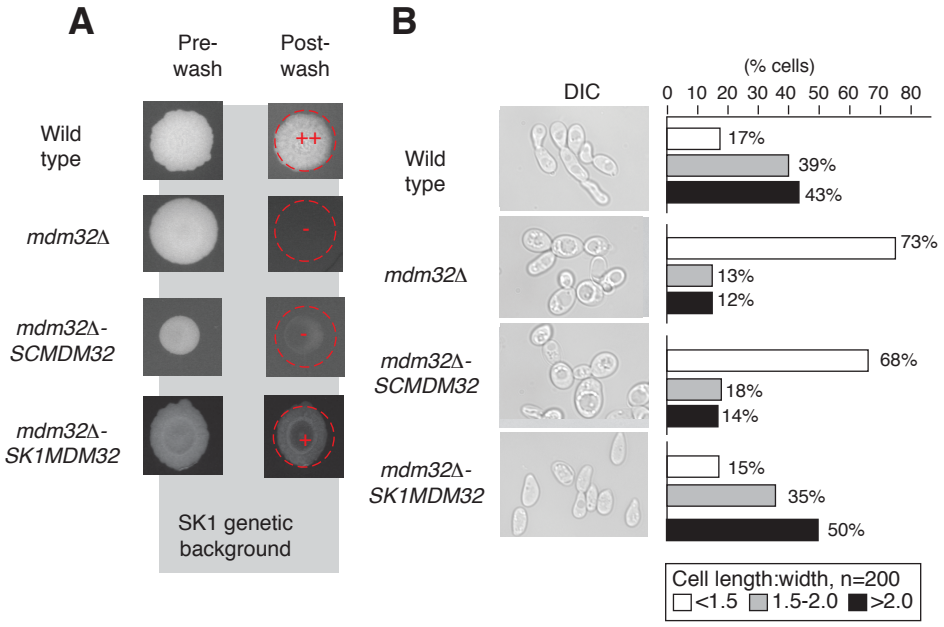

Figure 2.12. Respiratory growth assay. Wild type, *mdm32Δ*, *mdm32Δ-ScMDM32, and mdm32Δ-SK1MDM32* cells were grown overnight in glucose- containing medium. Then, 10-fold serial dilutions were spotted onto plates containing glucose (YPD) or glycerol (YPG) as carbon source. YPD plates were incubated for 2 d and YPG plates for 3 d at the indicated temperatures.

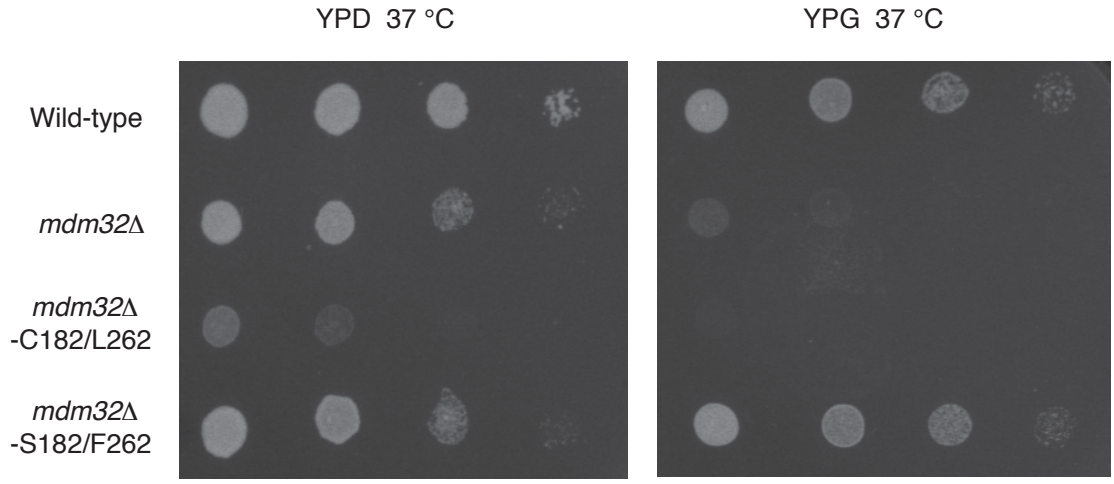

Figure 2.13. Mitochondria morphology in *mdm32Δ* mutant. Wild-type, *mdm32Δ*, *mdm32Δ-SCMDM32* and *mdm32Δ-SK1MDM32* cells were grown to log phase in SC medium and analyzed by fluorescence microscopy. (left) DIC, and (right) TRITC channel to visualize mito-tracker stained mitochondria morphology. *mdm32Δ*, *mdm32Δ-SCMDM32* cells display enlarged and spherical mitochondria, and *mdm32Δ-SK1MDM32* cells have normal mitochondria comparing to the wild-type.

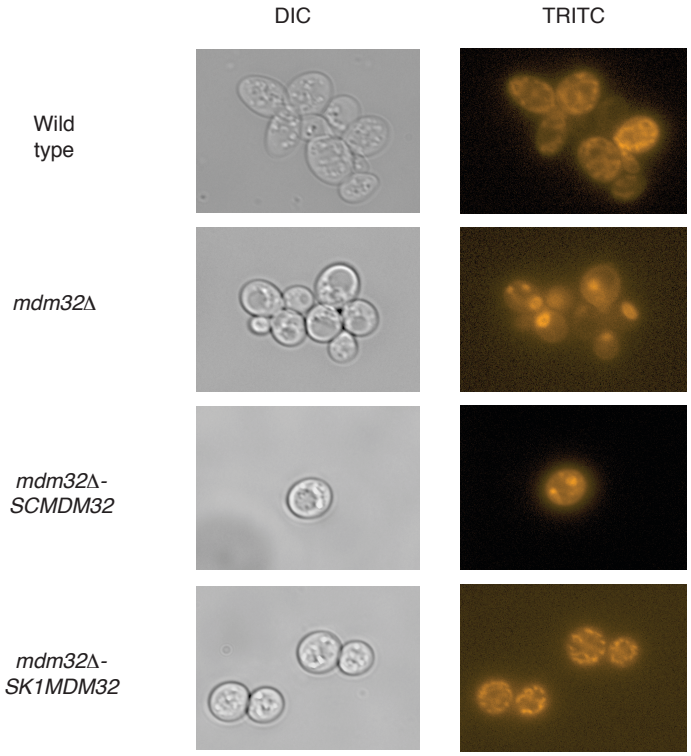

Figure 2.14. Analysis of Mdm32p and Mdm31p binding affinity by co-immunoprecipitation. The *MDM32* ORF was cloned into a GPD-eGFP Gateway plasmid, which has the GPD promoter and C-terminal eGFP tagging. The *MDM31* ORF was cloned into the GPD-TAP plasmid, which has GPD promoter and TAP tagging on the C-terminus. The resulting plasmids were transformed into *mdm32Δ* mutants. The binding affinity between Mdm32p and Mdm31p was revealed by IgG pull-down assay using Mdm31p-TAP as bait.

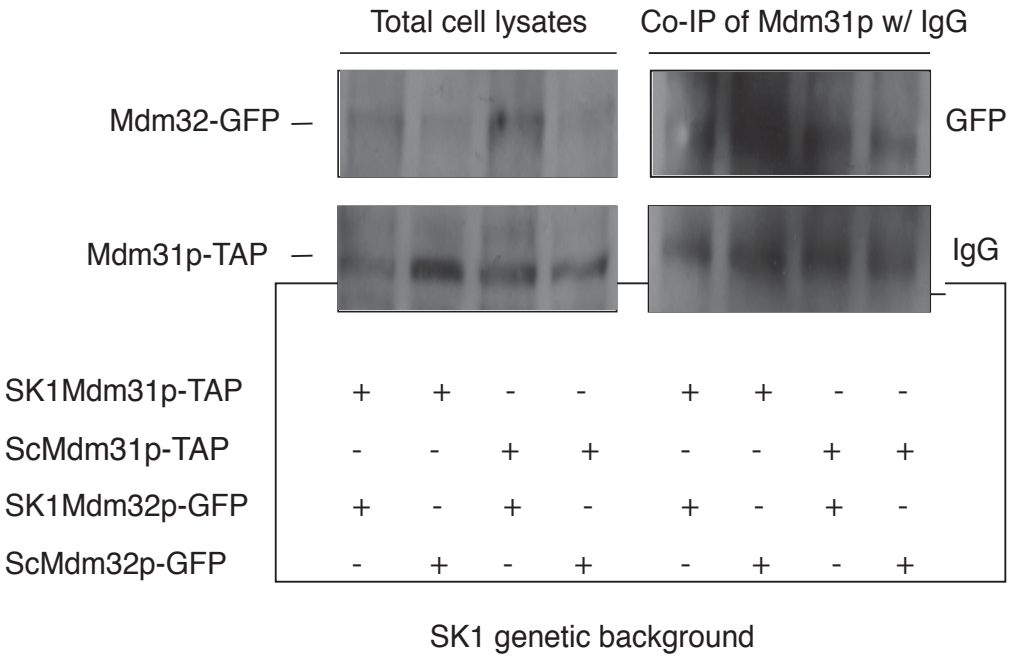

Table 2.1. Strains used in this study.

Strain	Genotype	Source
HLY337	*MATα ura3-52 trp1-1*	G. Fink (MIT, MA)
Y826	*MATα ura3-52 leu2Δ0*	M. Snyder (Stanford U., CA)
BY4741	*MATa his3Δ1 leu2Δ 0 met15Δ 0 ura3Δ0*	This study
SK1	*MATa ura3-52*	This study
SK1_modified	*MATa ura3-52 trp1Δ0*	This study
pea2Δ	*MATα pea2Δ leu2Δ0*	This study
pea2 409L	*MATα PEA2-409L leu2Δ0*	This study
rho2Δ	*MATα rho2Δ leu2Δ0*	This study
mdm32Δ	*MATα mdm32Δ trp1Δ0*	This study
mrpl23Δ	*MATα mrpl23Δ ura3-52*	This study
mpa43Δ	*MATα mpa43Δ ura3-52*	This study
idh2Δ	*MATα idh2Δ ura3-52*	This study
brr1Δ	*MATα brr1Δ ura3-52*	This study
sho1Δ	*MATα sho1Δ ura3-52*	This study
hal5Δ	*MATα hal5Δ ura3-52*	This study
gcy1Δ	*MATα gcy1Δ ura3-52*	This study
vps17Δ	*MATα vps17Δ ura3-52*	This study
yir021w-aΔ	*MATα yir02w-aΔ ura3-52*	This study

Table 2.2. Genes and corresponding allelic change identified in Σ1278b/S288c cross

Gene	Chromosome	Position	Allele change	Amino Acid change	LOD
UIP3	chrI	183875	T-C	W-R	3
ALT2	chrIV	678771	A-G	D-G	3.2
HPR1	chrIV	730732	A-G	K-E	3.6
PTP3	chrV	310095	A-T	K-N	3.2
AIM9	chrV	321040; 321397; 321775	C-T; T-C; A-G	A-V; V-A; N-S	3.6
FLO8	chrV	377186	T-C	x-W	17.4
YER148W-A	chrV	466241	G-T	S-I	3.1
DOT6	chrV	333269; 333440; 333615; 333665; 333684; 334212; 334228; 334313; 334739; 334746; 334877	C-A; C-A; G-A; G-C; T-C; G-A; A-C; T-C; C-T; G-A; A-G	T-N; A-D; G-S; S-T; C-R; V-I; R-S; I-T; A-V; A-T; N-S	5
YER076C	chrV	312722; 312806; 312830; 312962; 313202; 313340	G-T; G-A; G-A; C-G; G-T; C-G	G-V; G-E; S-N; A-G; S-I; S-C	4.6
AVT6	chrV	400477; 400832	A-G; G-A	N-S; A-T	14.5
YER046W-A	chrV	243718	G-T	R-L	4.1
YER121W	chrV	402396	A-T	K-M	15.1
YER084W	chrV	327359	A-C	D-A	3.4
YER077C	chrV	314585; 314943; 314975; 316218	G-A; G-C; G-A; G-A	R-H; V-L; R-K; A-T	3.6
PEA2	chrV	466241	C-A	L-M	3.1
DSE1	chrV	407953; 408140	C-A; G-C	N-K; G-A	14.7
YER076W-A	chrV	313483	T-A	I-N	3.9
GLO3	chrV	403553; 403774	A-G; A-G	K-E; N-S	15.3
YER084W-A	chrV	327966	G-A	G-S	5.1
YCK3	chrV	404920	T-G	C-G	15.4
YER119C-A	chrV	400886	C-T	R-W	14.3
SCC4	chrV	464044; 464098; 464159; 464159	C-T; G-A; C-T; G-T	T-I; C-Y; H-Y; G-E	3.4
ICP55	chrV	318305	A-G	M-V	3.1
SAK1	chrV	417316; 418486; 418864; 418870; 419264; 419532; 419564; 419627; 420275; 420428	A-G; A-G; A-G; G-A; G-A; T-G; G-A; T-G; A-G; A-G	N-D; I-V; T-A; G-S; S-N; I-M; R-H; I-R; Q-R; D-G	8.6
LCP5	chrV	415066; 415306	G-A; T-C	G-E; L-S	9.9
MUC1	chrIX	389946; 390272; 390741; 390776; 391025; 391760; 393114; 393135; 393153;	A-G; T-C; T-C; C-T; T-C; T-C; C-T; A-G; G-	I-V; L-P; S-P; T-I; I-T; V-A; H-Y; N-D; D-	4.2

		393333; 393356; 393392; 393420; 393654; 393656	T; A-G; G-A; G-A; G-C; A-G; C-T; T-C	Y; N-D; G-D; G-D; W-S; K-E; L-F; L-P	
YIR020C	chrIX	394368	G-C	V-L	4.4
YIR021W-A	chrIX	398580	G-C	A-P	4.1
YIR020W-A	chrIX	394989; 395008; 395133	A-G; T-C; A-G	T-A; V-A; T-A	3.2
SQT1	chrIX	379273	A-C	E-A	3.3
CAT8	chrXIII	827391; 829027	T-C; A-G	L-S; T-A	3.3
BUL1	chrXIII	815904; 818234; 818477	G-A; G-A; T-C	G-S; G-E; V-A	3.4
GAL80	chrXIII	171896	A-C	E-D	4.7
YMR290W-A	chrXIII	851619	T-A	S-T	3.2
DSK2	chrXIII	819064	C-G	A-G	3.1
RSE1	chrXIII	176006	G-A	R-K	3.6
RCE1	chrXIII	814437; 815080	G-A; A-C	V-I; L-F	3.9
RHO2	chrXIV	456838	T-G	F-C	3.3
NST1	chrXIV	455104	A-G	N-D	3.1
YNL089C	chrXIV	456838	A-C	K-Q	3.3
MET4	chrXIV	428863	T-C	I-T	3.2
YNL092W	chrXIV	450997	C-A	A-E	3.6
APP1	chrXIV	449116	G-A	A-T	4.2
MKT1	chrXIV	468490	A-G	K-R	3
NIS1	chrXIV	479818	T-G	L-W	3.3
POL1	chrXIV	433150; 433708	G-A; T-A	R-K; I-K	3.1
YNL095C	chrXIV	446679	C-G	S-C	3.6
CLN2	chrXVI	65676	G-A	M-I	3.2
TYW1	chrXVI	160842	C-T	S-L	3.6
ICY2	chrXVI	74459	G-T	M-I	3.1
FAS2	chrXVI	114050	G-A	S-N	3

Table 2.3. Genes and corresponding allelic change identified in SK1/S288c cross

Gene	Chromosome	Position	Allele change	Amino Acid change	LOD
SCM3	chrIV	211461	C-T	T-I	4.4
YDR524C-B	chrIV	1489710	C-G	R-G	4.3
NUP157	chrV	368702; 369116; 370467; 370846; 371298; 371852; 371855; 371982	T-C; G-A; G-A; G-A; A-G; A-C; G-A; A-G	F-S; G-E; A-T; M-I; N-D; K-T; R-K; I-V	4.6
RPS26B	chrV	424025	T-C	F-L	4.6
FLO8	chrV	375425; 376046; 376200	G-A; T-C; A-G	S-N; I-T; T-A	4.3
YER135C	chrV	438034	T-C	S-P	4.2
SCS2	chrV	401855	T-G	F-C	6.1
RPL23B	chrV	397397	A-G	L-L	7
SPR6	chrV	394353	T-C	C-R	4
COM2	chrV	421715; 422222	G-A; T-G	R-K; V-G	4.5
SLX8	chrV	385710; 395782; 396134	A-C; G-A; G-A	K-N; M-I; G-D	4.9
SSA4	chrV	366281	G-A	R-K	4.3
AVT6	chrV	400447	A-G	N-S	4.1
YER137C	chrV	441621; 441759	G-A; G-A	M-I; M-I	5.3
YER134C	chrV	437412	G-A	D-N	4.3
YER121W	chrV	402396	A-T	K-M	7.7
MAM1	chrV	372450; 373150	G-C; A-C	K-M; T-P	4.4
UBP5	chrV	458081; 458599; 459180; 459491; 459527; 459692; 459735; 459998	C-T; T-A; T-C; C-T; A-G; G-A; G-A; G-C	S-F; D-E; S-P; T-I; D-G; R-K; A-T; G-A	4.3
YER140W	chrV	452949	T-C	F-L	5
MAG1	chrV	455671	A-G	I-V	6.1
YER137W-A	chrV	441828; 441839; 441866	C-A; A-G; T-A	L-F; Y-C; I-K	4.8
PMD1	chrV	425330; 426273	T-C; A-T	S-P; Q-H	5.6
DSE1	chrV	407415; 407953; 408140	A-G; C-A; G-C	I-V; N-K; G-A	5.3
GLO3	chrV	403533; 403774; 404059	A-G; A-G; T-C	K-E; N-S; L-S	5.1
YCK3	chrV	404920	T-G	C-G	6.1
AST2	chrV	361783	A-C	E-A	5.2
YER119C-A	chrV	401102	C-A	G-V	5.5
YER133W-A	chrV	437262; 437412	T-C; C-T	F-L; R-C	4.3

SHO1	chrV	398971	A-C	K-N	4.7
SAK1	chrV	417316; 418509; 418870; 419224; 419532; 419564; 419627; 420275; 420592	A-G; A-T; G-A; G-C; T-G; G-A; T-G; A-G; C-A	N-D; K-N; G-S; A-P; I-M; R-H; I-R; Q-R; H-N	5.5
LCP5	chrV	415066; 415306; 415480	G-A; T-C; A-T	G-E; L-S; E-V	4.8
BOI2	chrV	392108; 393020; 393626	G-A; C-T; C-T	S-N; P-L; S-L	4.7
AAD6	chrVI	14848	T-C	L-P	4.2
MPH1	chrIX	357797; 359491	G-A; G-A	S-N;M-I	4.1
EPS1	chrIX	347114	A-G	I-V	4.2
AIM21	chrIX	361350	G-A	E-K	4.3
HSP150	chrX	120967	G-A	V-I	4.5
HAL5	chrX	108137	T-C	V-A	4.1
MPA43	chrXIV	180743	G-T	R-L	4.6
FOL1	chrXIV	165065; 165506; 165718; 165983; 166577; 166584	G-A; A-G; A-T; T-A; A-G; C-T	V-I; N-D; E-D; L-I; R-G; A-V	4.5
RTC4	chrXIV	168579	T-C	V-A	4.4
CAF120	chrXIV	113719	C-G	T-R	4.2
TEX1	chrXIV	170791	A-G	E-G	4
DSL1	chrXIV	159121; 159158; 159167	G-C; C-T; T-A	E-D; A-V; L-H	4.5
PRM1	chrXIV	111795	T-A	H-Q	4
SIP3	chrXIV	160631; 161278; 162495	G-C; T-C; G-T	A-P; M-T; L-F	4.6
PIK1	chrXIV	142664; 142665	G-A; G-A	G-S; G-D	4.2
YNL057W	chrXIV	516537	C-T	A-V	4.5
YNL277W-A	chrXIV	116758	G-A	G-E	4.5
POL2	chrXIV	154540	T-C	Y-H	5
TOF1	chrXIV	124765; 125950	G-A; G-A	G-D; G-E	4.6
YNL058C	chrXIV	516537	G-A	A-T	4.5
YIF1	chrXIV	147717	G-C	G-A	4.9
BOR1	chrXIV	119276; 119890	T-A; T-A	N-K; I-N	4.1
BNI1	chrXIV	130096; 132375	A-G; G-A	I-M; E-K	4.5
RAD50	chrXIV	176375; 177300; 178096; 178273	A-G; A-G; G-A; A-G	D-G; I-M; D-N; I-V	4.4
ATG2	chrXIV	191917	T-C	I-T	4.3
UBP2	chrXV	556317; 558129; 558498	A-G; A-T; C-T	D-G; D-V; T-I	5.8
MRPL23	chrXV	612124	G-A	R-K	5.7
IRC14	chrXV	580334	G-C	L-F	7.1
SFL1	chrXV	587207; 588023; 588410;	G-A; G-A;	E-L; V-M; Q-	7.8

		588537; 589133	C-T; T-C; A-G	x; L-P; T-A	
SPP2	chrXV	608819	A-T	K-M	5.6
AFI1	chrXV	568463; 569111	T-A; T-C	V-D; I-T	5.9
LEO1	chrXV	553519	A-C	K-N	4.1
MDM32	chrXV	607152; 607393	G-C; A-T	C-S; L-F	9
ARP8	chrXV	590261; 592239; 592386	T-A; G-A; G-A	D-E; G-E; G-D	6.7
SLP1	chrXV	625879	G-A	D-N	4.7
YOR139C	chrXV	587197; 587207	A-T; C-T	R-S; S-L	9.3
RUP1	chrXV	584519; 585809; 586077	G-A; A-G; T-A	E-K; T-A; D-E	7.3
PDR5	chrXV	619862	A-G	N-D	4
ADE2	chrXV	565892	A-G	R-G	4.7
RGA1	chrXV	562242; 562413; 563143; 563767	C-A; A-T; A-C; T-C	P-T; I-F; Y-S; V-A	5.5
SMP3	chrXV	609994; 610270; 610455; 610497	A-G; G-A; A-G; C-A	M-V; D-N; Q-R; T-N	4.9
BAG7	chrXV	578916	G-A	D-N	6
ORT1	chrXV	570760	A-G	I-V	5
CAT5	chrXV	559460	A-G	I-M	5.2
RIO1	chrXV	548996	G-A	G-R	4.9
SIA1	chrXV	581864	C-T	L-F	6.3
VPS17	chrXV	573249; 573359; 573378; 574379	A-G; A-G; A-G; G-A	D-G; I-V; E-G; A-T	5.5
ELG1	chrXV	603167; 603550; 604120; 604414; 604516; 604573; 604763; 604805	T-A; A-G; G-C; T-C; G-A; T-A; C-G; G-A	Y-N; E-G; S-T; V-A; R-H; F-Y; L-V; D-N	5.7
GCY1	chrXV	551235	A-G	T-A	4.1
BRR1	chrXVI	672812	G-C	E-D	4.1
OPI11	chrXVI	654754	G-A	G-S	4.2
RPL43A	chrXVI	654754	C-T	R-C	4.2
YPL277C	chrXVI	15418	G-C	R-P	4.4
YPR050C	chrXVI	665341	A-G	K-R	5.5
YPR045C	chrXVI	656529	C-A	H-Q	4.5
ATG11	chrXVI	662621; 663705	C-T; G-A	P-S; M-I	4.5

Table 2.4. Deletion mutants used in this study

Null mutant phenotypes with Sigma background

Gene	Chromosome	Invasive Phenotype
HPR1	IV	Invasive
DSE1	V	Invasive
SAK1	V	Invasive
PEA2	V	Decreased
YER121W	V	Invasive
YER046W-A	V	Invasive
YIR021W-A	IX	Decreased
CAT8	XIII	Invasive
DSK2	XIII	Invasive
CYT1	XV	Increased
RHO2	XIV	Decreased
YNL095C	XIV	Decreased
YNL092W	XIV	Invasive
APP1	XIV	Invasive
NIS1	XIV	Invasive
ICY2	XVI	Invasive

Null mutant phenotypes with SK1 background

Gene	Chromosome	Invasive Phenotype
SHO1	V	Decreased
BOI2	V	Invasive
HAL5	X	Decreased
MPA43	XIV	Decreased
GCY1	XV	Decreased
VPS17	XV	Decreased
SFL1	XV	Invasive
MDM32	XV	Decreased
MRPL23	XV	Decreased
IDH2	XV	Decreased
BRR1	XVI	Decreased

Reference

1. Gimeno CJ, Ljungdahl PO, Styles CA, Fink GR (1992) Unipolar cell divisions in the yeast S. cerevisiae lead to filamentous growth: regulation by starvation and RAS. Cell 68: 1077-1090.
2. Liu H, Styles C, Fink G (1993) Elements of the yeast pheromone response pathway required for filamentous growth of diploids. Science 262: 1741-1744.
3. Chandarlapaty S, Errede B (1998) Ash1, a Daughter Cell-Specific Protein, Is Required for Pseudohyphal Growth of Saccharomyces cerevisiae. Molecular and Cellular Biology 18: 2884-2891.
4. Erdman S, Snyder M (2001) A Filamentous Growth Response Mediated by the Yeast Mating Pathway. Genetics 159: 919-928.
5. Cullen PJ, Sprague GF (2012) The Regulation of Filamentous Growth in Yeast. Genetics 190: 23-49.
6. Lorenz MC, Cutler NS, Heitman J (2000) Characterization of alcohol-induced filamentous growth in Saccharomyces cerevisiae. Mol Biol Cell 11: 183-199.
7. Ma J, Jin R, Dobry CJ, Lawson SK, Kumar A (2007) Overexpression of Autophagy-Related Genes Inhibits Yeast Filamentous Growth. Autophagy 3: 604-609.
8. Starovoytova AN, Sorokin MI, Sokolov SS, Severin FF, Knorre DA (2013) Mitochondrial signaling in Saccharomyces cerevisiae pseudohyphae formation induced by butanol. FEMS Yeast Research 13: 367-374.
9. Cook JG, Bardwell L, Thorner J (1997) Inhibitory and activating functions for MAPK Kss1 in the S. cerevisiae filamentous-growth signalling pathway. Nature 390: 85-88.
10. Rupp S, Summers E, Lo HJ, Madhani H, Fink G (1999) MAP kinase and cAMP filamentation signaling pathways converge on the unusually large promoter of the yeast FLO11 gene. EMBO J 18: 1257-1269.
11. Hedbacker K, Carlson M (2008) SNF1/AMPK pathways in yeast. Front Biosci 13: 2408-2420.
12. Gagiano M, Van Dyk D, Bauer FF, Lambrechts MG, Pretorius IS (1999) Msn1p/Mss10p, Mss11p and Muc1p/Flo11p are part of a signal transduction pathway downstream of Mep2p regulating invasive growth and pseudohyphal differentiation in Saccharomyces cerevisiae. Molecular Microbiology 31: 103-116.
13. Peter M, Neiman AM, Park HO, van Lohuizen M, Herskowitz I (1996) Functional analysis of the interaction between the small GTP binding protein Cdc42 and the Ste20 protein kinase in yeast. EMBO J 15: 7046-7059.
14. Kataoka T, Powers S, McGill C, Fasano O, Strathern J, et al. (1984) Genetic analysis of yeast RAS1 and RAS2 genes. Cell 37: 437-445.

15. Mosch HU, Roberts RL, Fink GR (1996) Ras2 signals via the Cdc42/Ste20/mitogen-activated protein kinase module to induce filamentous growth in Saccharomyces cerevisiae. Proc Natl Acad Sci U S A 93: 5352-5356.
16. Abdullah U, Cullen PJ (2009) The tRNA Modification Complex Elongator Regulates the Cdc42-Dependent Mitogen-Activated Protein Kinase Pathway That Controls Filamentous Growth in Yeast. Eukaryotic Cell 8: 1362-1372.
17. Robertson LS, Fink GR (1998) The three yeast A kinases have specific signaling functions in pseudohyphal growth. Proceedings of the National Academy of Sciences 95: 13783-13787.
18. Pan X, Heitman J (1999) Cyclic AMP-dependent protein kinase regulates pseudohyphal differentiation in Saccharomyces cerevisiae. Mol Cell Biol 19: 4874-4887.
19. Robertson LS, Causton HC, Young RA, Fink GR (2000) The yeast A kinases differentially regulate iron uptake and respiratory function. Proc Natl Acad Sci U S A 97: 5984-5988.
20. Toda T, Cameron S, Sass P, Zoller M, Wigler M (1987) Three different genes in S. cerevisiae encode the catalytic subunits of the cAMP-dependent protein kinase. Cell 50: 277-287.
21. Kubler E, Mosch HU, Rupp S, Lisanti MP (1997) Gpa2p, a G-protein alpha-subunit, regulates growth and pseudohyphal development in Saccharomyces cerevisiae via a cAMP-dependent mechanism. J Biol Chem 272: 20321-20323.
22. Rupp S, Summers E, Lo H-J, Madhani H, Fink G (1999) MAP kinase and cAMP filamentation signaling pathways converge on the unusually large promoter of the yeast FLO11 gene. EMBO J 18: 1257-1269.
23. Vyas VK, Kuchin S, Berkey CD, Carlson M (2003) Snf1 kinases with different beta-subunit isoforms play distinct roles in regulating haploid invasive growth. Mol Cell Biol 23: 1341-1348.
24. Elbing K, McCartney RR, Schmidt MC (2006) Purification and characterization of the three Snf1-activating kinases of Saccharomyces cerevisiae. Biochem J 393: 797-805.
25. Borneman AR, Leigh-Bell JA, Yu H, Bertone P, Gerstein M, et al. (2006) Target hub proteins serve as master regulators of development in yeast. Genes & Development 20: 435-448.
26. Ahn SH, Acurio A, Kron SJ (1999) Regulation of G2/M progression by the STE mitogen-activated protein kinase pathway in budding yeast filamentous growth. Mol Biol Cell 10: 3301-3316.
27. Edgington NP, Blacketer MJ, Bierwagen TA, Myers AM (1999) Control of Saccharomyces cerevisiae filamentous growth by cyclin-dependent kinase Cdc28. Mol Cell Biol 19: 1369-1380.

28. Miled C, Mann C, Faye G (2001) Xbp1-Mediated Repression of CLB Gene Expression Contributes to the Modifications of Yeast Cell Morphology and Cell Cycle Seen during Nitrogen-Limited Growth. Molecular and Cellular Biology 21: 3714-3724.
29. Kron SJ, Styles CA, Fink GR (1994) Symmetric cell division in pseudohyphae of the yeast Saccharomyces cerevisiae. Mol Biol Cell 5: 1003-1022.
30. Jin R, Dobry CJ, McCown PJ, Kumar A (2008) Large-Scale Analysis of Yeast Filamentous Growth by Systematic Gene Disruption and Overexpression. Molecular Biology of the Cell 19: 284-296.
31. Sheu Y-J, Santos B, Fortin N, Costigan C, Snyder M (1998) Spa2p Interacts with Cell Polarity Proteins and Signaling Components Involved in Yeast Cell Morphogenesis. Molecular and Cellular Biology 18: 4053-4069.
32. van Drogen F, Peter M (2002) Spa2p Functions as a Scaffold-like Protein to Recruit the Mpk1p MAP Kinase Module to Sites of Polarized Growth. Current biology : CB 12: 1698-1703.
33. Lichius A, Yáñez-Gutiérrez ME, Read ND, Castro-Longoria E (2012) Comparative Live-Cell Imaging Analyses of SPA-2, BUD-6 and BNI-1 in *Neurospora crassa* Reveal Novel Features of the Filamentous Fungal Polarisome. PLoS ONE 7: e30372.
34. Lorenz MC, Heitman J (1998) Regulators of pseudohyphal differentiation in Saccharomyces cerevisiae identified through multicopy suppressor analysis in ammonium permease mutant strains. Genetics 150: 1443-1457.
35. Fichtner L, Schulze F, Braus GH (2007) Differential Flo8p-dependent regulation of FLO1 and FLO11 for cell–cell and cell–substrate adherence of S. cerevisiae S288c. Molecular Microbiology 66: 1276-1289.
36. Lo W-S, Dranginis AM (1998) The Cell Surface Flocculin Flo11 Is Required for Pseudohyphae Formation and Invasion by Saccharomyces cerevisiae. Molecular Biology of the Cell 9: 161-171.
37. Reynolds TB, Fink GR (2001) Bakers' yeast, a model for fungal biofilm formation. Science 291: 878-881.
38. Douglas LM, Li L, Yang Y, Dranginis AM (2007) Expression and characterization of the flocculin Flo11/Muc1, a Saccharomyces cerevisiae mannoprotein with homotypic properties of adhesion. Eukaryot Cell 6: 2214-2221.
39. Guo B, Styles CA, Feng Q, Fink GR (2000) A Saccharomyces gene family involved in invasive growth, cell-cell adhesion, and mating. Proc Natl Acad Sci U S A 97: 12158-12163.
40. Harris SD, Momany M (2004) Polarity in filamentous fungi: moving beyond the yeast paradigm. Fungal Genetics and Biology 41: 391-400.
41. Voynov V, Verstrepen KJ, Jansen A, Runner VM, Buratowski S, et al. (2006) Genes with internal repeats require the THO complex for transcription. Proc Natl Acad Sci U S A 103: 14423-14428.

42. Grossmann G, Malinsky J, Stahlschmidt W, Loibl M, Weig-Meckl I, et al. (2008) Plasma membrane microdomains regulate turnover of transport proteins in yeast. J Cell Biol 183: 1075-1088.
43. Alvarez FJ, Douglas LM, Rosebrock A, Konopka JB (2008) The Sur7 protein regulates plasma membrane organization and prevents intracellular cell wall growth in Candida albicans. Mol Biol Cell 19: 5214-5225.
44. Cullen PJ, Sprague GF, Jr. (2000) Glucose depletion causes haploid invasive growth in yeast. Proc Natl Acad Sci U S A 97: 13619-13624.
45. Santangelo GM (2006) Glucose signaling in Saccharomyces cerevisiae. Microbiol Mol Biol Rev 70: 253-282.
46. Aun A, Tamm T, Sedman J (2013) Dysfunctional Mitochondria Modulate cAMP-PKA Signaling and Filamentous and Invasive Growth of Saccharomyces cerevisiae. Genetics 193: 467-481.
47. Liu Z, Butow RA (2006) Mitochondrial Retrograde Signaling. Annual Review of Genetics 40: 159-185.
48. Goffeau A, Barrell BG, Bussey H, Davis RW, Dujon B, et al. (1996) Life with 6000 genes. Science 274: 546, 563-547.
49. Winzeler EA, Shoemaker DD, Astromoff A, Liang H, Anderson K, et al. (1999) Functional characterization of the S. cerevisiae genome by gene deletion and parallel analysis. Science 285: 901-906.
50. Giaever G, Shoemaker DD, Jones TW, Liang H, Winzeler EA, et al. (1999) Genomic profiling of drug sensitivities via induced haploinsufficiency. Nat Genet 21: 278-283.
51. Giaever G, Chu AM, Ni L, Connelly C, Riles L, et al. (2002) Functional profiling of the Saccharomyces cerevisiae genome. Nature 418: 387-391.
52. Bharucha N, Ma J, Dobry CJ, Lawson SK, Yang Z, et al. (2008) Analysis of the Yeast Kinome Reveals a Network of Regulated Protein Localization during Filamentous Growth. Molecular Biology of the Cell 19: 2708-2717.
53. Piccirillo S, Honigberg SM (2010) Sporulation patterning and invasive growth in wild and domesticated yeast colonies. Research in Microbiology 161: 390-398.
54. Baudin A, Ozier-Kalogeropoulos O, Denouel A, Lacroute F, Cullin C (1993) A simple and efficient method for direct gene deletion in Saccharomyces cerevisiae. Nucleic Acids Res 21: 3329-3330.
55. Gueldener U, Heinisch J, Koehler GJ, Voss D, Hegemann JH (2002) A second set of loxP marker cassettes for Cre-mediated multiple gene knockouts in budding yeast. Nucleic Acids Res 30: e23.
56. Birkeland SR, Jin N, Ozdemir AC, Lyons RH, Weisman LS, et al. (2010) Discovery of Mutations in Saccharomyces cerevisiae by Pooled Linkage Analysis and Whole-Genome Sequencing. Genetics 186: 1127-1137.
57. Alberti S, Gitler AD, Lindquist S (2007) A suite of Gateway® cloning vectors for high-throughput genetic analysis in Saccharomyces cerevisiae. Yeast 24: 913-919.

58. Bharucha N, Chabrier-Roselló Y, Xu T, Johnson C, Sobczynski S, et al. (2011) A Large-Scale Complex Haploinsufficiency-Based Genetic Interaction Screen in *Candida albicans*: Analysis of the RAM Network during Morphogenesis. PLoS Genet 7: e1002058.
59. Shively CA, Eckwahl MJ, Dobry CJ, Mellacheruvu D, Nesvizhskii A, et al. (2013) Genetic Networks Inducing Invasive Growth in Saccharomyces cerevisiae Identified Through Systematic Genome-Wide Overexpression. Genetics 193: 1297-1310.
60. Dimmer KS, Jakobs S, Vogel F, Altmann K, Westermann B (2005) Mdm31 and Mdm32 are inner membrane proteins required for maintenance of mitochondrial shape and stability of mitochondrial DNA nucleoids in yeast. The Journal of Cell Biology 168: 103-115.
61. Valtz N, Herskowitz I (1996) Pea2 protein of yeast is localized to sites of polarized growth and is required for efficient mating and bipolar budding. The Journal of Cell Biology 135: 725-739.
62. Mao K, Wang K, Liu X, Klionsky DJ (2013) The Scaffold Protein Atg11 Recruits Fission Machinery to Drive Selective Mitochondria Degradation by Autophagy. Developmental cell 26: 9-18.
63. Haber JE (2012) Mating-Type Genes and MAT Switching in Saccharomyces cerevisiae. Genetics 191: 33-64.
64. Bettinger BT, Clark MG, Amberg DC (2007) Requirement for the Polarisome and Formin Function in Ssk2p-Mediated Actin Recovery From Osmotic Stress in Saccharomyces cerevisiae. Genetics 175: 1637-1648.
65. Kang CM, Jiang YW (2005) Genome-wide survey of non-essential genes required for slowed DNA synthesis-induced filamentous growth in yeast. Yeast 22: 79-90.
66. Wang H, Jiang Y (2003) The Tap42-Protein Phosphatase Type 2A Catalytic Subunit Complex Is Required for Cell Cycle-Dependent Distribution of Actin in Yeast. Molecular and Cellular Biology 23: 3116-3125.

CHAPTER 3

The peripheral protein *YLR414C*/*PUN1* is required for filamentous growth in *S. cerevisiae*

3.1 Introduction

Under conditions of nitrogen stress, certain strains of *Saccharomyces cerevisiae* implement a dramatic change in growth form characterized by the development of multicellular pseudohyphal filaments[1-4]. In yeast, this form of filamentous growth is thought to constitute a foraging mechanism initiated under conditions of limited nutrient availability. During pseudohyphal growth, yeast cells delay in G_2/M, exhibit an elongated morphology, display an altered budding pattern, remain physically attached, and invade their growth medium[5-7]. The yeast cells also exhibit an altered pattern of budding in which daughter cells emerge from mother cells predominantly opposite the birth end, as opposed to the bipolar pattern of bud emergence observed in diploid cells under conditions of vegetative growth[8,9]. Thought to be a foraging mechanism, yeast filamentous growth has been studied extensively as a model for related hyphal growth transitions in the opportunistic human pathogen *Candida albicans*, where these growth transitions are required for virulence[9-12].

In *S. cerevisiae*, at least three signaling pathways regulate the initiation and maintenance of pseudohyphal growth: 1) the cyclic AMP-protein kinase A (PKA) pathway[13,14]; 2) the Kss1p mitogen-activated protein kinase (MAPK) cascade[15]; and 3) a pathway involving the 5′-AMP-activated protein kinase Snf1p[16,17]. During filamentous growth, nitrogen stress results in activation of the GTP-binding protein Ras2p, which acts upstream of both the PKA and MAPK signaling modules. Ras2p stimulates the adenylate cyclase Cyr1p, and the resulting increase in cAMP activates

Tpk2p, the catalytic subunit isoform of PKA[18,19]. Ras2p also acts through the G-protein Cdc42p and the p21-activated kinase Ste20p to initiate the MAPK cascade of Ste11p, Ste7p, and the MAPK Kss1p[20-22]. The Snf1p kinase is required for pseudohyphal growth and for growth on secondary carbon sources[23-25]. Snf1p is regulated by the kinase Sak1p during nitrogen signaling, and Snf1p pairs with its Gal83p β-subunit isoform to activate expression of downstream targets that enable pseudohyphal growth[17,26,27]. Recent genomic studies have identified additional signaling pathways and gene sets that contribute to yeast pseudohyphal growth, collectively indicating an extensive regulatory network controlling gene and protein activity during the filamentous growth transition.

Cell periphery proteins are a set of proteins located at the plasma membrane and cell wall[28-30]. They play critical roles in mediating cell-cell and cell-substrate adhesion, nutrient transport, and receptor-linked signaling events[31-34]. Previous studies have identified a group of cell periphery proteins that also contribute to filamentous growth in yeast. For example, the cell surface protein Flo11p is required for pseudohyphal growth, invasive growth, and biofilm formation in filamentous strains of *S. cerevisiae[33,35-37]*. *FLO11* expression is subject to extensive regulatory control. The PKA, Kss1p MAPK, and Snf1p pathways all regulate *FLO11* transcription, and epigenetic silencing through the histone deacetylase Hda1p further controls *FLO11* expression. Flo11p contributes to cell-substrate adhesion *in vivo*, exhibits homotypic adhesion *in vitro*, and is the only flocculin family member that is expressed in filamentous strains of *S. cerevisiae*. Other cell periphery proteins regulating filamentous growth include the membrane transporter Mep2p and the amino acid transporter homolog Ssy1p[32,38,39]. Therefore, proteins at the yeast cell periphery play critical roles in pseudohyphal growth. However, the mechanism through which protein composition at the plasma membrane and cell wall is differentially regulated during filamentation is still unclear. To address this, the Kumar laboratory initiated a global study of protein abundance profiles at the yeast cell periphery during filamentous growth.

In this study, quantitative proteomics was used to profile changes in protein abundance at the yeast cell periphery during pseudohyphal growth. For this work, plasma

membrane protein preparations were generated from yeast colonies under vegetative and filamentous growth conditions, and these samples were analyzed by mass spectrometry using isobaric iTRAQ reagents. Our analysis identified a set of proteins differentially abundant during pseudohyphal growth, revealing, in particular, an integral component of the plasma membrane compartment of Can1 (MCC)[40,41], Ylr414cp/Pun1p, which we found to be important for the pseudohyphal growth response. Ylr414cp/Pun1p, exhibits increased abundance under conditions of nitrogen stress and is required for wild-type filamentous growth and cell adhesion. *pun1Δ* mutants showed filamentous growth defects and mutant phenotypes in cell elongation, surface-spread colony filamentation and invasive growth on solid medium. Since Pun1p is a known member of the MCC, we further explored the function of other MCC proteins to identify any general role of the MCC during yeast filamentous growth. Overall, this work presents an informative data set of proteins that change abundance during pseudohyphal growth, while also identifying an essential, but previously unstudied role for a member of the MCC, *PUN1*, in the molecular events enabling the yeast filamentous growth transition.

3.2 Materials and Methods

3.2.1 Yeast Strains and Growth Conditions

All yeast strains were generated in the Σ1278b background. The genotype of haploid Y825 strain is *MATa ura3-52 leu2Δ0*; the genotype of the diploid Y825/6 strain is *ura3-52/ura3-52 leu2Δ0/ leu2Δ0[42,43]*. Haploid deletion mutants were constructed in strain Y825 by homologous recombination using the PCR-based strategy of Baudin *et al[44]*. Haploid mutants were independently constructed and mated to generate homozygous diploids. YLR414C was chromosomally tagged with the Venus variant of yellow fluorescent protein in Y825/6. Integrated alleles were generated by standard protocols using the vYFP-KanMX6 cassette from pBS7[45]. For co-localization analysis, MCC component genes were amplified by PCR; each open reading frame was amplified along with 1kb of upstream genomic DNA for induction into pDEST-mCherry[27]. Upon

cloning, the PCR product creates a transcriptional fusion between the 3' –end of the gene and mCherry.

Yeast strains were propagated on rich YPD medium or synthetic medium as described. Haploid filamentous growth was induced in standard medium (0.17% yeast nitrogen base without amino acids and ammonia, 2% glucose, and 5mM ammonium sulfate, with essential amino acids) supplemented with 1% butanol or on SLAD plate (0.17% yeast nitrogen base without amino acids and ammonium sulfate, 2% glucose, and 50μM ammonium sulfate, with essential amino acids) supplemented with 1% butanol[46]. Diploid filamentous growth was induced in liquid low nitrogen medium (0.17% yeast nitrogen base without amino acids and ammonia, 2% glucose, and 50μM ammonium sulfate, with essential amino acids) or on SLAD plates. Invasive growth was assayed on YPD medium (1% yeast extract, 2% polypeptone and 2% glucose).

3.2.2 Yeast Filamentous Growth Assay

Invasive growth of haploid strains was determined by the standard plate washing assay; mid-log phase cultures (5μL) were spotted onto YPD plates and incubated for 7 days at 30 °C[47], and surface cells were subsequently washed off under a gentle stream of water[48]. The mark on the plates was then photographed by BioRad gel document microscope. Colony morphology of deletion mutants was observed by streaking mid-log cultures grown in YPD onto SLAD plates (diploid strains) or SLAD supplemented with 1% butanol (haploid strains) and incubating at 30 °C for 10 days.

3.2.3 Yeast Microscopy

For fluorescence microscopy, overnight cultures were diluted to an absorbance (A_{600}) of 0.1 in synthetic medium lacking leucine. Yeast cells grown to an A_{600} of 0.6 were used for co-localization analysis. For assay of filamentous growth, cells were grown overnight, diluted to an A_{600} of 0.1, and grown in standard medium or inducing conditions as required. Filamentous growth in haploid strains was induced by inoculating

diluted cultures into standard growth medium supplemented with 1% butanol for 4h at 30°C. Diploid filamentous strains were induced as follows: overnight cultures were centrifuged, washed, and inoculated at an A_{600} of 0.1 in low nitrogen medium at 30°C for 4 hours before observation[42]. All images were taken on an upright Nikon Eclipse 80i microscope with a Cool SNAP E32 CCD (Photometrics, Tucson, AZ); and images were acquired by MetaMorph software package (Molecular Devices).

3.2.4 Plasma Membrane Protein Preparation

Plasma membrane proteins were prepared by cell fractionation on Renografin density gradients[49]. Around 17 A_{600} units of yeast cells were harvested from plates for each density gradient. Cells were then washed in Tris/EDTA buffer and treated with a mixture of protease inhibitors prior to cell lysis by vortexing with glass beads. After vortexing, the supernatant was reserved, and remaining unbroken cells were removed by centrifugation at 500g. The lysate was mixed with an equal volume of Renografin-76, Renocal-76, or Renografin-60 (Bracco Diagnostics, Inc., Princeton, NJ) and placed at the bottom of an SW 50.1 centrifuge tube. The lysate/Renografin mixture was overlaid with 2 volumes each of 34, 30, 26, and 22% Renografin prior to overnight centrifugation at 40,000 rpm. Following centrifugation, fractions from the top of the gradient were collected; the fractions were diluted with Tris/EDTA buffer, and Renografin was removed from these samples by centrifugation in an ultracentrifuge at 100,000*g* for 1 h.

3.3 Results

3.3.1 Identifying a set of differentially abundant proteins at the yeast cell periphery during pseudohyphal growth by mass spectrometry

To identify plasma membrane proteins that are differentially enriched during filamentous growth in yeast, a mass spectrometry-based approach was implemented

using differential isobaric tagging. In this study, we used a wild-type diploid strain Y825/6 that is derived from the Σ1278b genetic background. In most cases, standard *S. cerevisiae* strains don't undergo filamentous growth even under induction conditions. However, Σ1278b is able to perform an extensive and easily controlled transition from vegetative growth to filamentous growth, with the pseudohyphal growth response encompassing surface spread filamentation and invasive growth on solid medium. For this reason, Σ1278b is a preferred laboratory strain for studying filamentous growth. In this study, Y825/6 was plated on standard growth medium (SC complete medium with normal nitrogen concentration) and on pseudohypal growth induction medium (SC complete medium with low nitrogen concentration). Colonies were collected from standard medium and low nitrogen medium plates, and plasma membrane proteins were extracted using standard procedures. Sample proteins were tagged with isobaric reagents 114/115 for proteins harvested from cells under normal nitrogen conditions and reagent 116/117 for proteins harvested from cells under low nitrogen conditions. The different reagent tags will yield four uniquely reported ions (114-117) upon fragmentation in mass spectrometry[50,51]. Following mass spectrometry, the relative abundance of proteins in the vegetative and filamentous growth samples were determined (**Figure 3.1A**). Dr. Tao Xu, a former member of lab, performed most of this work in collaboration with Phil Andrews' laboratory.

In total, we analyzed 3968 peptides from plasma membrane samples and identified 2463 peptides, which correspond to 356 proteins. Among these possible identities, we discovered 65 plasma membrane proteins and 19 additional proteins that are localized to the yeast cell wall, cell periphery, and bud tips (**Figure 3.1B**). Moreover, this screen yields about 270 additional proteins that do not localize to the yeast cell periphery. These proteins were carried over in the plasma membrane preparations. This might be caused by the nature of the preparation procedures and by the similarities of these proteins to the plasma membrane proteins.

3.3.2 Plasma membrane protein Ylr414c/Pun1 mediates filamentous growth, cell growth and cell-cell adhesion

Among these 84 plasma membrane proteins, we identified a protein of unknown function, Ylr414c, which is localized in punctate patches in the MCC domain in the plasma membrane. Mass spectrometry analysis showed that Ylr414c was enriched 2.1-fold under pseudohyphal growth conditions as compared to vegetative growth conditions. The total ion confidence interval was 99.99%. To examine the functional significance of Ylr414c protein during filamentous growth, we generated homozygous diploid deletion mutants of *YLR414C* in the filamentous Σ1278b genetic background and assayed these mutants for filamentation. Under low nitrogen conditions, *ylr414cΔ/Δ* exhibits defects in surface spread pseudohyphal growth on solid agar plates, which phenotypically show smooth edges around the colonies, compared to the rough and irregular edges in the wild type filamentous strain (**Figure 3.2A**). This is the first result showing that Ylr414c is required for filamentous growth in *S. cerevisiae*.

To further define the role of *YLR414C* in enabling filamentous growth, we assayed a haploid *ylr414cΔ* mutant for surface spread filamentation, cell morphology, and invasive growth. Low nitrogen conditions can also trigger surface spread filamentation in haploids, and the phenotypic trait can be exaggerated upon addition of butanol or other short chain alcohols to low-nitrogen solid medium. The short-chain alcohols are end products of amino acid catabolism under nitrogen-deprivation conditions and likely mimics nitrogen stress. Deletion of *YLR414C* in a haploid strain of the filamentous Σ1278b genetic background results in the loss of surface spread filamentation on low nitrogen medium supplemented with 1% butanol (**Figure 3.2B**). Single cell morphological assays also show a more spherical cell morphology compared to the elongated, attached wild type pseudohyphal cells. Furthermore, the invasive wash assay shows that the *ylr414cΔ* mutant is defective in invasive growth on rich solid medium (**Figure 3.3**). Therefore, these results in combination indicate that *YLR414C* is required for haploid and diploid filamentous growth in *S. cerevisiae*. Because its protein abundance profile is increased during filamentation, we then named it *PUN1* (plasma membrane protein up-regulated during nitogen stress).

Most yeast filamentous strains, including Σ1278b and SK1, change their flocculation profile. Flocculation is calcium dependent cell-cell aggregation, and it is mediated by cell surface proteins referred to as flocculins. In both Σ1278b and SK1, *FLO11* is the only flocculin expressed on the cell membrane, and therefore, the Σ1278b and SK1 strains do not flocculate in the same manner as do non-filamentous yeast strains[37]. We discovered that the *ylr414cΔ* mutant in the Σ1278b genetic background sediments more slowly than the wild type Σ1278b strain and *flo11Δ* strains (**Figure 3.4**). Here we are not strictly assaying their flocculation function but rather their ability to sediment. This analysis still suggests that *YLR414C/PUN1* affects cell-cell adhesion in this strain. Furthermore, we examined whether *PUN1* can affect yeast cell growth under different conditions. We discovered that the homozygous diploid *pun1Δ* mutant exhibited a pronounced growth defect under conditions of nitrogen stress and a mild growth defect under conditions with normal nitrogen levels (**Figure 3.5**). This growth defect does not account for the observed filamentous growth phenotype, however, as the *pun1Δ* mutant is capable of forming colonies. In total, we found that *PUN1* is required for filamentous growth, cell-cell adhesion and cell growth in *S. cerevisiae*.

3.3.3 MCC domains are involved in yeast filamentous growth

MCC is an ergosterol-rich domain estimated to be about 300 nm in diameter, corresponding to sites of furrow-like invaginations of the plasma membrane. To date, the MCC consists of at least 9 proteins: 3 transporters with 12 predicted transmembrane domains each and 6 tetraspan proteins of unknown function (**Figure 3.6**). The MCC is known to represent a protective area within the plasma membrane controlling the turnover of transport proteins, although it may have additional unknown functions in other cell processes[52-54]. *PUN1* serves as a member of the MCC and is predicted to contain 4 transmembrane domains along with Fmp45, Ygr131w, Nce102, Sur7 and Ynl194c.

To determine the potential functions of MCC proteins in the yeast pseudohyphal growth response, we generated single deletion and overexpression mutants of each gene

encoding an MCC protein in strains of the Σ1278b genetic background and tested their phenotypes under filamentous induction conditions. Among the deletion mutants, we discovered that deletion mutants of *fur4,* encoding a uracil transporter, displayed loss of surface spread filamentation on low nitrogen supplemented with 1% butanol. Also, *FUR4* affects invasive filamentous growth because the *fur4Δ* mutant shows a defect in invasive growth on rich medium plates by the standard wash assay of Gimeno and colleagues[48]. To assay filamentous growth phenotypes resulting from overexpression, we cloned 8 ORFs of corresponding MCC genes into overexpression plasmids under control of the galactose-inducible promoter GAL1, and transformed these overexpression Gal plasmids into diploid strains of the Σ1278b genetic background. Strains were grown in low-nitrogen medium with galactose rather than glucose as carbon source. Overexpression of *TAT2[53]* resulted in exaggerated cell elongation and invasive growth, while overexpression of the remaining MCC genes yielded wild type cell and colony morphology (**Figure 3.7**). In total, these phenotypic results do not indicate an overall function for the MCC during pseudohyphal growth, but rather highlight the importance of specific MCC transporters and components in enabling the wild type filamentous growth response.

To study the localization of *PUN1* in yeast filamentous growth strains, we constructed a plasmid where the carboxy terminus of *PUN1* was fused with the Venus variant of yellow fluorescent protein and transformed the plasmid into strains of the Σ1278b genetic background. The subcellular localization of Pun1p-vYFP did not change in low-nitrogen medium supplemented with 1% butanol. The protein was primarily found localized in punctate patches at the plasma membrane. We subsequently co-localized Pun1p with other known components of the MCC to explore the spatial relationship of these proteins during pseudohyphal growth. The Sur7, Fmp45, and Ynl194c proteins were tagged with mCherry in chromosomes, and these strains were transformed with the Pun1p-vYFP plasmid. The results showed that Pun1p-vYFP co-localized with the other MCC components under filamentous growth conditions (**Figure 3.8**). Therefore, the MCC is very likely intact during pseudohyphal growth and houses Pun1p in both filamentous and non-filamentous stains.

3.4. Discussion

In this study, we tried to identify potential plasma membrane proteins involved in filamentous growth in *S. cerevisiae* by applying a mass spectrometry-based approach. By isobaric tagging of plasma membrane proteins with unique reagents, we were able to detect proteins that are differentially enriched during various filamentous growth stages. In total, we discovered 11 proteins that are differentially abundant under conditions of nitrogen stress and have been localized to the yeast cell periphery. Among these proteins, we were interested in a protein of unknown function localized to the MCC domain, Ylr414c. Deletion mutants of *YLR414C* in both haploid and diploid strains showed defects in surface spread filamentation, invasive growth on solid medium, cell-cell adhesion and cell growth under conditions of nitrogen stress. Overexpression of *YLR414C* results in exaggerated cell elongation, although invasive growth properties are not appreciably increased over wild type. These results indicate that *YLR414C* is required for wild type filamentous growth in yeast. Thus, we renamed the gene as *PUN1*. We further analyzed other proteins within the MCC domain to identify a general function for this compartment during pseudohyphal growth. From this work, we identified a phenotypic link between *TAT2* and *FUR4* and filamentous growth. Deletion mutants of *fur4* show a loss of surface-spread filamentation and invasive growth. Overexpression of *TAT2* resulted in exaggerated cell elongation. Moreover, we confirmed that the MCC domain does not change in a filamentous growth strain under conditions of nitrogen stress. Overall, this work profiles changes in protein abundance at the yeast cell periphery during filamentous growth and identifies a previously uncharacterized gene that is required for the wild type yeast filamentous response to nitrogen stress.

PUN1 is known as a component of the MCC domain, and it shares sequence similarity among *Candida glabrata*, *Emericella nidulans* and several other fungi. We discovered that *PUN1* is required for pseudohyphal growth in a filamentous strain of *S. cerevisiae*. Its function in other filamentous fungi is still unknown. Further studies in the Kumar laboratory of transcriptional profiles from deletion mutants of *PUN1* have unveiled 82 genes that exhibit increased transcript abundance and 48 genes that yield

decreased mRNA levels. In particular, the genes exhibiting decreased mRNA levels upon *PUN1* deletion were significantly enriched in genes contributing to amino acid biosynthesis. The up-regulated genes were enriched for genes known to contribute to nitrogen-stress responses in yeast. These results suggest that *PUN1* contributes to nitrogen stress through signaling pathways that regulate the expression of genes involved in amino acid biosynthesis. It is well known that nitrogen stress triggers a series of cellular response enabling cells to cope with conditions of nutrient limitation. These responses include changes in amino acid synthesis, mRNA transcription and protein translation. It is not surprising then that *PUN1* plays a role in mechanisms of amino acid biosynthesis. In total, *PUN1* may be characterized as part of the yeast cell response to environmental stress, rather than as strictly a filamentous growth component. *PUN1* mRNA levels are increased in a non-filamentous strain of *S. cerevisiae* under nitrogen stress, and *PUN1* transcripts also increase upon cell wall damage[55]. Deletion mutants for *PUN1* also exhibit impaired thermotolerance[56]. Collectively, this evidence suggests that *PUN1* may play a general role in the cell response to environment stress.

PUN1 is known as one of the components of the MCC domain. The MCC represents a protective area within the plasma membrane to control the turnover of transport proteins[53]. We discovered that several components of the MCC domain were also required for filamentous growth in yeast. *TAT2* and *FUR4* are amino acid transporters, while Fur4p transports uracil, and Tat2p transports tryptophan and tyrosine. This result is consistent with the general understanding that amino acid sensors and transporters play an important role in regulating filamentous growth in yeast. For example, the ammonium permease Mep2p is a known sensor of ammonium availability, exhibiting both transport functions and a regulatory role affecting the filamentous growth MAPK pathway. Therefore, the general function of the MCC domain is worthy exploring in the context of filamentous growth.

Although we confirmed that *PUN1* is linked to filamentous growth, the particular function of Pun1p is still unknown. We speculate that Pun1p may act as a transporter, as does Mep2p, Tat2p and Fur4p. However, our initial characterization has failed to identify the function of *PUN1* in amino acid transport, and additional studies will be

necessary to identify the molecular function of Pun1p. Nevertheless, this study identifies a new component required for filamentous growth and sheds light upon the potential additional function of the MCC domain in cell stress responses, with a particular emphasis on its role in the yeast pseudohyphal growth response.

3.5 Acknowledgements

We thank Damian Krysan (University of Rochester) and Robert Fuller (University of Michigan) for providing filamentous yeast strains. Mass spectrometry was performed at the Michigan Proteome Consortium in the Andrews laboratory (University of Michigan). We thank John Strahler and Angela Walker for assistance with the generation and analysis of mass spectrometry data.

Figure 3.1. Mass spectrometric analysis of yeast plasma membrane protein preparations under vegetative and filamentous growth conditions. ***A***, overview of steps in generating yeast plasma membrane protein preparations for isobaric labeling and mass spectrometry. A diploid strain was growth on solid medium to enable the full pseudohyphal response prior to plasma membrane protein extraction and mass spectrometry. *WT*, wild type; *LC MALDI-TOF*, liquid chromatography matrix-assisted laser desorption ionization time of flight. ***B***, summary of data from iTRAQ-based mass spectrometry. In total, 356 proteins were profiled, and within this set, proteins that localize to the indicated regions at the cell periphery are tallied in the rectangular inset.

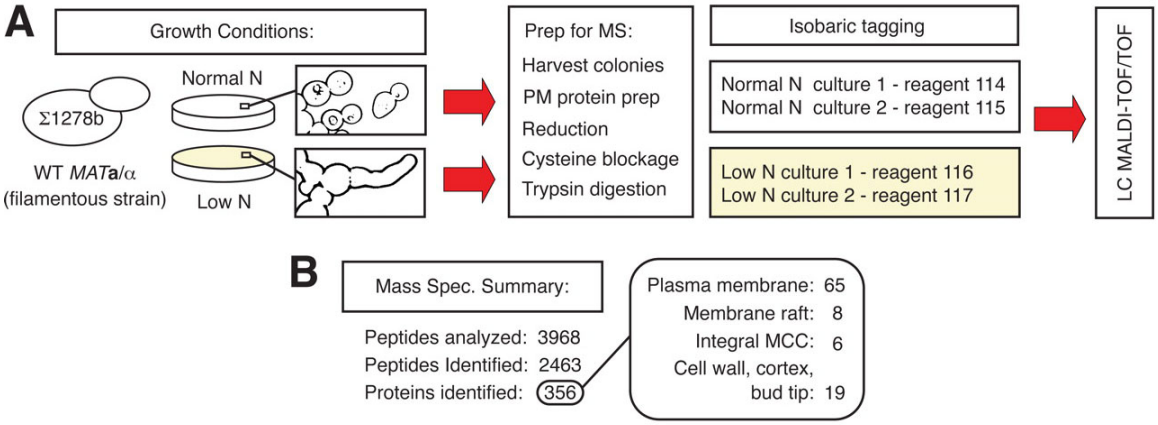

Figure 3.2. Surface-spread filamentation of *YLR414C*. *A,* colony morphology of homozygous diploid mutant of *YLR414C*. Yeast cells were grown on low ammonium medium (SLAD), and surface-spread filamentation was assessed. As indicated, *ylr414cΔ/Δ* exhibit defects in pseudohyphal growth on SLAD plates. ***B*,** haploid strain deleted for *YLR414C* exhibit reduced surface-spread filamentation, a loss of elongated cell morphology in SLAD medium supplemented with 1% butanol.

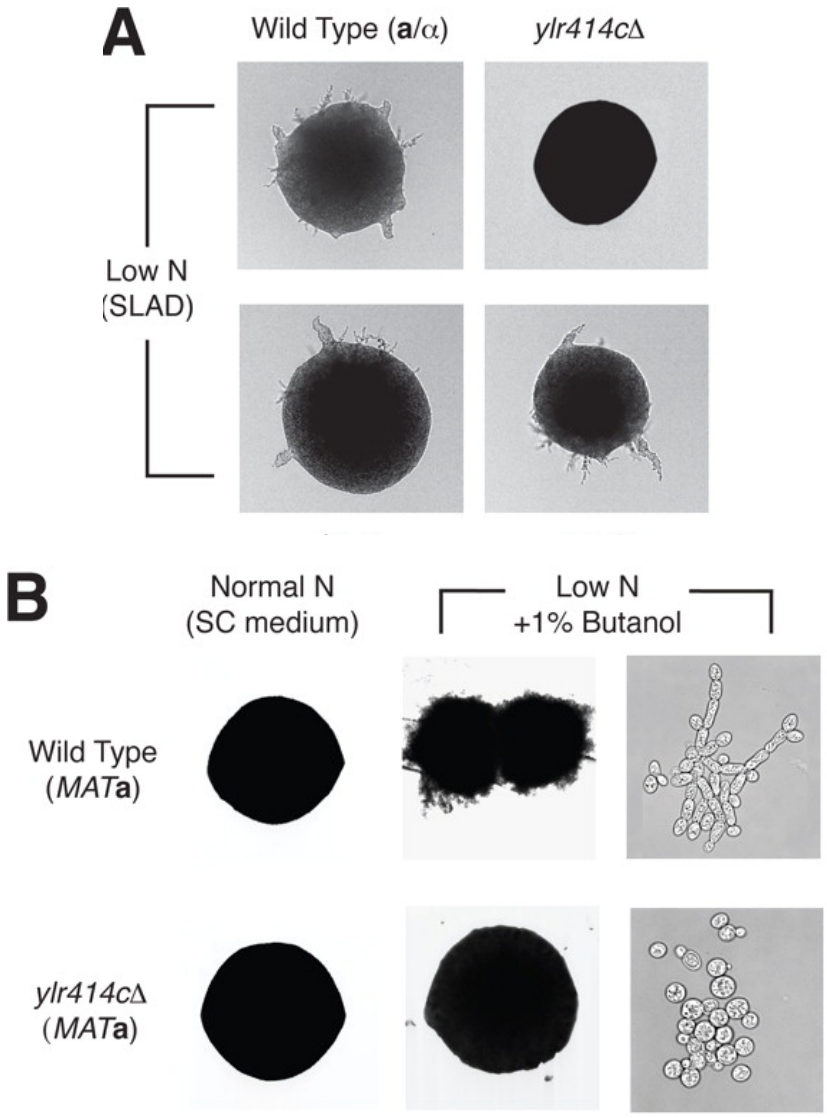

Figure 3.3. Invasive growth analysis of *YLR414C*. Reduced invasive growth, with the latter phenotype assessed by washing the plate surface under a gentle stream of water. Filamentous growth was induced in the haploid strain on low nitrogen plates supplemented with 1% butanol; cells from these colonies were scraped into a suspension in identical liquid media for analysis of cell morphology by differential interference contrast microscopy (see figure 3.2B).

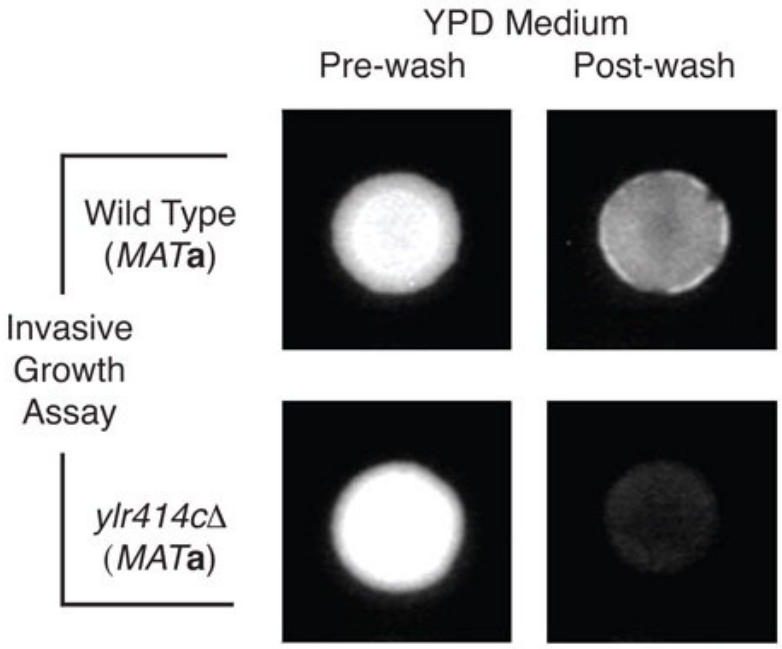

Figure 3.4. Sedimentation analysis of *YLR414C*. Haploid strain deleted for *YLR414C* sediments more slowly than a corresponding wild-type (*WT*) strain and haploid muc1Δ mutant. Dashed lines indicate levels of cells in test tube cultures. Normalized cultures of wild-type, *ylr414cΔ*, and *muc1Δ* cells were initially mixed and allowed to settle for 1 hour prior to imaging. To quantify the observed changes in cell sedimentation, a 1ml aliquot was withdrawn from the upper half of each test tube culture for determination of cell density of OD_{600}. Results from here measurement of independent biological replicates are shown to the bottom, and the increased cell density indicates decreased cell sedimentation.

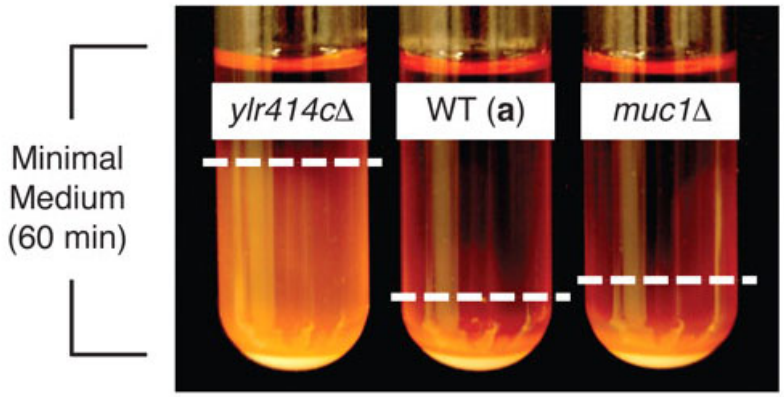

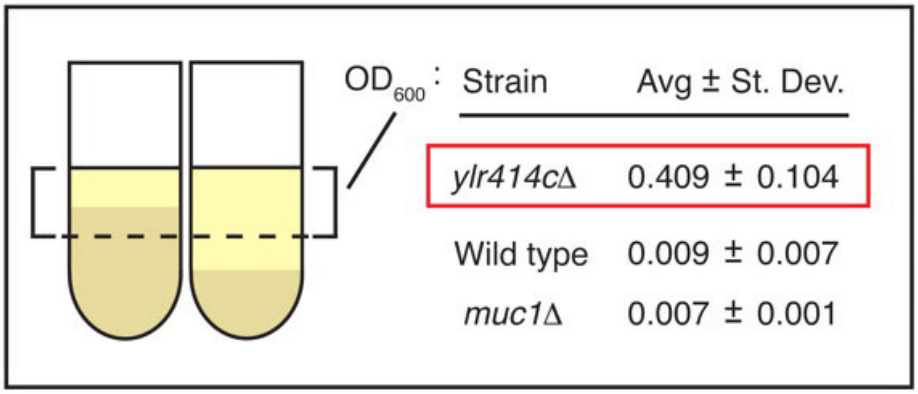

Figure 3.5. *ylr414cΔ* has growth defect. Homozygous diploid deleted for *ylr414c* exhibits a growth defect relative to wild type. As shown, the indicated cultures were normalized to OD_{600} 3.0 and serially diluted 5-fold onto normal (top) and low nitrogen (bottom) media. Concentrations at which differential growth is evident are boxed in red. The observed defect is more pronounced under conditions of nitrogen stress but evident under normal conditions in the filamentous Σ1278b strain as well.

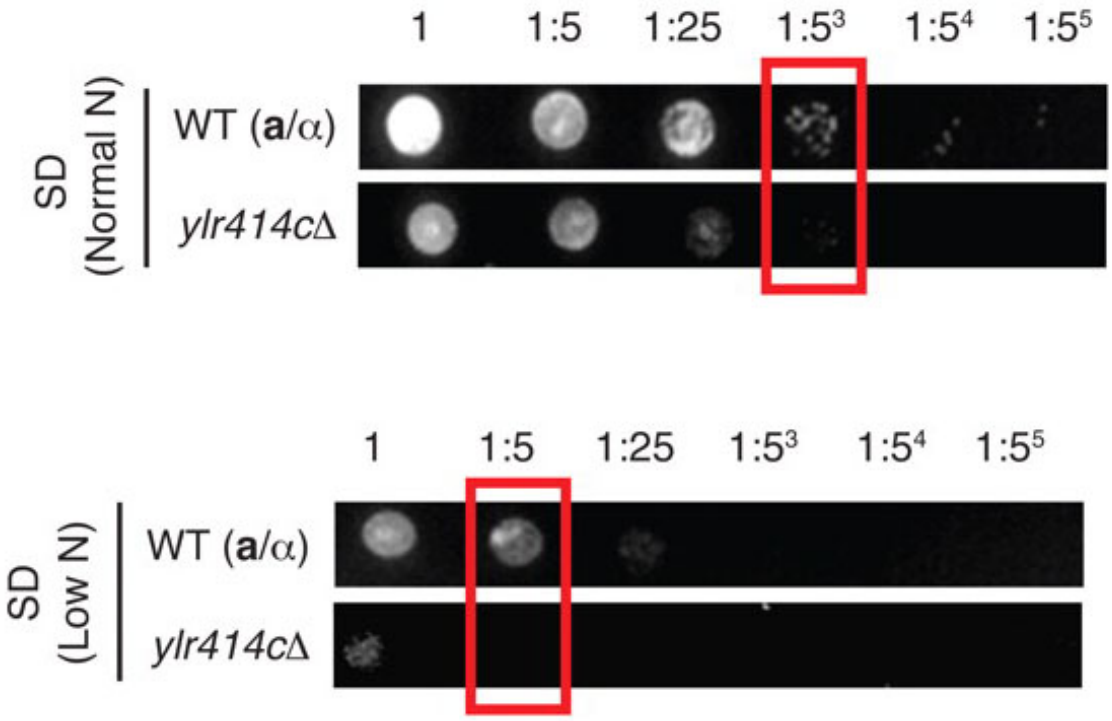

Figure 3.6. A diagrammatic overview of MCC plasma membrane subdomain. The MCC contains nine integral membrane proteins with either 4 or 12 predicted transmembrane domains (TMD). As predicted, Ylr414cp has four transmembrane domains. Can1p, Fur4p and Tat2p have 12 transmembrane domains.

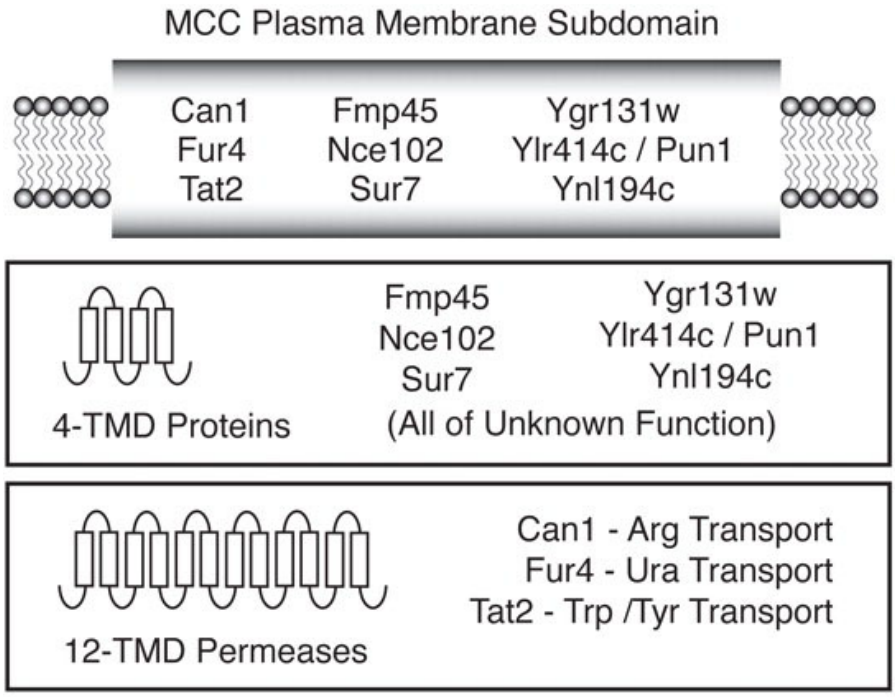

Figure 3.7. Phenotypic analysis of MCC proteins under filamentous growth conditions. Haploid deletion mutants were constructed in the filamentous Σ1278b background for all genes encoding plasma membrane proteins localized to the MCC. Colony morphology was assessed qualitatively under conditions that induce filamentous growth; results are summarized in the rectangular inset ("-" indicates reduced filamentous growth and "+" indicates wild type surface-spread filamentation), and an images of the surface-spread filamentation detect in *fur4Δ* was shown; and the known nonfilamentation *tec1Δ* mutant is shown as negative control. Cell morphology phenotypes upon gene overexpression are indicated in the lower panel. Plasmids carrying MCC component genes under transcriptional control of a galactose-inducible promoter were introduced into a diploid derivative of the filamentous Σ1278b strain, and the cell morphology are assessed upon galactose induction under conditions that induce filamentous growth. The results are summarized below ("+++" and "++" indicate exaggerated filamentous growth). The wild type strain for the control was transformed with empty vector pRS426.

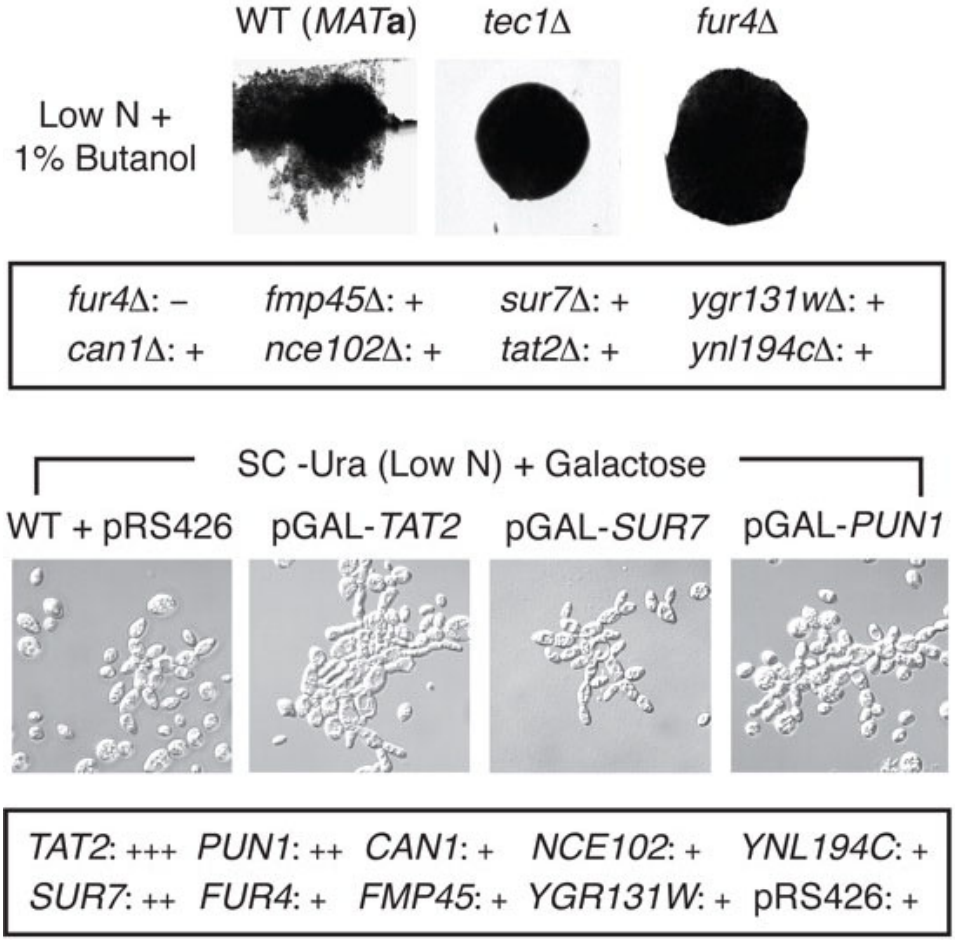

Figure 3.8. Localization of MCC proteins with filamentous Σ1278b genetic background strain under filamentous growth conditions. Localization of *Ylr414c* in the strain with Σ1278b genetic background was revealed using Ylr414c-vYFP fusion protein. The localization of Ylr414cp and other MCC component proteins is unchanged under filamentous growth conditions. Ylr414cp-vYFP localizes in punctate patches at the plasma membrane, consistent with the MCC domain, and co-localizes with Sur7p-mCherry, Fmp45p-mCherry, and Ynl194cp-mCherry under filamentous growth conditions.

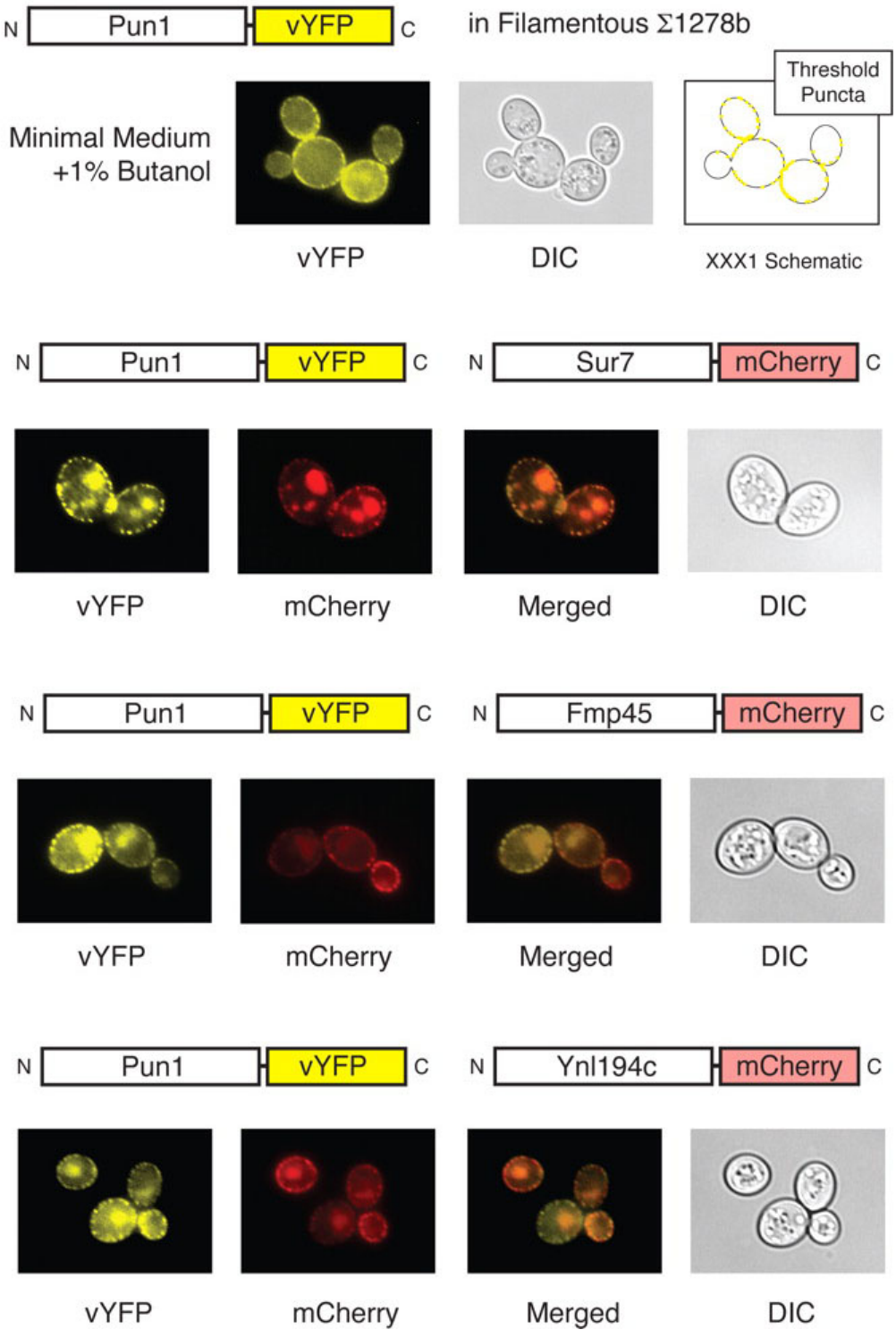
N
Pun1
vYFP
C
in Filamentous Σ1278b
Minimal Medium
+1% Butanol
Threshold
Puncta
vYFP
DIC
XXX1 Schematic
N
Pun1
vYFP
C
N
Sur7
mCherry
C
vYFP
mCherry
Merged
DIC
N
Pun1
vYFP
C
N
Fmp45
mCherry
C
vYFP
mCherry
Merged
DIC
N
Pun1
vYFP
C
N
Ynl194c
mCherry
C
vYFP
mCherry
Merged
DIC

Reference

1. Gimeno CJ, Ljungdahl PO, Styles CA, Fink GR (1992) Unipolar cell divisions in the yeast S. cerevisiae lead to filamentous growth: regulation by starvation and RAS. Cell 68: 1077-1090.
2. Liu H, Styles C, Fink G (1993) Elements of the yeast pheromone response pathway required for filamentous growth of diploids. Science 262: 1741-1744.
3. Chandarlapaty S, Errede B (1998) Ash1, a Daughter Cell-Specific Protein, Is Required for Pseudohyphal Growth of Saccharomyces cerevisiae. Molecular and Cellular Biology 18: 2884-2891.
4. Erdman S, Snyder M (2001) A Filamentous Growth Response Mediated by the Yeast Mating Pathway. Genetics 159: 919-928.
5. Ahn SH, Acurio A, Kron SJ (1999) Regulation of G2/M progression by the STE mitogen-activated protein kinase pathway in budding yeast filamentous growth. Mol Biol Cell 10: 3301-3316.
6. Edgington NP, Blacketer MJ, Bierwagen TA, Myers AM (1999) Control of Saccharomyces cerevisiae filamentous growth by cyclin-dependent kinase Cdc28. Mol Cell Biol 19: 1369-1380.
7. Miled C, Mann C, Faye G (2001) Xbp1-Mediated Repression of CLB Gene Expression Contributes to the Modifications of Yeast Cell Morphology and Cell Cycle Seen during Nitrogen-Limited Growth. Molecular and Cellular Biology 21: 3714-3724.
8. Kron SJ, Styles CA, Fink GR (1994) Symmetric cell division in pseudohyphae of the yeast Saccharomyces cerevisiae. Mol Biol Cell 5: 1003-1022.
9. Berman J, Sudbery PE (2002) Candida Albicans: a molecular revolution built on lessons from budding yeast. Nat Rev Genet 3: 918-930.
10. Csank C, Makris C, Meloche S, Schroppel K, Rollinghoff M, et al. (1997) Derepressed hyphal growth and reduced virulence in a VH1 family-related protein phosphatase mutant of the human pathogen Candida albicans. Mol Biol Cell 8: 2539-2551.
11. Kelly MT, MacCallum DM, Clancy SD, Odds FC, Brown AJ, et al. (2004) The Candida albicans CaACE2 gene affects morphogenesis, adherence and virulence. Mol Microbiol 53: 969-983.
12. Berman J (2006) Morphogenesis and cell cycle progression in Candida albicans. Curr Opin Microbiol 9: 595-601.
13. Pan X, Heitman J (1999) Cyclic AMP-Dependent Protein Kinase Regulates Pseudohyphal Differentiation in Saccharomyces cerevisiae. Molecular and Cellular Biology 19: 4874-4887.

14. Aun A, Tamm T, Sedman J (2013) Dysfunctional Mitochondria Modulate cAMP-PKA Signaling and Filamentous and Invasive Growth of Saccharomyces cerevisiae. Genetics 193: 467-481.
15. Rupp S, Summers E, Lo HJ, Madhani H, Fink G (1999) MAP kinase and cAMP filamentation signaling pathways converge on the unusually large promoter of the yeast FLO11 gene. EMBO J 18: 1257-1269.
16. Kuchin S, Vyas VK, Carlson M (2002) Snf1 Protein Kinase and the Repressors Nrg1 and Nrg2 Regulate FLO11, Haploid Invasive Growth, and Diploid Pseudohyphal Differentiation. Molecular and Cellular Biology 22: 3994-4000.
17. Vyas VK, Kuchin S, Berkey CD, Carlson M (2003) Snf1 Kinases with Different β-Subunit Isoforms Play Distinct Roles in Regulating Haploid Invasive Growth. Molecular and Cellular Biology 23: 1341-1348.
18. Mosch HU, Roberts RL, Fink GR (1996) Ras2 signals via the Cdc42/Ste20/mitogen-activated protein kinase module to induce filamentous growth in Saccharomyces cerevisiae. Proc Natl Acad Sci U S A 93: 5352-5356.
19. Kubler E, Mosch HU, Rupp S, Lisanti MP (1997) Gpa2p, a G-protein alpha-subunit, regulates growth and pseudohyphal development in Saccharomyces cerevisiae via a cAMP-dependent mechanism. J Biol Chem 272: 20321-20323.
20. Peter M, Neiman AM, Park HO, van Lohuizen M, Herskowitz I (1996) Functional analysis of the interaction between the small GTP binding protein Cdc42 and the Ste20 protein kinase in yeast. EMBO J 15: 7046-7059.
21. Cook JG, Bardwell L, Thorner J (1997) Inhibitory and activating functions for MAPK Kss1 in the S. cerevisiae filamentous-growth signalling pathway. Nature 390: 85-88.
22. Abdullah U, Cullen PJ (2009) The tRNA modification complex elongator regulates the Cdc42-dependent mitogen-activated protein kinase pathway that controls filamentous growth in yeast. Eukaryot Cell 8: 1362-1372.
23. Carlson M, Osmond BC, Botstein D (1981) Genetic evidence for a silent SUC gene in yeast. Genetics 98: 41-54.
24. Celenza JL, Carlson M (1984) Structure and expression of the SNF1 gene of Saccharomyces cerevisiae. Mol Cell Biol 4: 54-60.
25. Celenza JL, Carlson M (1984) Cloning and genetic mapping of SNF1, a gene required for expression of glucose-repressible genes in Saccharomyces cerevisiae. Mol Cell Biol 4: 49-53.
26. Elbing K, McCartney RR, Schmidt MC (2006) Purification and characterization of the three Snf1-activating kinases of Saccharomyces cerevisiae. Biochem J 393: 797-805.
27. Ma J, Jin R, Dobry CJ, Lawson SK, Kumar A (2007) Overexpression of Autophagy-Related Genes Inhibits Yeast Filamentous Growth. Autophagy 3: 604-609.

28. Sarma NJ, Yaseen NR (2013) Dynein Light Chain 1 (DYNLT1) Interacts with Normal and Oncogenic Nucleoporins. PLoS One 8: e67032.
29. Bendezu FO, Martin SG (2013) Cdc42 explores the cell periphery for mate selection in fission yeast. Curr Biol 23: 42-47.
30. Gonzalez-Sandoval A, Towbin BD, Gasser SM (2013) The formation and sequestration of heterochromatin during development: delivered on 7 September 2012 at the 37th FEBS Congress in Sevilla, Spain. FEBS J 280: 3212-3219.
31. Lorenz MC, Heitman J (1998) The MEP2 ammonium permease regulates pseudohyphal differentiation in Saccharomyces cerevisiae. EMBO J 17: 1236-1247.
32. Lorenz MC, Heitman J (1998) Regulators of pseudohyphal differentiation in Saccharomyces cerevisiae identified through multicopy suppressor analysis in ammonium permease mutant strains. Genetics 150: 1443-1457.
33. Lo W-S, Dranginis AM (1998) The Cell Surface Flocculin Flo11 Is Required for Pseudohyphae Formation and Invasion by Saccharomyces cerevisiae. Molecular Biology of the Cell 9: 161-171.
34. Guo B, Styles CA, Feng Q, Fink GR (2000) A Saccharomyces gene family involved in invasive growth, cell–cell adhesion, and mating. Proceedings of the National Academy of Sciences 97: 12158-12163.
35. Gagiano M, Van Dyk D, Bauer FF, Lambrechts MG, Pretorius IS (1999) Msn1p/Mss10p, Mss11p and Muc1p/Flo11p are part of a signal transduction pathway downstream of Mep2p regulating invasive growth and pseudohyphal differentiation in Saccharomyces cerevisiae. Molecular Microbiology 31: 103-116.
36. Fichtner L, Schulze F, Braus GH (2007) Differential Flo8p-dependent regulation of FLO1 and FLO11 for cell–cell and cell–substrate adherence of S. cerevisiae S288c. Molecular Microbiology 66: 1276-1289.
37. Douglas LM, Li L, Yang Y, Dranginis AM (2007) Expression and characterization of the flocculin Flo11/Muc1, a Saccharomyces cerevisiae mannoprotein with homotypic properties of adhesion. Eukaryot Cell 6: 2214-2221.
38. Ramsook CB, Tan C, Garcia MC, Fung R, Soybelman G, et al. (2010) Yeast cell adhesion molecules have functional amyloid-forming sequences. Eukaryot Cell 9: 393-404.
39. Forsberg H, Hammar M, Andreasson C, Moliner A, Ljungdahl PO (2001) Suppressors of ssy1 and ptr3 null mutations define novel amino acid sensor-independent genes in Saccharomyces cerevisiae. Genetics 158: 973-988.
40. Douglas LM, Wang HX, Li L, Konopka JB (2011) Membrane Compartment Occupied by Can1 (MCC) and Eisosome Subdomains of the Fungal Plasma Membrane. Membranes (Basel) 1: 394-411.

41. Stradalova V, Stahlschmidt W, Grossmann G, Blazikova M, Rachel R, et al. (2009) Furrow-like invaginations of the yeast plasma membrane correspond to membrane compartment of Can1. J Cell Sci 122: 2887-2894.
42. Bharucha N, Ma J, Dobry CJ, Lawson SK, Yang Z, et al. (2008) Analysis of the Yeast Kinome Reveals a Network of Regulated Protein Localization during Filamentous Growth. Molecular Biology of the Cell 19: 2708-2717.
43. Jin R, Dobry CJ, McCown PJ, Kumar A (2008) Large-Scale Analysis of Yeast Filamentous Growth by Systematic Gene Disruption and Overexpression. Molecular Biology of the Cell 19: 284-296.
44. Baudin A, Ozier-Kalogeropoulos O, Denouel A, Lacroute F, Cullin C (1993) A simple and efficient method for direct gene deletion in Saccharomyces cerevisiae. Nucleic Acids Res 21: 3329-3330.
45. Nagai T, Ibata K, Park ES, Kubota M, Mikoshiba K, et al. (2002) A variant of yellow fluorescent protein with fast and efficient maturation for cell-biological applications. Nat Biotechnol 20: 87-90.
46. Lorenz MC, Cutler NS, Heitman J (2000) Characterization of alcohol-induced filamentous growth in Saccharomyces cerevisiae. Mol Biol Cell 11: 183-199.
47. Shively CA, Eckwahl MJ, Dobry CJ, Mellacheruvu D, Nesvizhskii A, et al. (2013) Genetic Networks Inducing Invasive Growth in Saccharomyces cerevisiae Identified Through Systematic Genome-Wide Overexpression. Genetics 193: 1297-1310.
48. Gimeno CJ, Ljungdahl PO, Styles CA, Fink GR (1992) Unipolar cell divisions in the yeast S. cerevisiae lead to filamentous growth: Regulation by starvation and RAS. Cell 68: 1077-1090.
49. Chang A (2002) Plasma membrane biogenesis. Methods Enzymol 351: 339-350.
50. Gingras AC, Aebersold R, Raught B (2005) Advances in protein complex analysis using mass spectrometry. J Physiol 563: 11-21.
51. Ranish JA, Yi EC, Leslie DM, Purvine SO, Goodlett DR, et al. (2003) The study of macromolecular complexes by quantitative proteomics. Nat Genet 33: 349-355.
52. Young ME, Karpova TS, Brugger B, Moschenross DM, Wang GK, et al. (2002) The Sur7p family defines novel cortical domains in Saccharomyces cerevisiae, affects sphingolipid metabolism, and is involved in sporulation. Mol Cell Biol 22: 927-934.
53. Grossmann G, Malinsky J, Stahlschmidt W, Loibl M, Weig-Meckl I, et al. (2008) Plasma membrane microdomains regulate turnover of transport proteins in yeast. J Cell Biol 183: 1075-1088.
54. Alvarez FJ, Douglas LM, Rosebrock A, Konopka JB (2008) The Sur7 protein regulates plasma membrane organization and prevents intracellular cell wall growth in Candida albicans. Mol Biol Cell 19: 5214-5225.

55. Rodriguez-Pena JM, Perez-Diaz RM, Alvarez S, Bermejo C, Garcia R, et al. (2005) The 'yeast cell wall chip' - a tool to analyse the regulation of cell wall biogenesis in Saccharomyces cerevisiae. Microbiology 151: 2241-2249.
56. Mir SS, Fiedler D, Cashikar AG (2009) Ssd1 is required for thermotolerance and Hsp104-mediated protein disaggregation in Saccharomyces cerevisiae. Mol Cell Biol 29: 187-200

Chapter 4

Haploinsufficiency Based Genetic Interaction Screening in *Candida albicans*

4.1 Introduction

Candida albicans is a member of the resident flora of the gastrointestinal tract and is the most common fungal pathogen in humans[1-3]. The most severe manifestations of candidiasis occur in immunocompromised patients and include debilitating mucosal disease such as oropharyngeal candidiasis as well as life-threatening disseminated infections of the bloodstream and major organ systems. Candida infections are difficult to treat. Even with first-line antifungal therapy, candidiasis has an associated mortality of up to 50% in some patient populations[4,5]. Common treatment generally involves the administration of fluconazole or itraconazole. However, the recurrent nature of the disease leads to the development of antifungal-resistance *C. albicans*. Therefore, *C. albicans* is an important organism to study, both from a medical and biological perspective. Animal studies have shown that the pathogenic potential of *C. albicans* is associated with its ability to transition between three morphological states: yeast, pseudohyphae, and hyphae[6-8]. Further insights into the contributions of the different morphotypes to pathogenesis have emerged from studies with *C. albicans* strains that allow the conditional induction of filamentation *in vivo*.

C. albicans is known to exist in multiple growth forms: yeast, pseudohyphal and true hyphal form. Morphogenesis is triggered by a number of environmental factors, such as temperature, pH value and nutrition supply. It is commonly understood that the virulence of *C. albicans* is associated with its ability to switch between yeast and hyphal growth. However, this relationship is not a simple one. One line of evidence is that

deletion of *C. albicans ACE2* results in defects in cell separation, increased invasion of solid agar medium and inappropriate pseudohyphal growth[9]. The *ACE2* deletion strain is also avirulent in a mouse model. In addition, Noble *et al.* generated a bar-coded collection of homozygous deletion mutants and used it in a signature-tagged mutagenesis study of infectivity in a mouse model[10]. Mutants with defects in morphogenesis were more likely to have decreased infectivity; however, a significant portion of mutants with severe morphogenesis defects retained the ability to cause infection. Noticeably, this study assayed for infection and not for disease; therefore it does not necessarily indicate the relationship between morphogenesis and *Candida* pathogenesis. Furthermore, their work serves to highlight the fact that additional studies will be required to fully understand the complex relationship between morphogenesis and pathogenesis in *C. albicans*.

Unlike *S. cerevisiae*, *C. albicans* usually exists in diploid form and lacks a classical meiotic cycle[11]. This fact makes the mating-based genetic strategies used to create genome-wide libraries of double mutant strains in *S. cerevisiae* are not applicable. Consequently, genetic interaction studies in *C. albicans* have been limited to gene-by-gene analyses. To date, molecular genetic studies of *C. albicans* have largely relied on *S. cerevisiae* as an experimental model based on the similarity between the two species. Uhl *et al*. developed a haploinsufficiency-based genetic analysis and used it to perform a screen for genes involved in hyphal development[12]. Haploinsufficiency describes the situation when mutation in one allele of a given gene results in a measurable phenotype. Complex haploinsufficiency (CHI) develops from a special case of unlinked non-complementation where a strain with two heterozygous mutations displays a more severe phenotype than either single mutant. This method can be successfully used to identify genes with similar function. Haarer *et al*. have identified about 208 actin interacting genes by using this approach[13]. They started with a parental strain that was a heterozygous actin mutant (*ACT1/act1Δ*) and further mutated a second set of genes in this strain. Double mutants were then assayed for growth defects compared to heterozygotes and the wild-type *ACT1* strain. The double mutants displayed CHI, meaning that the second mutated gene synthetically interacts with *ACT1* and has similar function.

Therefore, CHI can provide a useful strategy for the large-scale analysis of synthetic genetic interactions in *C. albicans*.

In this study, the Kumar laboratory presents the first large-scale synthetic genetic interaction screen in *C. albicans*. This work involved a CHI-based screening strategy applied to the identification of genes that interact with the RAM signaling network during *C. albicans* filamentation[14,15]. Cbk1p is the key serine/threonine protein kinase, which mediates many of the functions of the RAM network through its regulation of the transcription factor Ace2[16]. RAM pathway mutants in *C. albicans* show two distinct filamentation phenotypes. *CBK1* null mutants are unable to form filaments on Spider Medium (SM) or serum-containing medium, while *ACE2* null mutants are constitutively pseudohyphal and form true hyphae on serum[9]. In total, this CHI screen identified 151 genes showing decreased hyphal growth relative to the *CBK1* heterozygote, including 44 genes that genetically interact with *CBK1*. The results have also established a possible connection between the RAM and PKA pathways in hyphal development, while also identifying 17 putative targets of the RAM network transcription factor, Ace2p.

4.2 Materials and Methods

4.2.1 Strains, media and growth conditions

All strains were derived from CAI4 (*ura3Δ::imm434/ura3Δ::imm434*). CAMM-292 (*ura3*Δ::*imm*434/*ura3*Δ::*imm*434/*cbk1*-Δ1::*his*G/*CBK1*) was used as the parental strain for the transposon mutagenesis[17]. Standard yeast media was used for growth strains in this study. Yeast peptone dextrose supplemented with 80mg/L uridine, synthetic dextrose medium lacking uracil, and Spider Medium were prepared using standard recipes. Induction of filamentous growth in *C. albicans* was carried out using Spider Medium plates at 37°C for 3 days or liquid Spider Medium at 37°C for 3 hours[6,12]. All phenotypes were confirmed on Spider Medium plates supplemented with uracil to control for possible positional effects of *URA3* expression.

4.2.2 Transposon Mutagenesis

C. albicans strain WO-1 pEMBLY23 genomic DNA library [18](NIH AIDS Research & Reference Reagent Program) was used as the starting material for the transposon mutagenesis. Mutagenesis was performed *in vitro* using the GPS3-Mutagenesis system from NEB, with 80ng of DNA library and 20ng of donor plasmid. The donor plasmid was first modified to contain the Candida-specific *URA3-dpl200* cassette [19]at the *Spe*I restriction site. A total of nine independent mutagenesis reactions were performed. The transposon-inserted library plasmids were transformed into DH5α cells and selected on LB+Amp+Kan plates. Plasmids were recovered by Maxiprep (Qiagen), digested with *Pvu*II to release the genomic DNA fragments and transformed into *C. albicans* strain CAMM-292 using a standard lithium acetate transformation protocol. Slight modifications of this protocol were used, namely heat shock temperature of 44°C for 20 minutes [20] before plating. Each fragment integrates into the genome via homologous recombination. The resultant double heterozygotes were selected on SC-URA plates.

4.2.3 Screening for hyphal growth phenotypes

The resulting transgenic strains were grown overnight in liquid SC-URA medium in 96-well plates and replica-plated using a hand-pinning tool onto Spider Media in duplicate. Plates were incubated at 37°C for 5 days. Images were obtained using BioRad gel document camera. Colonies with altered hyphal growth relative to the starting strain CAMM-292 were scored as positive. These were retested on Spider plates and incubated as before to confirm the phenotype.

4.2.4 Identifying transposon insertion sites

Transposon insertion sites were amplified by 3' RACE (rapid amplification of cDNA ends). Total cellular RNA of the transposon-inserted strains was extracted and was reverse transcribed into cDNA with MMLV reverse transcriptase (Invitrogen) and a 3' RACE adapter. A fragment containing the URA3 marker was generated by standard PCR procedure using primers complementary to the ends of URA3 gene and the 3' RACE adaptor. The fragment was then cloned into a TA vector and was sequenced by University of Michigan Sequencing Core. The insertion sites were then identified by BLSTN searches using the Candia Genome Database (CGD)

4.2.5 Confirmation of synthetic interactions

CBK1 was re-integrated into each double heterozygote using plasmid pMM4, which carries the entire *CBK1* ORF and its promoter region. Since the selectable marker in pMM4 is *URA3*, similar to the transposon marker used, we had to cure the strain of this marker before reintroducing *CBK1*. To do this, we used the standard 5'FOA (5' fluoroorotic acid) selection method[21]. 5'FOA is a compound that is converted to fluorodeoxyuridine, a toxic intermediate, by yeast cells containing a wild type *URA3* gene. Thus only cells that do not possess a wild type *URA3* gene are able to survive on media containing 5'FOA with uracil added exogenously. The double heterozygotes were first grown in liquid YPD with 80mg/l uridine for 48 hours to encourage loss of the *URA3* marker[22]. A dilution was then plated on Synthetic Complete media containing 80mg/l uridine and 1mg/ml 5'FOA. Colonies were picked at random and replica plated onto YPD + uridine plates and SC-Ura plates. Colonies on YPD + uridine plates that did not grow on SC-URA were scored as positive i.e. they had lost the *URA3* marker. These were then picked as candidates for transformation of *CBK1*.

For the *CBK1* transformation, pMM4 was linearized with *BsrG*I and transformed into each transposon-inserted Ura- strain. The resultant *CBK1*-integrated transformants were selected on SC-URA. These were then screened on Spider medium as earlier and an increase in hyphal growth compared to that of the double heterozygote was scored as

positive. Integration of *CBK1* was confirmed by standard PCR amplification of a fragment of *CBK1*.

4.3 Results

4.3.1 Transposon mutagenesis of *C. albicans* genomic DNA library

To identify potential targets that are haploinsufficient with *CBK1*, a transposon insertion library was constructed in *C. albicans* using the *cbk1*Δ/*CBK1* background. The overall outline of the CHI-based screening strategy is presented in **Figure 4.1.** As a resource for large-scale screening, transposon insertion mutants offer both advantages and disadvantages. The advantage of using transposon-mediated gene disruption is that the mutagenic event is not biased towards annotated genes, so uncharacterized open reading frames (ORFs) are also disrupted. The limitation of this approach is that the transposon insertion collection is not comprehensive. Transposition is a random process, making it difficult to obtain an insertion affecting each yeast gene. Therefore, the insertion site might not be in a functional gene. In this study, a donor plasmid was derived from the bacterial element Tn7. The Tn*7* system has been used extensively for *in vitro* mutagenesis[23,24], with low reported insertion site specificity. For purposes of this screen, the Tn*7* element was modified to contain a recyclable allele of the *Candia* specific *URA3* marker; specifically, the *URA3-dpl200* allele was inserted into Tn*7* sequence encoded in the donor plasmid pGPS3. The advantage of *URA3-dpl200* is to allow recombinational excision of the *URA3* gene under counter-selection with 5-fluoro-orotic acid (5-FOA)[19]. Subsequently, this modified transposon was used in an *in vitro* mutagenesis reaction with a *C. albicans* genomic DNA library derived from the WO-1 strain. The genomic library was mutagenized to yield an estimated 20,000 independent insertions. The resulting insertion library was recovered in *E. coli*, and genomic DNA inserts were released by enzyme digestion for introduction into the *C. albicans cbk1*Δ/*CBK1* heterozygote strain. By homologous recombination, the mutagenized genomic DNA fragment will replace its native chromosomal locus, thereby generating a

heterozygous insertion mutant in the parent *cbk1*Δ/*CBK1* strain. In total, the approach yielded 6,528 independent Ura+ transformants (also see **Figure 4.4**).

4.3.2 CHI screening of the *cbk1Δ/CBK1* mutant

In contrast to wild type *C. albicans* filamentous strain CAI-4, *cbk1*Δ/*CBK1[17]* heterozygotes show defects in true hyphal growth, whereas the colonies show a decreased area of central wrinkling and a more prominent ring of peripheral filamentation on Spider medium at 37°C (**Figure 4.2**). We used this parental strain for testing haploinsufficiency for two reasons. First, it provided increased sensitivity in that the strain was already deficient for filamentation. Second, it could also improve specificity because weak phenotypes of non-interacting, transposon-derived mutants would be hidden by the *cbk1*Δ/*CBK1* phenotype.

In total, 6,528 insertion mutants for alterations in hyphal growth were identified by spotting cultures on 96-well format plates in duplicate and incubating them for 5 days on Spider plates. Hyphal growth phenotypes were compared to the original *CBK1* heterozygous strain. A decrease in hyphal growth indicated by a reduction or absence of peripheral hyphae or wrinkling at the center was scored as positive. Clones showing defects in hyphal growth were re-tested in the second screen. After retesting these strains in duplicate as earlier, 441 out of 1,810 showed consistent hyphal growth defects and were considered as our final set of putative *CBK1* interactors. In total, these 441 transposon insertion mutants correspond to 139 insertion sites and 42 unique genes

URA3 is a conserved gene and encodes for orotidine-5'-phosphate decarboxylase, a pyrimidine biosynthesis enzyme[19]. Previous studies have shown that differences in expression of this gene can lead to hyphal growth defects. To eliminate the possibility that the effect is caused by the *URA3* marker, identified insertion mutants were tested on Spider medium containing uridine. All the mutants tested showed hyphal growth defects, just as on the original Spider plates, confirming that *URA3* expression was not responsible for the phenotypes.

To confirm that the genes identified were true synthetic interactors of CBK1/RAM network, *CBK1* was re-integrated at its chromosomal position using plasmid pMM4. 41 candidate CHI strains with integration of *CBK1* showed increased hyphal growth, indicating that the observed phenotypes were dependent on the *cbk1* mutation and were likely due to a synthetic genetic interaction between *cbk1*Δ/*CBK1* and the transposon insertion. Among the 41 candidates, 22 genes were previously reported to relate to the RAM signaling pathway, and 14 were related to cAMP/PKA signaling, suggesting potential interaction between the RAM and PKA pathways during filamentous growth in *C. albicans*.

4.3.3 Deletion analysis and Cbk1p-dependent localization of *C. albicans* Rgd3p

To confirm the morphogenesis profile of *rgd1* mutants identified by CHI screening, we used the method developed by Fonzi *et al[17]*. to delete *RGD3* in wild type and *CBK1/cbk1Δ* strains. The *RGD3* heterozygote (*RGD3/rgd3Δ*) and *RGD3 CBK1* double mutant (*CBK1/cbk1Δ; RGD3/rgd3Δ*) showed similar phenotypes to the strains generated from transposon-based insertional mutagenesis (**Figure 4.3**). These results confirmed the synthetic interaction between *CBK1* and *RGD3*.

To further investigate the possible localization shift of Rgd3p in *CBK1*deletion strains, we generated a cassette in which *RGD3* was tagged with GFP in the C terminus and transformed into wild type, *CBK1/cbk1Δ*, and *cbk1Δ/Δ* strains. The construct could replace wild-type *RGD3* and allow the expression of Rgd3p-GFP. Transformed strains contain the URA+ element and are able to grow in SC-URA selection medium. Cells were grown overnight in SC-URA medium at 30°C to maintain vegetative growth. Fluorescence microscopy then was used to detect localization of Rgd3p.

We observed localization of Rgd3p to the septum in yeast stages, and the localization of Rgd3p depends on the presence of Cbk1p. We failed to localize Rgd3p in *CBK1/cbk1Δ* and *cbk1Δ/Δ* strains (**Figure 4.5**).

4.4 Discussion

In this study, a large-scale genetic analysis was performed in *Candida albicans*. Our approach was based on a CHI strategy, and, like other large-scale genetic analyses of *C. albicans*, we employed transponson-mediated insertional mutagenesis to generate a large collection of double heterozygous mutants derived from a parental strain containing a heterozygous null mutation of the RAM pathway kinase CBK1. This library was then used to screen for genes that interacted with *CBK1* during SM-induced morphogenesis. In total, we identified 41 genes that were true synthetic interactors of the *CBK1*/RAM network[14,15].

The transposon insertion library yields 6,238 independent insertions sites within the *C. albicans* genome. Although there are some limitations of transposon mutagenesis, this is still a large collection of mutants spread over much of the *C. albicans* genome. Since both coding and non-coding regions may be disrupted depending upon the site of insertion; the phenotypic consequences of disrupted regulatory regions, like promoters and terminators, can also be studied. The Tn7 plasmid system is easy to maintain, transfer, and transform into genetic backgrounds of interest[23,24]. Thus, it is a great resource for the further study of *C. albicans* genomics.

This research is the first using CHI-based genetic interaction screening for genetic analysis of the obligate diploid yeast *C. albicans*. It also confirms that CHI-based genetic screening is effective in identifying genes that interact with the query gene through a variety of mechanisms. The screen reveals a set 41 proteins with synthetic interactions with *CBK1*. These proteins have various functions in cell mechanisms, including the *ACE2* transcription targets *ENO1* and *PGK1*; potential *CBK1*-interactors *RGD3* and *VPS13*; and protein chaperones *HSP70*. Rgd3p is a putative fungal specific Rho GTPase GAP protein based on its genetic similarity to Rgd2p in *S. cerevisiae[25,26]*. The protein structure and function have not been characterized. Preliminary results showed that Rgd3p localized to the septum in vegetative growth conditions, which is the same as Rho4p localization. Deletion of *RGD3* showed negative effects in hyphal growth. This result could suggest a general role of the RhoGTPase family in hyphal growth in filamentous yeast. Among the 41 unique genes showing synthetic interactions with *CBK1*,

22 were involved in the RAM pathway, and 14 were regulated by the cAMP/PKA pathway. This result suggests a potential link between the RAM network and the cAMP-dependent PKA pathway, with both pathways functioning in parallel to regulate hyphal development in this species.

4.5. Acknowledgements

We thank Damian Krysan (University of Rochester) for providing reagents and for helpful comments in this project. We also thank William Fonzi (Georgetown University) and Geraldine Bulter (University of Dublin, Ireland) for providing strains and constructs.

Figure 4.1. Schematic of screening strategy. In vitro mutagenesis of C. albicans genomic library WO-1 using a Tn7-based transposon containing the *CaURA3-dpl200* auxotrophic marker yielded a library of plasmids from which genomic inserts were released by restriction endonuclease digestion and transformed into a *cbk1Δ/CBK1* heterozygote strain. The resulting library was screened on Spider Medium for altered filamentation relative to the parental strain.

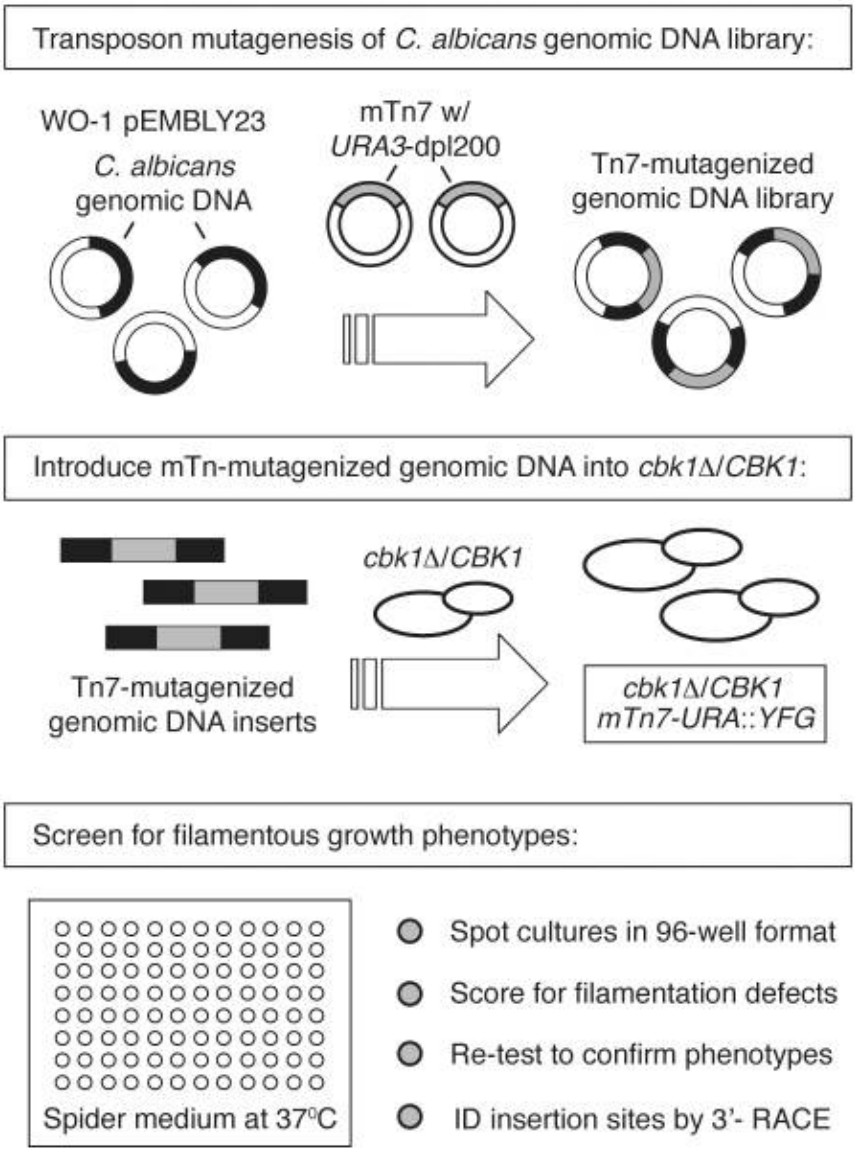

Figure 4.2. Screening of Tn7 transposon-inserted transformants on Spider plates for hyphal growth phenotypes. Transformants were grown overnight in SC-Ura medium and then spotted in 96-well format using a hand pinning tool on Spider medium. Plates were incubated at 37°C for 5 days. Colonies showing reduced or null hyphae as compared to *cbk1Δ/CBK1* were scored as positive (example of such colonies shown by the pointed arrow). These were retested on Spider medium as earlier to confirm hyphal growth phenotypes.

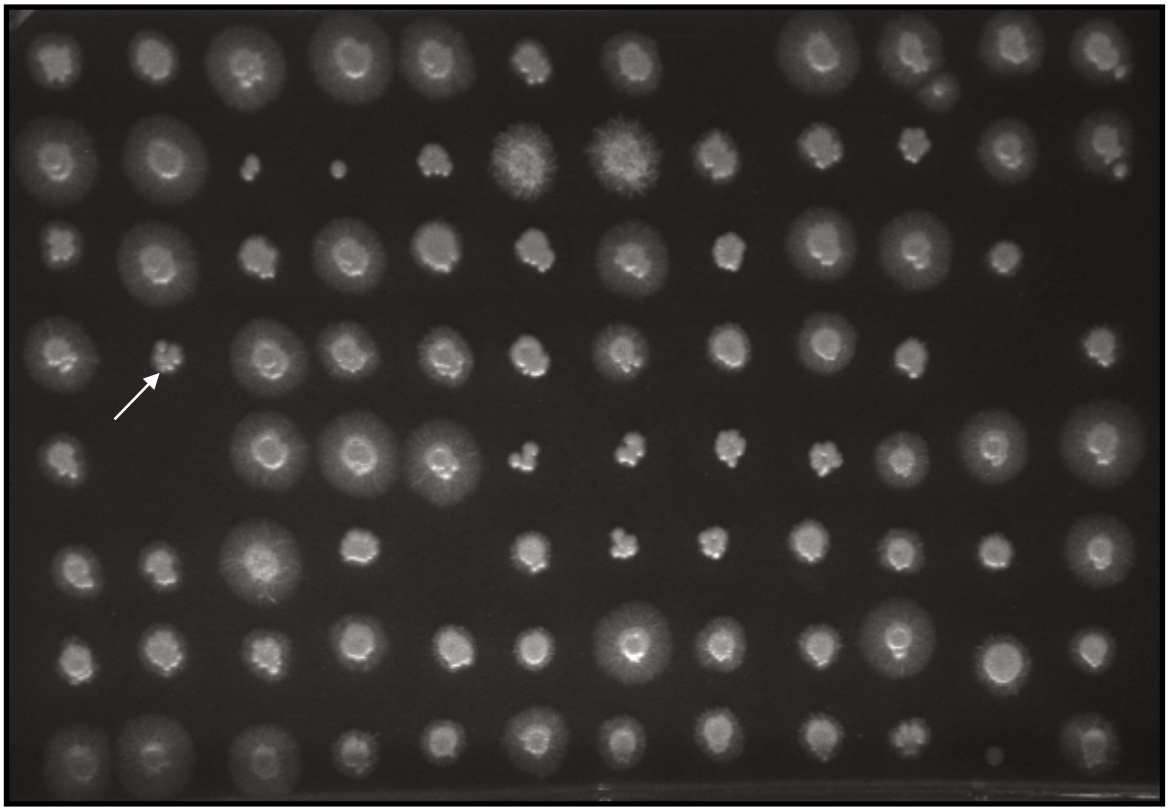

Figure 4.3. CHI-based screening identifies synthetic genetic interactions with CBK1 during morphogenesis. ***A***. Examples of primary screening data for complex heterozygotes showing synthetic genetic interactions with CBK1, as shown in Figure 4.2, each strain was spotted on Spider Medium and incubated at 37°C for 3 days. Mutants with decreased peripheral invasion and decreased central wrinkling were selected. Representative positive scoring mutants from the primary screen are shown here. ***B***. Representative examples of independently constructed complex heterozygote strains showing complex haploinsufficient genetic interaction with *cbk1Δ*.

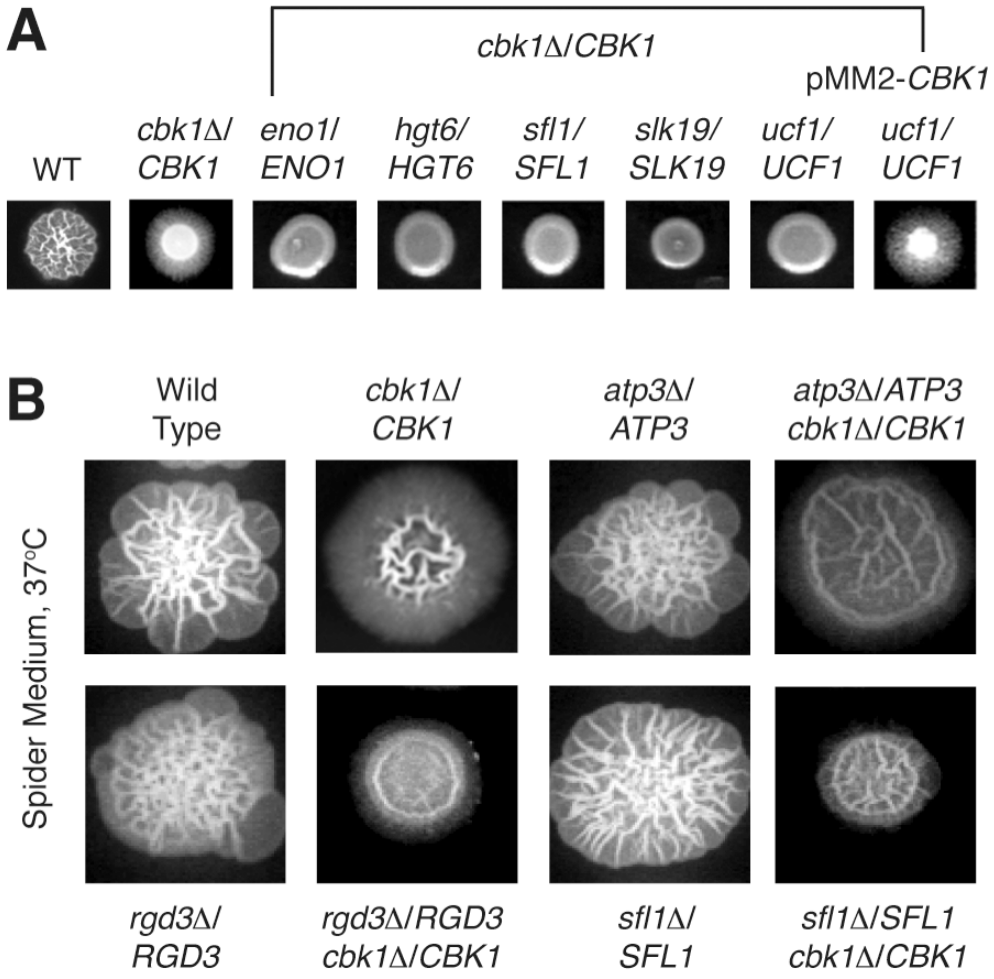

Figure 4.4. Summary of analysis of screening data. In total, 41 unique genes were identified showing synthetic interaction with *CBK1*.

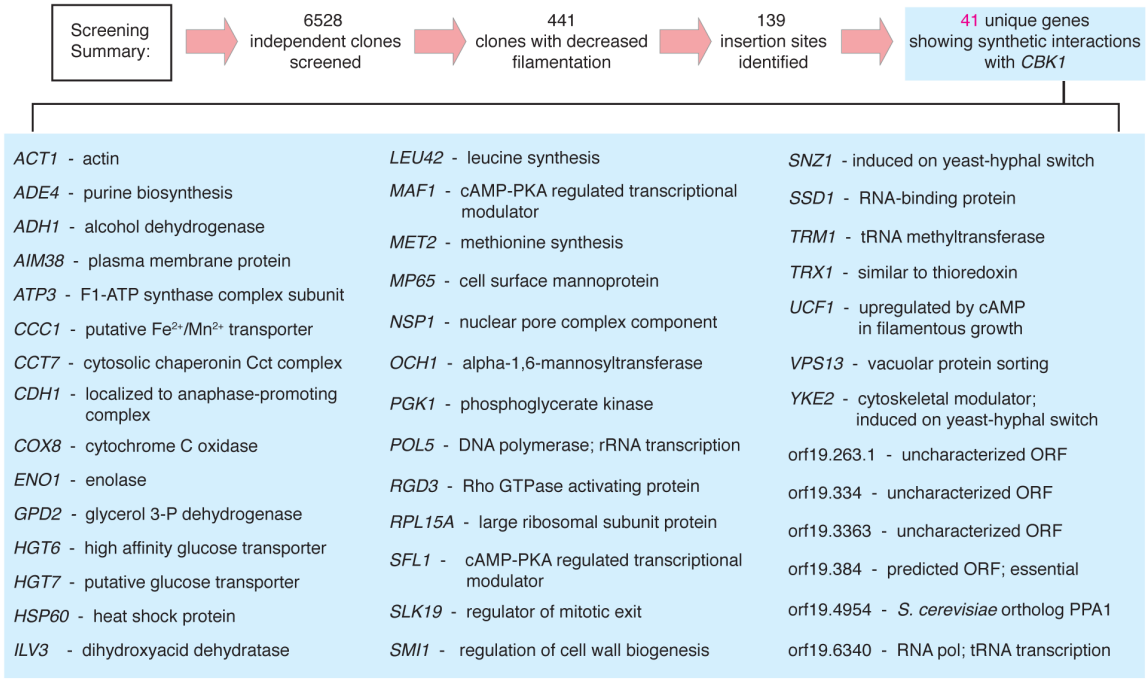

Figure 4.5. Localization of Rgd3p-GFP in wild type and *CBK1* deletion strains. In yeast form, Rgd3p localized in septal site or budding neck region while they failed to concentrate in *CBK1* deletion strains. In hyphal form, Rgd3p defused in whole cell, but the phenotype of *cbk1Δ/Δ* is unique. In this case, Rgd3p concentrated to one budding neck region when cells failed to separate and were unable to form true hyphae.

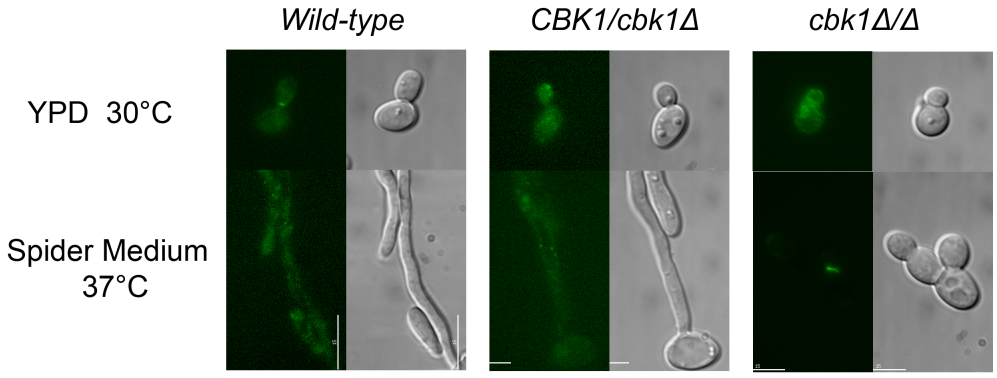

Reference

1. Whiteway M, Oberholzer U (2004) Candida morphogenesis and host-pathogen interactions. Curr Opin Microbiol 7: 350-357.
2. Csank C, Makris C, Meloche S, Schroppel K, Rollinghoff M, et al. (1997) Derepressed hyphal growth and reduced virulence in a VH1 family-related protein phosphatase mutant of the human pathogen Candida albicans. Mol Biol Cell 8: 2539-2551.
3. Bismay K, Mathew A, Rajesh R, Kurian G, Unni VN, et al. (2012) Disseminated candidiasis 18 years after renal transplantation. Indian J Nephrol 22: 462-465.
4. Lopez C, Bulacio L, Espejo T, Paz M, Pairoba C, et al. (2012) Prevalence of chronic hyperplasic candidiasis. Its association to risk factors in an Oral Medicine Service in Rosario, Argentina. J Mycol Med 22: 35-41.
5. Anwar KP, Malik A, Subhan KH (2012) Profile of candidiasis in HIV infected patients. Iran J Microbiol 4: 204-209.
6. Sudbery P, Gow N, Berman J (2004) The distinct morphogenic states of Candida albicans. Trends Microbiol 12: 317-324.
7. Berman J (2006) Morphogenesis and cell cycle progression in Candida albicans. Curr Opin Microbiol 9: 595-601.
8. Jayatilake JA, Samaranayake YH, Cheung LK, Samaranayake LP (2006) Quantitative evaluation of tissue invasion by wild type, hyphal and SAP mutants of Candida albicans, and non-albicans Candida species in reconstituted human oral epithelium. J Oral Pathol Med 35: 484-491.
9. Kelly MT, MacCallum DM, Clancy SD, Odds FC, Brown AJ, et al. (2004) The Candida albicans CaACE2 gene affects morphogenesis, adherence and virulence. Mol Microbiol 53: 969-983.
10. Noble SM, Johnson AD (2007) Genetics of Candida albicans, a Diploid Human Fungal Pathogen. Annual Review of Genetics 41: 193-211.
11. Berman J, Sudbery PE (2002) Candida Albicans: a molecular revolution built on lessons from budding yeast. Nat Rev Genet 3: 918-930.
12. Uhl MA, Biery M, Craig N, Johnson AD (2003) Haploinsufficiency-based large-scale forward genetic analysis of filamentous growth in the diploid human fungal pathogen C.albicans. EMBO J 22: 2668-2678.
13. Haarer B, Viggiano S, Hibbs MA, Troyanskaya OG, Amberg DC (2007) Modeling complex genetic interactions in a simple eukaryotic genome: actin displays a rich spectrum of complex haploinsufficiencies. Genes Dev 21: 148-159.
14. Song Y, Cheon SA, Lee KE, Lee SY, Lee BK, et al. (2008) Role of the RAM network in cell polarity and hyphal morphogenesis in Candida albicans. Mol Biol Cell 19: 5456-5477.

15. Nelson B, Kurischko C, Horecka J, Mody M, Nair P, et al. (2003) RAM: a conserved signaling network that regulates Ace2p transcriptional activity and polarized morphogenesis. Mol Biol Cell 14: 3782-3803.
16. Jansen JM, Barry MF, Yoo CK, Weiss EL (2006) Phosphoregulation of Cbk1 is critical for RAM network control of transcription and morphogenesis. J Cell Biol 175: 755-766.
17. McNemar MD, Fonzi WA (2002) Conserved serine/threonine kinase encoded by CBK1 regulates expression of several hypha-associated transcripts and genes encoding cell wall proteins in Candida albicans. J Bacteriol 184: 2058-2061.
18. Slutsky B, Staebell M, Anderson J, Risen L, Pfaller M, et al. (1987) "White-opaque transition": a second high-frequency switching system in Candida albicans. J Bacteriol 169: 189-197.
19. Wilson RB, Davis D, Enloe BM, Mitchell AP (2000) A recyclable Candida albicans URA3 cassette for PCR product-directed gene disruptions. Yeast 16: 65-70.
20. Walther A, Wendland J (2003) An improved transformation protocol for the human fungal pathogen Candida albicans. Curr Genet 42: 339-343.
21. Boeke JD, Trueheart J, Natsoulis G, Fink GR (1987) 5-Fluoroorotic acid as a selective agent in yeast molecular genetics. Methods Enzymol 154: 164-175.
22. Monteoliva L, Sanchez M, Pla J, Gil C, Nombela C (1996) Cloning of Candida albicans SEC14 gene homologue coding for a putative essential function. Yeast 12: 1097-1105.
23. Biery MC, Stewart FJ, Stellwagen AE, Raleigh EA, Craig NL (2000) A simple in vitro Tn7-based transposition system with low target site selectivity for genome and gene analysis. Nucleic Acids Res 28: 1067-1077.
24. Kumar A, Seringhaus M, Biery MC, Sarnovsky RJ, Umansky L, et al. (2004) Large-scale mutagenesis of the yeast genome using a Tn7-derived multipurpose transposon. Genome Res 14: 1975-1986.
25. Fernandes H, Roumanie O, Claret S, Gatti X, Thoraval D, et al. (2006) The Rho3 and Rho4 small GTPases interact functionally with Wsc1p, a cell surface sensor of the protein kinase C cell-integrity pathway in Saccharomyces cerevisiae. Microbiology 152: 695-708.
26. Dunkler A, Wendland J (2007) Candida albicans Rho-type GTPase-encoding genes required for polarized cell growth and cell separation. Eukaryot Cell 6: 844-854.

Chapter 5
Discussions and Future Studies

The budding yeast *Saccharomyces cerevisiae* is an ideal eukaryotic microorganism for biological studies. It has been widely used in biological research and is a popular model organism for genomics and proteomics, cell biology and biochemistry. It possesses a small size, minimal nutritional requirements, and is non-pathogenic in nature. *S. cerevisiae* also exhibits a short doubling time of 90 minutes and stable haploid and diploid cell forms, easing experimental data collection,. Recent developments in yeast genetics and proteomics have facilitated research in *S. cerevisiae* addressing the cellular mechanisms, developmental events, and post-translational modifications that enable pseudohyphal growth. In this thesis, I have utilized various methods in genomics and proteomics to explore more fully the mechanisms that regulate filamentous growth.

Chapter 1 introduces budding yeast as a model for eukaryotic cell biology and genetics and illustrates genomic and proteomic studies that have been carried out by various groups. In this chapter, I will also briefly discuss filamentous growth in the principal human fungal pathogen, *Candida albicans*, highlighting recent and relevant discoveries.

Filamentous growth in *Saccharomyces cerevisiae* and *Candida albicans* has been well studied through the application of genomic and proteomic technologies. As a form of cellular morphological change, filamentous growth is closely related to other cell mechanisms regulating morphology, including regulatory mechanisms that control apical cell growth, budding site selection and cell-cell adhesion. Moreover, since it is induced by nutrient limitation in the surrounding environment, filamentous growth has been found to be related to cellular energy-providing systems, such as mitochondrial metabolism and RNA processing mechanisms. Filamentous growth in *S. cerevisiae* is mediated by several signaling pathways. Classic studies from numerous laboratories have identified at least

three signaling pathways that regulate filamentous growth: the MAPK pathway, the Ras/PKA pathway, and the Snf1p kinase pathway. While these essential signaling pathways play key roles in regulating filamentous growth transitions in *S. cerevisiae*, the full genetic basis of yeast filamentation is very broad. *Candida albicans* is the most prominent fungal pathogen in humans. It belongs to the fungal kingdom and shares multiple similarities with *S. cerevisiae*. It is one of the major causes of candidiasis, which is fairly dangerous and commonly seen within patients whose immune system is compromised. Pervious studies have suggested that the virulence of *C. albicans* is strongly associated with its ability to switch between yeast and hyphal growth. It has been suggested that the yeast form is important for dissemination, and the hyphal form is required to invade host tissue. The well-studied signaling pathways regulating hyphal growth in *C. albicans* includes the MAPK pathway, cAMP/PKA pathway and RAM pathway.

Although much has been discovered regarding the molecular basis of filamentous growth, important questions remain concerning the fundamental genetic differences between filamentous and non-filamentous strains. In Chapter 2, I integrated pooled segregant analysis with next-generation sequencing techniques to identify alleles linked with invasive growth. In total, we identified 522 allelic differences within 201 genes that relate to haploid invasive growth. In particular, our work identified allelic variation in the *PEA2* and *MDM32* genes linked with invasive growth phenotypes in the Σ1278b and SK1 genetic backgrounds, respectively. The results indicate Pea2p, a key component in the cell polarisome complex, plays a critical role in regulating filamentous growth through the MAPK signaling pathway in yeast. We found that Pea2p primarily interacts with the scaffolding protein Spa2p to alter haploid axial budding to a unipolar pattern during invasive growth in filamentous strains, suggesting a strong connection between filamentous growth and bud site selection mechanisms. In addition, a mitochondrial structural protein Mdm32p was also linked to filamentous growth, revealing the possible role of general mitochondrial function and cell respiratory mechanisms during filamentous growth.

In this chapter, I discuss several studies that could be undertaken to further advance the research presented in this thesis. In my thesis work, I have focused principally on two hits from the linkage analysis screen. In total, this screen revealed more than 200 genes that are putatively linked to filamentous growth. As a follow up to this study, it would be informative to carry out a thorough analysis of the remaining genes, or a fraction thereof. The data from such a study would no doubt help in forming a better picture of the network of regulated proteins that enable pseudohyphal growth. Some proteins such as Sfl1p, Rho2p, and Yir021w-A, which is a small protein of unknown function, are especially worthy of further investigation. In fact, there were large sets of genes of unknown function within both screens, and it would be informative to check their relationships with respect to known signaling pathways that regulate filamentous growth.

Through the study of Pea2p presented in this dissertation, I proposed a working model of cell polarisome complex function regulating filamentous growth in haploid cells (Figure 5.1). It is interesting that different forms of Pea2p can alter its protein-protein interaction with Spa2p from distinct genetic backgrounds. It would be interesting to study further the mechanism through which the polarisome complex mediates filamentous growth. The Snyder group has suggested that the polarisome may interact with key components within MAPK signaling pathways, like Ste7p or Ste11p. Plus, my results indicate that Pea2p affects filamentous growth through the Kss1p MAPK pathway. Further, the role of the presumed scaffolding protein Bni1p in this process remains unclear. Thus, it would be informative to determine whether Bni1p affects filamentous growth. Additionally, a protein-protein interaction study using yeast two-hybrid or co-immunoprecipitation methods could be implemented to identify whether Bni1p from different genetic backgrounds may modulate respective binding affinities, potentially even affecting the overall integrity of the polarisome complex. In traditional views of the Kss1p MAPK pathway, Cdc42p as a Rho GTPase interacts with the MAPKKK Ste20p to initiate the signaling cascade. In the aforementioned linkage screen, I identified another member of the Rho GTPase family, Rho2p, that also affects filamentous growth. The overall function of Rho2p is still unclear; thus, it would be interesting to test its substrates to see whether Rho2p plays a role in regulation of the MAPK pathway.

Another possible study may be implemented to understand the connection between mitochondria and filamentous growth. The SK1/S288c screen reveals a set of mitochondrial genes, including *MDM32*, *MPA43*, *MRPL23*, and *IDH2* (Figure 5.2). Strains individually deleted for each of these genes exhibit impaired filamentous growth, and plasmid complementation with genes from the S288c genetic background cannot rescue the defective phenotypes. Therefore, it would be useful to identify the functional consequence of allelic variation between these genes and their encoded protein products. These findings could then be applied to general mitochondrial genes, potentially revealing novel mitochondrial regulatory functions during filamentous growth in yeast.

Finally, our linkage screen reveals a set of genes with alleles from a filamentous genetic background that are associated with non-invasive offspring (Figure 5.3). This indicates that the S288c genetic background is not uniformly repressive with respect to filamentation, and vise versa. This finding also suggests that the filamentous growth mechanism may exist in numerous yeast strains, with remnants present in non-filamentous strains from an evolutionary point of view. Interestingly, *BNI1* was identified in this set of genes, making it a good candidate for the following research. It would also be interesting to study the function of the polarisome complex within the SK1 genetic background. To date, the fundamental nature of filamentous growth is still unclear; we do know that pseudohyphal growth is a dramatic morphological change requiring a large amount of energy. Furthermore, pseudohyphal growth only exists in a fraction of tested natural strains. So it is still debatable whether it pseudohyphal growth is an ability of natural strains that has been generally lost during evolution or a gain of function during natural selection by environmental pressure. Here, I studied two widely used filamantous strains, Σ1278 and SK1, to establish our results. It would be really intriguing, however, to study more natural strains from the evolutionary tree to enable better and more informative comparisons, advancing our understanding of this important morphogenetic mechanism.

Chapter 3 describes an application of mass spectrometry identifying proteins with different abundance profiles during filamentous growth. By isobaric tagging of plasma membrane proteins with unique reagents, we were able to detect proteins that are

differentially enriched during various filamentous growth stages. In total, we discovered 11 proteins that are differentially abundant under conditions of nitrogen stress and have been localized to the yeast cell periphery. Among these proteins, we were interested in a protein of unknown function localized to the MCC domain, Ylr414c, renamed as Pun1p. Deletion mutants of *PUN1* in both haploid and diploid strains showed defects in surface spread filamentation, invasive growth on solid medium, cell-cell adhesion and cell growth under conditions of nitrogen stress. Overexpression of *PUN1* results in exaggerated cell elongation, although invasive growth properties are not appreciably increased over wild type. These results indicate that *PUN1* is required for wild type filamentous growth in yeast.

PUN1 is known as a component of the MCC domain. The MCC represents a protective area within the plasma membrane to control the turnover of transport proteins. We discovered that several components of the MCC domain were also required for filamentous growth in yeast. *TAT2* and *FUR4* are amino acid transporters, while Fur4p transports uracil, and Tat2p transports tryptophan and tyrosine. However, other membrane proteins are yet to be tested. Thus it would be interesting to test those genes to further categorize the function of the MCC during filamentous growth. Transcriptional profiles of a strain deleted for *PUN1* have unveiled 82 genes that exhibit increased transcript abundance and 48 genes that yield decreased mRNA levels. In particular, the genes exhibiting decreased mRNA levels upon *PUN1* deletion were significantly enriched in genes contributing to amino acid biosynthesis. Thus, it would be interesting to examine these gene sets to identify proteins which could further contribute to the extensive and intricately regulated filamentous growth transition.

Figure 5.1. Working model of polarisome regulating filamentous growth. Spa2p, Pea2p and Bud6p form a polarisome that regulates filamentous growth by interacting with MAPKKK Ste11p, suggesting the connection between MAPK pathway and polarisome. The function of Bni1p and Rho2p is unclear at this stage.

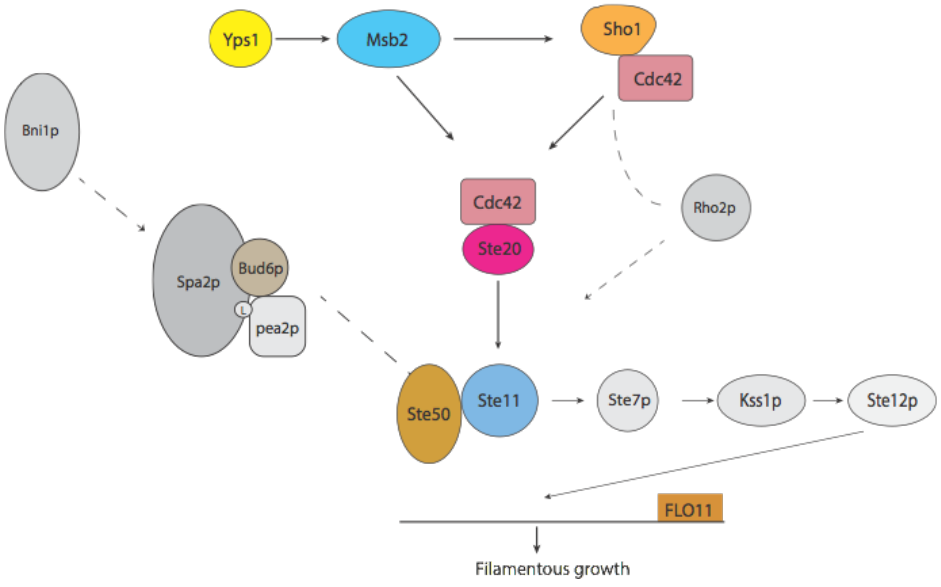

Figure 5.2. Mitochondrial genes identified within SK1/S288c cross. Deletion mutants of MDM32, MPA43, MRPL23 and IDH2 all exhibit impaired filamentous growth. Plasmid complementation using genes with S288c genetic background didn't rescue the defective phenotype.

gene	chromosome	S288c position (nt)	nt allele change (S288c to SK1)	amino acid change (S288c to SK1)	LOD score
MDM32	Chr. XV	607152; 607393	G-C; A-T	C-S; L-F	9
MPA43	Chr. XIV	180743	G-T	R-L	4.6
MRPL23	Chr. XV	612124	G-A	R-K	5.7
IDH2	Chr. XIV	580334	C-G	L-F	7

Figure 5.3. Allelic changes that correspond to non-invasive offspring. A set of genes that the Σ1278b allelic change is associated with non-invasive offspring, suggesting S288c genetic background is not uniformly repressive with respect to filamentation, and vise versa. Also, we observed the same in SK1/S288c cross.